Electrochemical Gasification in a Direct Carbon Fuel Cell

Author
T.V. Ottevanger BSc.

Supervisors
Dr. L.M. Kamp
Dr. K. Hemmes

Master
Sustainable Energy Technology

Faculty
Technology, Policy and Management

2021

Abstract

Electricity generation in a Direct Carbon Fuel Cell has thermodynamic advantages over conventional methods, because the DCFC is not limited by the Carnot efficiency. This thesis analyzes and models a DCFC where the electrochemical oxidation of carbon to carbon monoxide is taken into account, which is an endothermic reaction. The heat necessary for this reaction is converted directly into electricity, so the DCFC can achieve a theoretical reversible efficiency of >100%. The heat is provided by a solar reactor, which converts methane into hydrogen and solid carbon by thermal decomposition. The formed solid carbon particles is fuel for the DCFC. The produced CO at the anode of the DCFC is used in a WGS reactor where it reacts with steam to form hydrogen. In this way we present a Multi-Source Multi-Product energy system.

The MSMP energy system is modelled in Cycle Tempo and we use the modelling results to perform a feasibility study and exergy analysis. The exergy analysis showed that the solar reactor contributes the most to the total exergy losses in the system.

Considering the fact that the WGS reactor is a mature technology, the solar reactor is based on existing technology (CSP), and solutions to challenges in heat handling and mass transfer are available in the process industry, the MSMP energy system has high potential to be technically feasible. We calculated that the unknown costs of the MSMP energy system need to be lower than 29.8 €/MWh$_p$ to be competitive with conventional hydrogen production methods and need to be lower than 34.8 €/MWh$_p$ to be competitive with a gas fired plant. Based on current market prices for methane, hydrogen and electricity in Algeria and based on the fact that we were able to determine the costs of the majority of components in the MSMP energy system, it is likely that the unknown costs will not exceed our determined maximum unknown costs. This shows the economic feasibility potential. We calculated that the MSMP energy system emits 37% less CO2 than hydrogen production by steam reforming which indicates the sustainable potential. We concluded that the concept favors a geographical location with high solar density, good gas infrastructure and stable politics. Algeria seemed to meet all those demands. Therefore we conclude that our MSMP energy system has high potential to be socially feasible.

We concluded that our MSMP energy system has high potential to be technically, economically and socially feasible.

Executive Summary

This thesis analyzes multiple angles of approach of electrochemical gasification in a direct carbon fuel cell, based on the multi-source multi-product concept. As the name tells us, the MSMP concept include multiple components in an energy system, consuming multiple sources and producing multiple products.

Our concept is a combination of a solar reactor, direct carbon fuel cell and water-gas-shift reactor. The solar reactor is fed with natural gas (for simplification we use methane) and by focusing solar irradiation to a central receiver, the gas is heated up to temperatures where thermal decomposition of methane occur. The methane is converted into hydrogen and carbon particles and the carbon particles are used as fuel for the DCFC. The DCFC generates electricity and at the anode, a mix of CO and CO2 is produced. The CO is fed to a WGS reactor, where it reacts with steam to form hydrogen and CO2. With this concept, methane and solar power are the sources and hydrogen and electricity are the products: A MSMP energy system.

In Chapter 2 we present an overview of current technologies relevant to our concept. Here we try to determine state-of-the-art technologies relevant to our concept, which clarifies where further technological development is needed for the MSMP energy system. It seemed that both the solar reactor and the DCFC are immature technologies. Although combined solar power (CSP) has a similar working principle as the solar reactor and is applied on an industrial scale, a difference can be found in the receiver. In the receiver of a CSP plant only heat transfer occurs, but in the receiver of a solar reactor also a chemical reaction (thermal decomposition) occurs. This makes the solar reactor more advanced than CSP.

An even less mature technology is the DCFC. Literature reports a couple of experimental setups, but they are all focused on a DCFC where pure CO2 is produced at the anode. Our research focuses on a DCFC where both CO and CO2 is produced at the anode, which involves two other (electro)chemical reactions compared to the conventional DCFC. Such a DCFC is not tested yet in practice, indicating that the current state of technology is immature.

The WGS reactor is operational at an industrial scale, so we can say that this is a mature technology.

In Chapter 3 we present in detail the theory of the solar reactor, the DCFC and the WGS reactor. The solar reactor desires a temperature of > 1500 K for a > 99% methane thermal decomposition. With a solar tower configuration, where multiple heliostat mirrors are focused on one receiver, this temperature is possible to achieve. The aerosol fluid wall reactor and the vortex flow reactor showed results with good potential in an experimental setup.

The DCFC is based on the molten carbonate fuel cell, since it has the same molten carbonate electrolyte. However, the DCFC is fed with solid carbon as fuel. Carbon has a high energy density and if we take the reactions in the fuel cell into account we notice the potential of this type of fuel cell. At the anode with temperatures higher than 700 °C, the 4-electron electrochemical reaction oxidation of C to CO2, the 2-electron electrochemical oxidation of C to CO and CO2 and the chemical Boudouard reaction where C reacts with CO2 to form CO take place simultaneously. Since the 2-electron electrochemical reaction is endothermic, an external source is demanded to stabilize the cell voltage. In our case, the thermal source is the solar reactor. This means that heat is directly converted into electricity, so theoretically a reversible efficiency >100% would be possible for the DCFC.

The WGS reactor favors a temperature of 200 °C with a high steam to CO ratio. With these operating conditions, almost a 100% conversion of H20 and CO to H2 and CO2 can be achieved.

In Chapter 4 we present the MSMP energy system modelled in Cycle Tempo. Our model was limited by the fact that the fuel cell apparatus in Cycle Tempo only had the 4-electron electrochemical reaction taken into account. Therefore we had to rewrite the Cycle Tempo fuel cell subroutine to add the 2-electron electrochemical reaction. Also the Boudouard reaction was not implemented in the DCFC apparatus, so we modelled a separate Boudouard reactor fed by the anode. The solar reactor was modelled as a gasifier, since there was no solar reactor apparatus available in Cycle Tempo. Given the complexity of the model, we neglected pumps, valves, heat exchangers and blowers in the model. Losses by these components are therefore not taken into account.

Our aim was to tune the input variables of the DCFC in such a way that an expected I-V curve could be established, which we could use to determine the maximum power density. Unfortunately the voltage of the 2-electron DCFC turned out to be almost independent of temperature and the voltage of the 4-electron DCFC turned out to be dependent of temperature, while we expected the contrary based on the theory of the DCFC. Since we were unable to solve or explain this, we chose to determine the maximum power density based on literature and to tune the input variables such that the DCFC operates at this maximum power density. With these input variables our model showed what was expected. This was a measure of reliability, so that we could use the modelling results for the feasibility studies.

We also performed an exergy analysis. Although a negative exergy loss was shown, which is not possible in practice, we can say that the solar reactor showed the highest contribution to the total exergy loss of the system. This tells us that this is the part where most significant improvements are to be found.

With the help of the technology status, theory and modelling results we performed a feasibility study from a technical, economic and social perspective.

In Chapter 5: Technical feasibility we analyzed what technical limitations there would be if the MSMP energy system was built in practice and present solutions how to overcome the limitations. Challenges in heat were present, given the fact that the solar reactor (>1200 °C) and the fuel cell (700 – 800 °C) have high operation temperatures. By using graphite and stainless steel alloys as materials for the components in the system, proper thermal resistance can be expected. We presented a stepwise heat exchange solution, where multiple types of heat exchangers are connected based on the operation temperature. We proposed a solution for heat transfer where the molten carbonate electrolyte is heated by the solar reactor and is transferred to the fuel cell in order to provide the necessary heat.

For the large mass transfers in the system, solutions where available in the process industry where large pumps and blowers at high temperatures are operated. Only for the transport of the molten carbonate at our desired temperature no pumps were found in literature that operate at such scale and temperature, although we found an experimental setup where molten carbonate was successfully transported by a centrifugal pump. Considering the fact that the WGS reactor is a mature technology, the solar reactor is based on existing technology (CSP), the DCFC showed already its potential in experimental setups and we presented solutions to challenges in heat handling and mass transfer, we conclude that our MSMP energy system has high potential to be technically feasible.

In Chapter 6 we analyzed the economic feasibility, based on literature and the modelling results. Since no MSMP energy system is operational, we could not calculate or determine the developing, manufacturing and operation and maintenance costs based on practical data. Therefore we calculated the costs and revenue of the sources and products, based on current and local market prices (in our case in Algeria, based on the social feasibility). We determined the cost of parts in our MSMP energy system which we were able to determine, such as the mirrors of the solar reactor, WGS reactor and the MCFC (which shares the same electrolyte with the DCFC). All other non-determinable costs were called unknown costs. It turned out that the unknown costs need to be lower than 37.8 €/MWh for the MSMP energy system to stay profitable. We then analyzed the costs of competing hydrogen producers and electricity generators, in order to determine what the maximum unknown costs need to be for the MSMP energy system to compete with these competing technologies. We determined that the unknown costs need to be lower than 29.8 €/MWh_p to compete with the most common hydrogen production method, steam reforming. To compete with gas fired power plants the unknown costs need to be lower than 34.8 €/MWh_p . We have to acknowledge that our modelling results neglect certain losses in the system and that the we had to make some design choices which can be beneficial for the economic feasibility. But based on current market prices for methane, hydrogen and electricity in Algeria and based on the fact that we were able to determine the costs of the majority of components in the MSMP energy system, it is likely that the unknown costs will not exceed our determined maximum unknown costs. Therefore we can conclude that our proposed MSMP energy system has the potential to be economically feasible.

In Chapter 7 we performed a social feasibility study. We analyzed the sustainable potential and we analyzed where our MSMP energy system could be implemented. Based on the modelling results we calculated that our model emitted 37% less CO2 for hydrogen production than steam reforming, which is currently the most common method of hydrogen production. It is fair to say that the neglected losses by our model would account for a higher CO2 emission. However, the losses by this equipment were calculated by Houwing et al. in a similar MSMP energy system and the contribution of these losses were approximately 12.5% to the total exergy loss in the system. Therefore the contribution of these losses will probably not eliminate the 37% reduction of CO2 emission, compared to steam reforming.

We also explored where our MSMP energy system could be installed. Since our system highly depends on solar power, a country with high solar density was desired. We also desire a country with good gas infrastructure and stable politics. It turned out that Algeria meets all demands of our MSMP energy system. They do not have significant international conflicts, have an abundancy of natural gas resources, have good connection with the European gas grid, have renewable energy targets and have a very high solar density. Based on the modelling results we calculated that our MSMP energy system is more sustainable than conventional technology and we found a country that meets all demands for the MSMP energy system to be operational. Therefore we can conclude that our MSMP energy system has high potential to be socially feasible.

Based on existing technologies, the theory and modelling results we performed a technical, economic and social feasibility study. We presented our findings and discussed the uncertainties. Based on our research we conclude that our proposed MSMP energy system has high potential to be feasible.

Acknowledgement

Five and a half years ago I started my master study Sustainable Energy Technology. Never had I thought that it would take me four years to finish my master's thesis. But here I am, without a doubt very proud of what I achieved.

I met Dr. Kas Hemmes during my second year at TU Delft, as we had an introductory conversation about a possible subject for my master thesis. I was a little nervous, but I do remember as soon as I entered the office of Dr. Hemmes I immediately was relaxed. His office looked like a vintage jungle and his first question was what kind of music I liked. He put up some catchy saxophone music I suggested and that was the point that I knew he would be my thesis supervisor.

I cannot thank Dr. Kas Hemmes enough for his sharing of knowledge and his enthusiastic way of telling about super boring subjects. At first I did not know what he was talking about, but somehow he managed to make me believe that fuel cells and especially fuel cells in a MSMP energy system are very interesting. I want to thank him for his patience, because he understood that my working career I started during the second year of my master study had importance too. But I want to thank him especially for his will to supervise me after his retirement. Dr. Hemmes, I hope you will not be too busy with students like me during your retirement and I wish you good health and all the best!

I also want to thank Ir. Theo Woudstra for his help with Cycle Tempo. It was one hell of a job to rewrite the subroutine of the fuel cell, but you helped me understand the program properly. Without your help I was probably still trying to figure out Cycle Tempo.

I want to thank Dr. Linda Kamp. Last summer I decided that my thesis took too long and the summer holiday would be my last try, whether or not I succeeded. I did not, so I almost had given up my master study. But then I received an email by Dr. Linda Kamp, why it took me so long to graduate? She was willing to be my second supervisor and her approach was exactly what I needed. She let me make a project plan and gave me deadlines for a stepwise finish of my thesis. Dr. Kamp was able to give me renewed energy to finish my thesis. Thank you Dr. Kamp for your positivity and very useful feedback!

Last but not least I want to thank my parents, my brothers and especially my fiancé Christie for all your patience these years. All your motivational speeches gave me the energy to combine my working career and my master study. Thank you!

Sincerely,

Thomas Ottevanger

Dordrecht, February 11th, 2021

Table of contents

List of Figures

List of Tables

List of abbreviations

DCFC	Direct carbon fuel cell
MSMP	Multi-Source Multi-Product
CHP	Combined heat and power
CSP	Combined solar power
MCFC	Molten carbonate fuel cell
PEMFC	Polymer exchange membrane fuel cell
SOFC	Solid oxide fuel cell
WGS	Water-gas-shift
C	Carbon
CO	Carbon monoxide
CO2	Carbon dioxide
$CO3^{2-}$	Carbonate
H2	Hydrogen
CH4	Methane
H2O	Water
O2	Oxygen
e	Electron
K	Kelvin
°C	Degrees Celsius
kg	Kilo gram
m	Meter
m^3	Cubic meter
HHV	Higher heating value
kWh	Kilowatt hour
LHV	Lower heating value
MW	Megawatt
MWh	Megawatt hour
MWh_p	Megawatt hour produced (hydrogen equivalent)
A	Current density
V	Voltage
η	Efficiency
T	Temperature
H	Enthalpy
S	Entropy
s	Second
G	Gibbs free energy
F	Faraday constant
n	Number of electrons
E	Equilibrium voltage / Nernst voltage
E^0	Open circuit voltage
Ex	Exergy
Q	Heat
OCV	Open circuit voltage
P	Pressure
R	Steam to carbon monoxide ratio

1 Introduction

It has been commonly known that conventional power production, in the form of fossil fueled power plants, contributes significantly to the annual greenhouse gas emissions and therefore to global warming. Although commercial power plants are becoming more efficient over the decades and thus emit less GHG, they are limited by the Carnot efficiency: $\eta = 1 - \frac{T_2}{T_1}$ (Park and Kim, 2014). The conventional principle is always the same: Generation of heat by firing fossil fuel and convert the heat by work into electricity.

Contrary to fossil fueled systems, fuel cells eliminate the necessity of moving parts such as turbines. Fuel cells can convert the fuel directly into electricity and heat, without the heat-to-work conversion step. This thesis considers a Direct Carbon Fuel Cell (DCFC), which electrochemically oxidizes solid carbon. A common DCFC produces carbon dioxide (CO2) as product and this electrochemical reaction is nearly independent of temperature. Therefore the DCFC is not limited by the Carnot efficiency and theoretically can achieve a reversible efficiency of 100%.

Not commonly known is a DCFC operating at higher temperature, where we notice that also carbon monoxide (CO) is produced at the anode. The electrochemical oxidation of carbon to CO is an endothermic reaction, so the reaction demands an external thermal source. This means that heat is converted directly into electricity, so theoretically a reversible efficiency >100% is possible. Other than CO2, the produced CO is an energy carrier and can react with hot steam in a Water-Gas-Shift (WGS) reactor to produce hydrogen (H2) and CO2.

As external thermal source for the DCFC, a sustainable source is favored. Here we introduce the solar reactor. The solar reactor reflects and focusses solar irradiation with multiple mirrors onto a central receiver, where a certain medium is heated. This medium can be transferred to the DCFC to function as the external heat source. Under the right conditions the solar reactor is able to acquire a temperature where methane (CH4) can be converted into H2 and carbon particles at a high conversion efficiency. These carbon particles can be fed to the DCFC as fuel.

If we consider the three introduced systems (solar reactor, DCFC, WGS-reactor), we notice that we deal with a multi-dimensional system with multiple sources and multiple products. That is where we introduce the Multi-Source Multi-Product (MSMP) energy system.

The MSMP term is introduced by (Hemmes, 2009) and for a better understanding we will explain the basics of less dimensional systems. Energy conversion, specifically a form of energy converting into another form of energy (i.e. heat to electricity), can be seen as a one-dimensional system. In the past, taking into account a one-dimensional energy system, by-products of an energy conversion were seen and treated as waste. Conventional power plants have in most cases one energy source (coal, gas, etc) which is converted by gasification via a turbine into power. The necessary cooling water is treated as waste and therefore dissipated into the environment. Another example is a solar panel producing only electricity. Solar panels will heat up in the sun so it is reasonable to say they produce heat too (Jubayer, Siddiqui, *et al.*, 2016). However, the produced heat is not used which makes a solar panel a one-dimensional energy system.

One step further we can introduce a two-dimensional system, of which co-generation is a perfect example. Co-generation can be defined as an energy generation unit that simultaneously produces electricity and heat from one energy source. The Public Utility Regulatory Policies Act (PURPA) adds to this definition that the two products can be of any form of useful energy (Isa, Tan, *et al.*, 2016). A combined heat and power (CHP) plant is a perfect example of co-generation, which have already been used in the early 1880s for industrial plants in a time where steam was the primary source of energy (Frogoupoulos, 1996). Nowadays, conventional electricity production reaches efficiencies in the order of 40% which means that 60% of the energy input is lost to heat (Hemmes, 2009). It is imaginable that the efficiency of a CHP unit improves significantly when this lost heat is purposely used.

One step further than co-generation is tri-generation or poly-generation. Tri-generation can be defined as a combined heat, cold and power (CHCP) system that can produce electricity and both heat and cold. Co-, tri- or poly-generation energy systems still use only one source of energy. When multiple sources of energy are being used, we can introduce the MSMP energy system.

The MSMP energy system takes these multi-generation systems to another level, by using multiple energy sources. Therefore, as the name already tells us, the MSMP energy system is defined by the use of multiple energy sources, producing multiple products. A side note to this definition is that air does not qualifies as energy input, since a conventional power plant uses fuel + air as input. Figure 1 shows the sources and products of the MSMP energy system presented in this thesis.

Figure 1: In- and output sources and products in our MSMP energy system

With our proposed MSMP energy system we present a more sustainable method for both electricity generation and hydrogen production compared to conventional fossil fueled methods.

1.1 Problem statement

The DCFC is able to use solid carbon as fuel, and the commonly known occurring reaction is the electrochemical oxidation of carbon to CO2. The entropy change of this reaction is near zero, so the conversion is almost independent of temperature. Therefore the theoretical reversible efficiency can reach 100%. But at the anode, other (electro)chemical reactions are possible. The solid carbon can also be electrochemically oxidized to CO and this reaction has a positive entropy change, so the theoretical reversible efficiency is >100%. In order to stabilize the voltage, this positive entropy change must be compensated by an external source of thermal energy. In our case this external source of thermal energy is the solar reactor, where solar irradiation is reflected by heliostat mirrors and focused on one point where the heat is collected. The DCFC is able to directly convert the solar heat into power and is therefore not limited by the Carnot efficiency. Fact is that little or no research has been done towards a DCFC where CO as product is desired and that such a DCFC has not been manufactured and tested in practice. Our problem statement is that it is unknown if the theoretical advantages are achievable in practice.

This thesis tries to overcome this problem by presenting a feasibility study. The feasibility study will answer the question whether the proposed MSMP energy system is technically, economically and socially feasible or not. We present a Cycle Tempo model of the system which helps us study the energy and exergy balance, the energy and exergy flows and the system efficiency. The design and off design input parameters can be varied, in order to analyze the effect on the global system. We will use the modelling results for the feasibility studies.

1.1.1 Knowledge gap

Although the Molten Carbonate Fuel Cell on which the DCFC is based on has been studied for a long time, the DCFC has been neglected for many years. In the last two decades, interest in DCFC technology has been increased which is graphically shown in Figure 2 by the number of publications per year related to DCFC technology. However, most studies towards DCFC’s focus on the electrochemical process where only CO2 is produced. There is very little research towards the DCFC proposed in this thesis, where CO production is favored. Similarly the solar reactor presented in this thesis has not been studied very much.

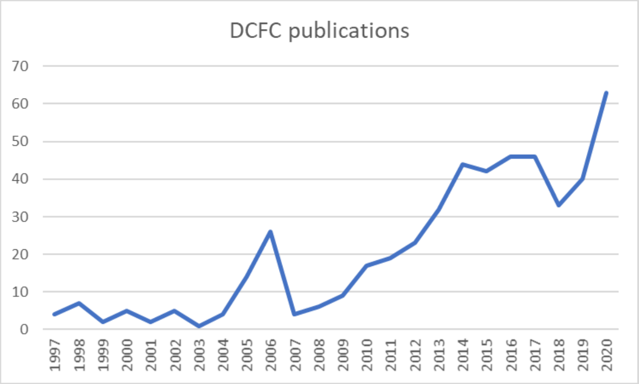

Figure 2: Number of publications related to DCFC research (ScienceDirect)

Therefore the purpose of this thesis is to present a feasibility study of the proposed MSMP energy concept. We will define the feasibility into three subjects, which are the technical, economic and social feasibility.

1.2 Research questions

The main research question of this thesis is formulated as follows:

Is a Direct Carbon Fuel Cell – Multi-Source Multi-Product energy system feasible?

The sub questions related to the main question are:

1. Is the MSMP energy system technically feasible?
2. Is the MSMP energy system economically feasible?
3. Is the MSMP energy system socially feasible?

At first the current state-of-the-art technology related to this thesis is reviewed to understand which technologies are available, how they work and what their barriers are. Second, the detailed theory is presented. Here the thermodynamics and reactions of the solar reactor, fuel cell and WGS-reactor are analyzed. In the theory we will present a modelling section where we simulate the MSMP energy system in the flow sheet modelling program Cycle-Tempo. The modelling results help us analyzing the energy balance, mass flows and efficiencies of the system. We also present an exergy analysis, where we try to analyze where we can improve our system. The technology and theory chapters are the foundation for the feasibility study.

In the technical feasibility the technical applicability of the MSMP energy system is analyzed. We basically imagine that we want to build the system in practice and we analyze what challenges there are to build and operate the system.

The economic feasibility is an analysis of the costs and benefits of our model. We will use the results of the Cycle Tempo model to estimate the value of the input fuel and output products. Then we analyze competing technologies to investigate what the developing and manufacturing costs of our MSMP energy system need to be in order to be competitive with conventional methods in terms of economics.

In the social feasibility we will focus more on the sustainable aspect. With the use of theoretical potential and the results of the Cycle Tempo model we will analyze if the concept has the potential to contribute to sustainable energy. We also focus on the location where the concept is applicable, as we analyze geo-politics and infrastructure.

After the feasibility studies we will draw the final conclusion of this thesis. Lastly, we will present a discussion and recommendations for further research.

1.3 Research methods

This paragraph presents a detailed understanding of the sub questions and what methods are used to answer these.

1.3.1 Is the MSMP energy system technically feasible?

For a better understanding of what we are studying precisely, we will do a literature study towards both DCFC technology and the MSMP energy system. Based on literature, we will present in Chapter 2 state-of-the art technologies relevant for our thesis. This overview helps us to analyze which technological barriers can be overcome with existing technology.

We will base our technological barriers on the theory and the Cycle Tempo model, Chapter 3 and 4 respectively. For example, the theory tells us what temperatures are to be expected and the Cycle Tempo model gives an estimation of the mass flows in the system. In the technical feasibility we will discuss whether the proposed MSMP energy system can be build and be operated under the desired conditions or not. This will answer if the concept is technically feasible.

1.3.2 Is the MSMP energy system economically feasible?

To determine the economic feasibility of our proposed MSMP energy system, we are limited to theoretical results. Practical results are not known, since our proposed model does not exists in practice and therefore cannot be tested to acquire empirical results. Also the lack of economic studies towards this kind of fuel cell technology limits the references for this sub question. Therefore we cannot estimate both developing and manufacturing costs.

Alternatively, we will do a literature research towards the economics of competing technologies and with the help of the Cycle-Tempo modelling results, we will analyze the value of the input and output products. In this way we are able to determine what the maximum developing and manufacturing costs of our MSMP energy system are, to be economically competitive with other conventional technologies.

By analyzing these costs we will determine if the concept is economically feasible.

1.3.3 Is the MSMP energy system socially feasible?

This sub question focusses on the non-technological and non-economical subjects of the proposed MSMP energy system.

We will focus on the sustainable contribution of the system. We will analyze if the generated electricity and produced hydrogen in the MSMP energy system is more sustainable than conventional electricity and hydrogen.

Our social feasibility study focusses also on location, thus where our proposed MSMP energy system is applicable. For example, the solar reactor is dependent on solar power, which differs from one place to another. Or taking into account that the concept in dependent on gas and produced hydrogen, a proper infrastructure of natural gas and hydrogen at the intended geographical location is desired.

Also the characteristics of local policy are of importance, because if local policy is not suited to implement our MSMP energy system it cannot be realized.

Research to both the sustainable potential and the geographical location answers the sub question.

1.4 Thesis outline

Chapter 1	Consists of the general introduction to the subject of this thesis. The research problem, knowledge gap, research questions and research methods are introduced.
Chapter 2	Gives an overview of state of the art technology relevant to the proposed MSMP energy system.
Chapter 3	Presents the detailed theory of the solar reactor and the Direct Carbon Fuel Cell.
Chapter 4	Presents the Cycle Tempo model and analyzes the modelling results and exergy analysis. The modelling results will be used for the feasibility studies.
Chapter 5	Presents the technical feasibility. In this chapter we will analyze what challenges there are when the concept will be built in practice and solutions to these challenges are presented.
Chapter 6	Presents the economic feasibility. In this chapter we will analyze the economics of our system and we will compare it with competing technologies.
Chapter 7	Presents the social feasibility. Here we analyze the sustainable potential of the concept and we determine preferred conditions for a country where the system could be implemented.
Chapter 8	In this chapter we will discuss the findings of the modelling results and the feasibility studies.
Chapter 9	Presents the conclusion of this thesis, based on the feasibility studies and the discussion.
Chapter 10	In this chapter we present recommendations for further research.

2 Technology

In this chapter we will present an overview of state-of-the-art technology and their current status relevant to this thesis.

2.1 Introduction

The MSMP energy system presented in this thesis has three main components: The solar reactor, the DCFC and the WGS-reactor. Both the solar reactor and the DCFC are immature technologies, both based on existing technology. To understand at what level the technology is developed and where innovations are needed, we will present and discuss in this chapter the state-of-the-art technology relevant for this thesis. The WGS-reactor is a more developed technology which is not the main focus of this thesis, therefore the WGS-reactor is not analyzed in detail.

Although we have introduced the MSMP energy system in Chapter 1: Introduction, we will present the concept in this chapter more in detail to understand which state-of-the art technologies are relevant.

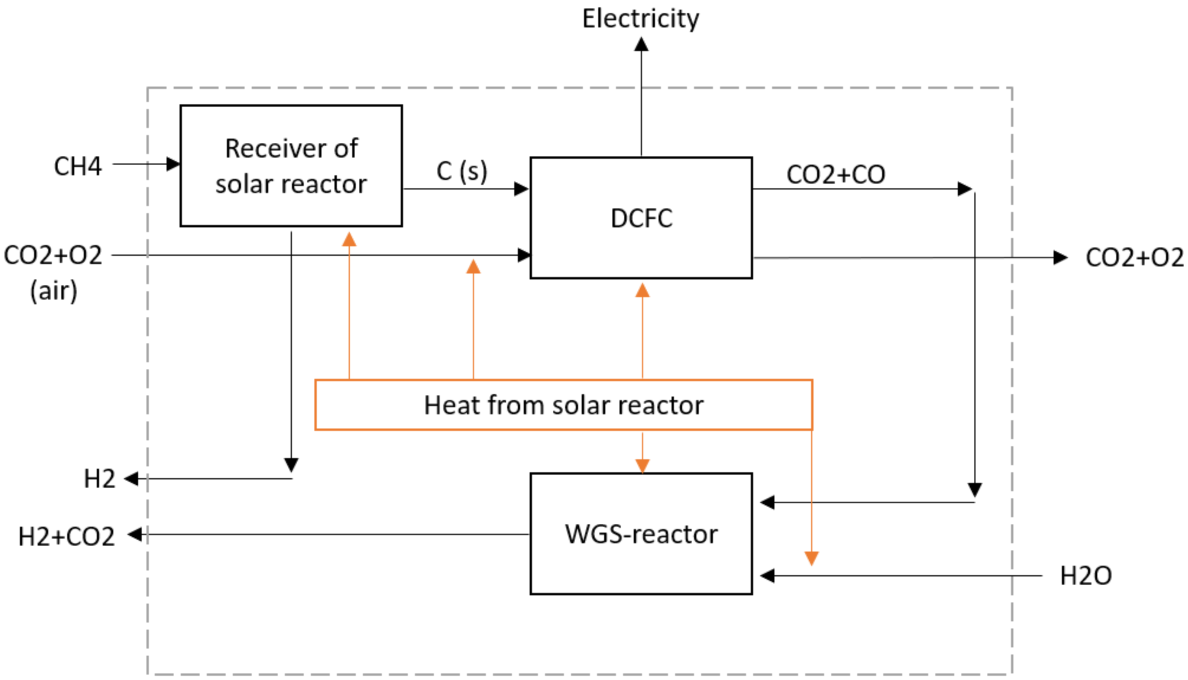

Figure 3: Schematic overview of a DCFC implemented in a MSMP energy system

The MSMP energy system presented in Figure 3 shows all main components involved in the system. Natural gas in the form of methane enters the system to a methane cracking unit, where the methane is converted by thermal decomposition into hydrogen and solid carbon particles. The necessary heat for this reaction is provided by a solar reactor, a device collecting the heat from the sun by reflecting solar irradiation with focused mirrors onto a central receiver where the methane is heated to temperatures needed for thermal decomposition.

The solid carbon formed by thermal decomposition is then fed to the DCFC at the anode. At the cathode, a mix of CO2 and O2 (it can be fed with air as well, since it contains both CO2 and O2) is fed to the DCFC. The cathode input is preheated to the desired DCFC operation temperature by (waste) heat of the solar reactor.

The DCFC produces both CO2 and CO at the anode and, dependent of the DCFC fuel utilization, can maintain particles of solid carbon. For simplification, the scheme in Figure 3 neglects this fact. As explained in Chapter 1: Introduction, the DCFC needs a thermal source for the endothermic electrochemical oxidation of C to CO. This heat is provided by the solar reactor.

The anode product gas, a CO/CO2 mixture, is transported to the water-gas-shift reactor, where it reacts with steam according to the water-gas-shift reaction. The WGS-reactor produces a gas mixture of H2 and CO2. In this way, both at the WGS-reactor and at the solar reactor H2 is produced.

Now that the MSMP energy system is introduced in detail, we will analyze different technologies relevant .

2.2 Solar reactor

The first step in our MSMP energy system is where the fuel (methane) enters the system and is heated by the solar reactor to temperatures where thermal decomposition of methane is possible in order to convert the methane into C and H2. A solar reactor appears to be a promising method for the production of hydrogen compared to conventional methods (Cinti and Hemmes, 2011a) (Ozalp, Kogan, *et al.*, 2009) (Keipi, Tolvanen, *et al.*, 2018). The difference between the methods lies within the supply of heat required for thermal decomposition.

We have partial combustion, where part of the input methane is used for combustion to produce the heat required for the thermal decomposition of the remaining methane. There is Power-to-Carbon, where electricity is used to provide the heat required for methane conversion in the form of electrical heating elements or with a plasma torch. Another method is the catalytic fluidized bed, where part of the produced carbon is used for regeneration of the catalyst needed for catalytic decomposition of methane (Keipi, Hankalin, *et al.*, 2016).

These conventional methods use either partial combustion of the input gas or an electrical heating element for the required heat. Our MSMP energy system favors a sustainable heat source and the solar reactor fits perfectly since it only uses solar power for the required heat.

Although the solar reactor seems promising, it is not a mature technology. It is based on the same working principle of a combined solar power (CSP) plant, where mirrors reflect solar irradiation to a central unit to heat a certain medium. However, the difference between a CSP plant and the solar reactor is that CSP plants use the heat to generate electricity in a steam cycle and the solar reactor uses the heat for thermal decomposition of methane. So in a CSP plant, at the central unit on which the mirrors focus the reflected solar irradiation, there is only heat transfer and no chemical conversion reaction is present. This difference has consequences for the desired operating temperature of the solar reactor. In a typical CSP plant, an operating temperature of 400 – 600 °C is expected (Dowling, Zheng, *et al.*, 2017). But in a solar reactor, a temperature >1200 °C is desired to acquire proper thermal decomposition of methane (Cinti and Hemmes, 2011a).

There are CSP plants operational. In fact, in 2017, the cumulative capacity of CSP plants was 4.9 GW (Omri, Chtourou, *et al.*, 2019). Most CSP plants are installed in Spain and the US, who are leaders in CSP technology. Other regions to find CSP plants are Morocco, China and the Middle-East.

Contrary to CSP plants, there are no solar reactors operational. If we consider literature, we notice that research towards the solar reactor is mainly focused on the optimization of heat supply to acquire a high temperature and on the optimization of the heat transfer rate in the reactor (Jia, Cao, *et al.*, 2020).

In order to supply the heat required for thermal decomposition there are two solar reactor configurations described by (Ozalp, Kogan, *et al.*, 2009) which are applicable and can supply the heat demands. The first is the solar tower, which is not more than a construction to house either the reflector or receiver of the solar reactor (Ozalp, Kogan, *et al.*, 2009). Figure 4 shows the solar tower configuration. The solar tower is surrounded by Fresnel reflectors, also called heliostats. These heliostats are all oriented in a way that all solar beams facing the heliostats are reflected towards the receiver.

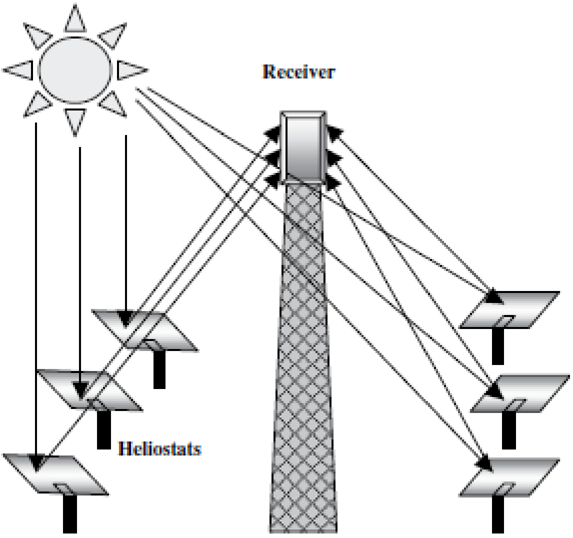

Figure 4: Solar tower with receiver on top and surrounded by heliostats (Ozalp, Kogan, *et al.*, 2009)

In commercial solar tower plants an external tube receiver is used (Breeze and Breeze, 2016a). The solar beams are reflected towards the external tube receiver and hit the outside of the tube, which carries a heat transportation fluid. The heat is then conducted from the heat transportation fluid through the inner fluid for processing.

Another configuration is the solar dish. The solar dish configuration uses a parabolic reflector focused on the receiver on top, as shown in Figure 5. The optical axis (from the middle of the dish towards the focal point) follows the sun's azimuth (Ozalp, Kogan, *et al.*, 2009).

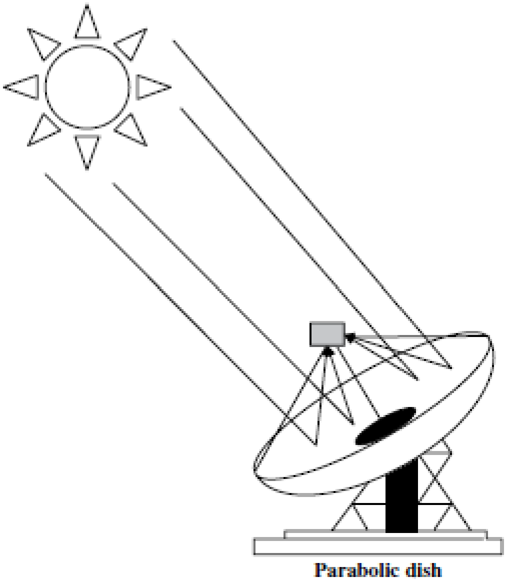

Figure 5: Solar parabolic dish focused on the receiver (Ozalp, Kogan, *et al.*, 2009)

When the solar irradiation is reflected towards the receiver, it heats up a medium. The receiver is by far the most complex part in a solar reactor since it needs to handle very high temperatures. In literature, an example of a receiver design is presented at the University of Colorado where a triple-tube reactor design in a fluid-wall aerosol flow reactor without a catalyst is used (Dahl, Buechler, *et al.*, 2004). (Dahl, Buechler, *et al.*, 2004) uses an aerosol flow reactor because it is able to achieve very fast heating rates. Their reactor has graphite tubes which absorb the reflected sunlight and the tubes radiate the heat to the carbon particles which reradiate the heat to the methane. (Xiaowei, Jean-Charles, *et al.*, 2004) reports that carbon can oxidize at such conditions, but this can be prevented by adding an argon stream.

An alternative reactor design is presented by the ETH-Swiss Federal Institute of Technology. They designed a vortex flow reactor (Hirsch and Steinfeld, 2004), which exposes the methane directly to the solar irradiation. In this receiver the methane and carbon particles are flowing in a vortex through the receiver, which collects and 'traps' the solar irradiation via a concentric nozzle.

(Abanades and Flamant, 2005) tested different geometries of the nozzle. The results showed that the geometry of the nozzle influences the methane conversion very much.

The current status of the solar reactor is still in the developing phase. CSP plants, on which the solar reactor is based, are operated at an industrial scale. However, for the solar reactor only prototypes have been tested and no industrial solar reactors are operational (yet).

2.3 Fuel Cell

DCFC technology has not been developed as much as other high temperature fuel cells, such as the Molten Carbonate Fuel Cell (MCFC) and the Solid Oxide Fuel Cell (SOFC). Where these fuel cells have been developed in the early 20th century, the interest in the DCFC has increased only since the last two decades (Giddey, Badwal, *et al.*, 2012).

The DCFC proposed in this thesis uses solid carbon as fuel, which is preferably electrochemically oxidized to CO. This electrochemical reaction is endotherm, so the fuel cell needs an external heat source which in our case is the solar reactor described in the previous paragraph. If we consider literature, we notice that most DCFC studies are focused on a fuel cell which electrochemically oxidizes carbon to CO2.

(Peelen, Hemmes, *et al.*, 1998) proposed as one of the first a DCFC where the electrochemical conversion of C to CO is desired. They reported its thermodynamic advantages and the interesting fact that the produced CO can be used to produce syngas. (Li, Zhu, *et al.*, 2009) demonstrated that a complete oxidation of carbon to CO2 can be achieved at temperatures of 873 – 973 K, but for temperatures higher than 973 K a mixture of CO2 and CO is produced. (Liu, Tian, *et al.*, 2010) proposed a model that simulates electrochemical reaction dynamics and kinetic mechanisms of a CO2 producing DCFC, where they studies the effect of varying the size of the carbon particles on the performance of the cell. They revealed that the electrochemical oxidation of carbon has relatively slow kinetics.

At the Lawrence National Laboratory, Cooper and coworkers have developed a number of DCFC designs (Giddey, Badwal, *et al.*, 2012). They constructed a DCFC with a tilted orientation design, which is showed in Figure 6. They tested different carbon fuels, such as acetylene black, coal derived carbon and carbon black. Power densities of up to 100 mW/cm^2 where achieved, with an efficiency of 80%. They concluded that both the carbon structure and the presence of sulphur has a significant effect on the performance of the DCFC.

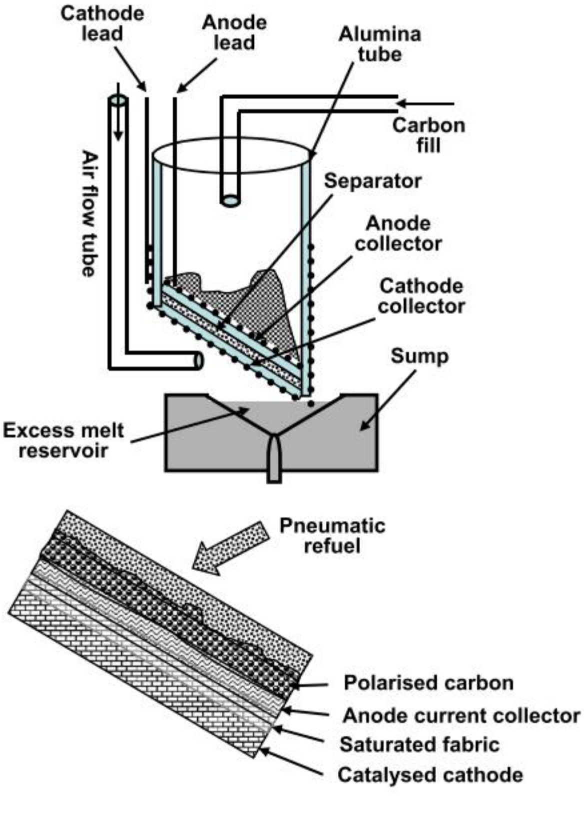

Figure 6: The basic tilted cell configuration of LLNL (Giddey, Badwal, *et al.*, 2012)

The Korean Institute of Science and Technology tested a DCFC at temperatures 873 – 1073 K and reported the formation of CO at temperatures higher than 973 K (Badwal, Ju, *et al.*, 2017). (Ido and Kawase, 2020) developed a tubular DCFC and noticed that the CO/CO2 ratio increased with increasing temperature.

Although little research towards the DCFC has been performed, there are a couple of experimental setups. These experimental results showed what was expected in theory. However, we have to take into account that all setups are on a very small scale and no DCFC is currently operational. In practice DCFC technology is in its infancy.

2.4 WGS-reactor

The last main component of our MSMP energy system is the water-gas-shift (WGS) reactor, which takes the last step of our system into account. The product gas at the anode of the DCFC is a CO/CO2 mixture and the content of CO is mixed with steam in the WGS reactor to form H2 and CO2. Contrary to the solar reactor and the DCFC, the WGS reactor is a more mature technology. Currently the water gas shift reaction is operated on an industrial scale, because with this reaction high purity H2 can be produced (Karagöz, Tsotsis, *et al.*, 2020). With increasing interest in H2 applications such as PEM fuel cells, the demand for H2 gas with a high purity is increasing because they are intolerant to impurities in the fuel.

In 1780, Italian physicist Felice Fontana discovered the WGS reaction where CO was mixed with steam, which converted to a mixture of CO2 and H2 (Reddy and Smirniotis, 2015). Traditionally, the WGS reaction is performed on an industrial scale in a heterogeneous catalytic reactor. This reactor is based on a two-step method, with two WGS reactions involved; a high temperature and low temperature catalyst bed. With the two-step method, a near 100% CO conversion can be achieved (Reddy and Smirniotis, 2015).

Another industrially used method to perform the WGS reaction is in a membrane catalytic reactor, which firstly was reported in 1866 (Saeidi, Fazlollahi, *et al.*, 2017). This cylindric reactor contains an inner and outer tube, where the inner tube is a porous membrane. With a membrane cylindrical reactor it is possible to achieve a near 100% CO conversion in single stage. (Saw, Nandong, *et al.*, 2018) achieved a H2 purity of 99,87% in an experimental setup, in order to prove that a near 100% CO conversion is possible.

(Rosner, Chen, *et al.*, 2019) studied the effect of steam requirement in the WGS reactor and they concluded that a lower steam requirement generally benefits the efficiency.

Recently the interest in WGS reactors have also increased in the methanol and ammonia industry. For example, one of the largest ammonia producers Linde patented the Linde Ammonia Concept (Rosner, Chen, *et al.*, 2019), using an isothermal WGS reactor.

If we consider literature we can conclude that the WGS reactor is a technology that has been tested and applied in practice significantly. The WGS reaction, where the WGS reactor is based on, is applied at an industrial scale and the interest will increase because of the increasing demand for high purity H2.

2.5 Conclusion

In this chapter we reviewed state-of-the-art technology relevant for our proposed MSMP energy system in order to draw a conclusion on the current status of technology.

Although CSP plants, on which the solar reactor is based, are operational we notice that the desired solar reactor for our MSMP energy system is an immature technology. The main difference with conventional CSP plants is that in the receiver of a CSP plant only heat transfer occurs, while in the receiver of the solar reactor both heat transfer and thermal decomposition takes place. Therefore the receiver of the solar reactor operates at higher temperature than CSP, to establish proper thermal decomposition. This technology is only tested in experimental setups.

The DCFC is an even less mature technology. The basic principles have been known for a long time, but interest is increasing only in the last 20 years. Side note is that most publications are based on a DCFC where a pure CO2 output is desired. Very few publications consider a DCFC which produces a CO/CO2 mixture. There are some known experimental setups, of which the Lawrence National Laboratory setup is mostly reviewed in literature. This setup was performed at temperatures where only CO2 is formed, so the formation of CO was not investigated in practice.

The WGS reactor is based on the WGS reaction and we have noticed that the interest in this reaction is increasing, because the demand for high purity H2 is increasing. The WGS reaction is applied in many industrial applications and is therefore a mature technology.

We can conclude that the WGS reactor is a mature technology, but both the solar reactor and the DCFC are immature technologies.

3 Theory

This chapter presents in detail the thermodynamic and (electro)chemical processes of the DCFC, solar reactor and WGS reactor.

3.1 Introduction

In the previous chapter we have presented the basic concept of the MSMP energy system and relevant state-of-the art technology. In this chapter we focus on the theory of the concept in more detail as we analyze the thermodynamics and (electro)chemical processes of the solar reactor, fuel cell and in less detail the WGS reactor. The analysis of the detailed theory helps us understand how the components in the MSMP energy system work, what challenges there are and helps us motivate why our concept is promising. The reactions taking place in the DCFC are specifically in our scope of research, because here we find the knowledge gap which is explained in the introduction of this thesis. We will explain which reaction takes place in the fuel cell and which is favored under what conditions.

The structure of this chapter is similar to Chapter 2, as we analyze the MSMP energy system step by step following the main components. First the theory of the solar reactor is presented in detail, followed by the fuel cell. Lastly, in less detail the theory of the WGS reactor is presented. This chapter gives a better understanding how our MSMP energy system works and on what theory it is based.

3.2 Solar reactor

In our MSMP energy system heat is desired for thermal decomposition of methane, for the endotherm reaction in the DCFC and for the WGS reactor. This heat can be provided by the solar reactor. Where conventional external thermal sources consume fossil fuels in order to generate the required heat, the solar reactor uses the irradiation of the sun as heat source and is therefore fossil fuel free. Similarly, the solar reactor does not have greenhouse gas emissions, thus is a sustainable alternative for the necessary external thermal source.

In Chapter 2, the basic principles of the solar reactor are explained. In this chapter we will present a more detailed analysis. First we will focus on the process of thermal decomposition, followed by an overview of the two main types of solar reactors where we will motivate which type suits more in our MSMP energy system. Lastly we will focus on the receiver/reactor where the process of thermal decomposition takes place.

3.2.1 Thermal decomposition

The main function of the solar reactor is to convert methane into solid carbon particles and hydrogen. This conversion reaction can be acquired by thermal decomposition, which is endothermic (Keipi, Hankalin, *et al.*, 2016). This conversion can be described by the following (simplified) reaction:

$$CH_4 \rightarrow C + 2H_2 \quad \Delta H_r^0 = 76\ kJ/mol_{CH_4} \tag{1}$$

Thermal decomposition is dependent on temperature, which is shown in the equilibrium curve where the degree of methane conversion increases with increasing temperature (Keipi, Hankalin, *et al.*, 2016). The equilibrium curve is presented in Figure 7. The Figure shows a grey vertical marker which marks the temperature where we can assume a 100% conversion of methane to hydrogen and carbon (Li, Li, *et al.*, 2011).

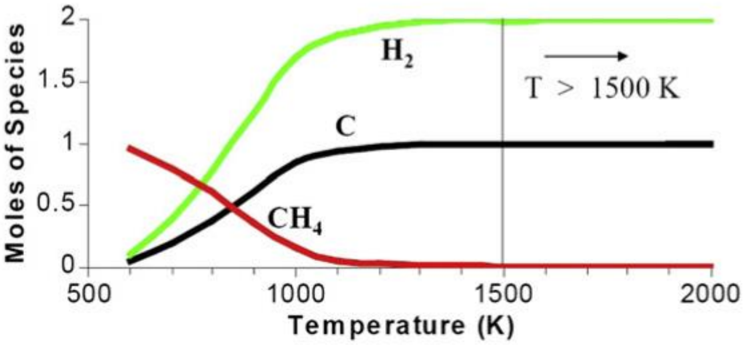

Figure 7: Methane decomposition equilibrium products P=0.1 MPa (Cinti and Hemmes, 2011b).

According to (Ozalp, Kogan, *et al.*, 2009) a high conversion via thermal decomposition depends on two main components:

1. Optics configuration of the solar collector
2. Design of the solar receiver.

In the following sub-paragraph we will describe the possible optics configuration of the solar reactor with the goal to motivate the preferred configuration for our solar reactor in the MSMP energy system.

3.2.2 Optics configuration

We can distinguish three configurations of the solar collector, which are the trough, tower and dish configuration respectively. Although the trough configuration of the solar collector optics can reach high efficiencies, the maximum achievable temperature is approximately 700 K (Ozalp, Kogan, *et al.*, 2009). According to Figure 7, this temperature will not reach a proper conversion and is therefore not preferred for our desired methane conversion process. Therefore the trough configuration will not be analyzed in this thesis.

The solar tower configuration is not more than a construction to house either the reflector or receiver of the solar reactor (Ozalp, Kogan, *et al.*, 2009). The standard configuration is with the receiver on top of the tower, but often the reflector is applicated to save construction and maintenance costs (Segal and Epstein, 2003). In case of a reflector the solar irradiation is reflected downwards to a ground-level receiver, which is easy to access for maintenance. Figure 4 shows the solar tower configuration of a solar reactor. As shown in Figure 4, the solar tower is surrounded by Fresnel reflectors, also called heliostats. These heliostats are all oriented in such a way that all solar beams facing the heliostats are reflected towards the receiver.

Another configuration is the solar dish. The solar dish configuration uses a parabolic reflector focused on the receiver on top, as shown in Figure 5. The optical axis (from the middle of the dish towards the focal point) follows the sun's azimuth (Ozalp, Kogan, *et al.*, 2009). Contrary to a solar tower, the size of the solar dish is limited. Commercial solar dishes are often limited to a diameter of 10m, although one commercial solar dish with a diameter of 25m has been build (Breeze and Breeze, 2016b). According to (Breeze and Breeze, 2016b), the limitation in size means as a general guide that a 10m diameter solar dish can achieve a maximum output power of 25 kW.

The solar tower can be assembled with a large receiver surrounded by many reflectors, in able to have sufficient power output from one receiver. The solar dish too can achieve sufficient power output by coupling multiple dishes. Amongst all solar methods, the solar dish can achieve the highest solar flux concentration ratio which allows a very high conversion efficiency (Ozalp, Kogan, *et al.*, 2009). However (Cinti and Hemmes, 2011b) mentions that the solar tower can reach the highest temperatures. They refer to practical results, where lower methane conversion efficiencies were measured than was expected. Therefore the highest possible temperature is desired and in combination of the limited size of a solar dish, the solar tower configuration is favored for the solar reactor in our MSMP energy system.

3.2.3 Receiver/ reactor

The receiver is where the solar irradiation needs to be collected to heat a certain medium. As mentioned before, to achieve very high conversion efficiencies a temperature >1500 K is desired, which means that the receiver needs to handle an extreme heat flux.

The external tube receiver described in Chapter 2 reflects the solar beams towards an external tube receiver and hit the outside of the tube, which carries a heat transportation fluid (Breeze and Breeze, 2016a). The heat is then conducted from the heat transportation fluid through the inner fluid for processing. This is the working principle for a CSP plant, where heat is transferred to another medium to be stored or used somewhere else. In our case, the heat does not need to be transferred somewhere else but needs to be used to heat gaseous methane for thermal decomposition. Therefore the receiver is basically a reactor where a conversion process takes place.

If we change the transportation fluid from the external tube receiver by methane gas, the receiver becomes a reactor. Although (Ozalp, Kogan, *et al.*, 2009) concludes that a (metal) external tubular reactors are not practical for high temperature methane conversion, there are studies presenting a feasible solution. An example is the reactor developed by the University of Colorado, described in Chapter 2. They designed a triple-tube reactor in a fluid-wall aerosol flow reactor (Dahl, Buechler, *et al.*, 2004), showed in Figure 8. They noticed that an aerosol flow reactor is able to achieve very fast heating rates.

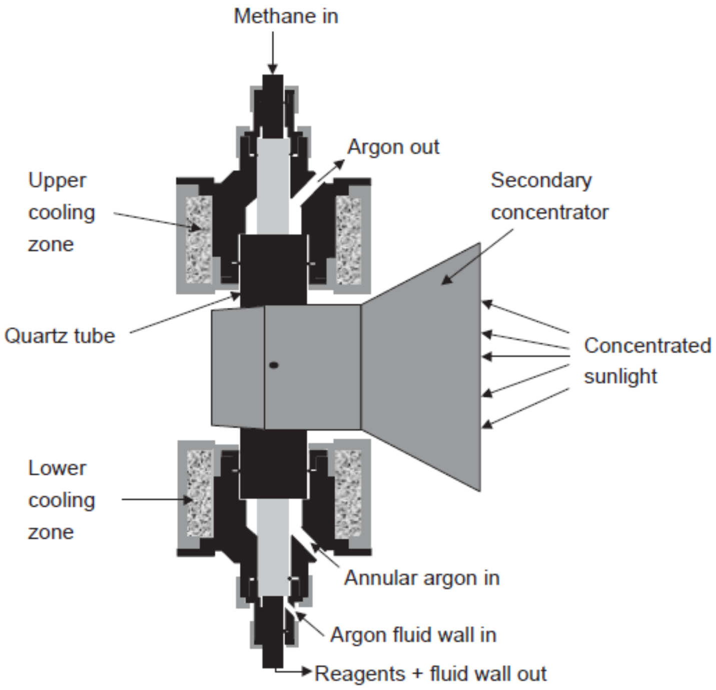

Figure 8: Schematic overview of the aerosol fluid wall reactor presented by (Dahl, Buechler, *et al.*, 2004).

This reactor has three inner concentric tubes of graphite and an outer tube made out of quartz. The center solid graphite tube is heated by the reflected sunlight, in our case by heliostats. The heat from the solid center tube is then radiated to the porous second tube and furthermore the carbon particle present in the gas stream absorb the radiation from the porous tube. These carbon particles, formed by reaction, heat up the gas stream. The residence time of methane in the solar reactor presented by (Dahl, Buechler, *et al.*, 2004) is $0.01s$ at a temperature of $> 2000K$. The study of (Xiaowei, Jean-Charles, *et al.*, 2004) shows that the formed solid carbon particles oxidize at such temperatures, with a rate depending on the residence time. The study shows that the oxidizing rate is minimal at the residence time used by (Dahl, Buechler, *et al.*, 2004), however it is unwanted for the carbon to oxidize at all. Therefore argon is fed into the annular region between the carbon and quartz tube. With this method an inert atmosphere is created which prevents the carbon from oxidizing.

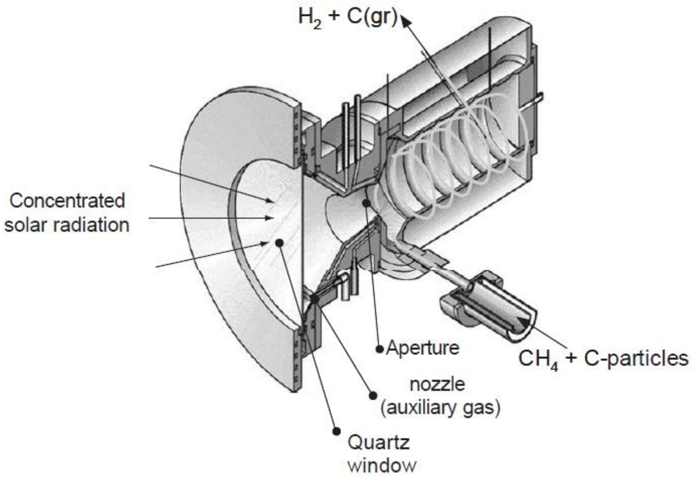

Figure 9: Schematic overview of a vortex flow reactor, laden with carbon particles (Hirsch and Steinfeld, 2004)

The alternative reactor design described in Chapter 2 is presented by the ETH-Swiss Federal Institute of Technology. They designed a vortex flow reactor (Hirsch and Steinfeld, 2004). A schematic overview of this reactor type is shown in Figure 9. The concentrated solar power enters the vortex reactor at the aperture, a windowed opening in the cylindrical cavity. Tangent to the cylindrical reactor, the methane stream is injected through an inlet port right behind the aperture. The injected methane is lead via vortex flow through the reactor along a helical path. The product stream (H2 and C) exits the cavity at the tangential outlet port at the rear. (Hirsch and Steinfeld, 2004) show with the vortex configuration an efficient radiation heat transfer to the reaction site, by exposing the carbon particles directly to the high-flux irradiation. They conclude that the carbon particles serve both efficiently as radiant absorbers and as nucleation sites for the decomposition of methane.
At the aperture, the quartz window is cooled by an injected auxiliary gas flow. This injected gas flow also keeps the quartz window clear of particles, reducing re-radiation losses and consequently increasing the conversion efficiency (Ozalp, Kogan, *et al.*, 2009). A major challenge in designing this reactor is to reduce or prevent the cavity effect. Multiple internal reflections inside the cavity may lead to a portion of the incoming solar irradiation being absorbed by the cavity, exceeding the surface absorption. (Steinfeld, Brack, *et al.*, 1998) presents a solution to minimize this portion, by optimizing the cavity diameter and depth to the cavity diameter. The cavity receiver can approach a blackbody absorber when the ratio between aperture- and cavity diameter is increased. However, a decrease in diameter of the aperture decreases re-radiation losses but requires the need for a higher

concentration. (Steinfeld, Brack, *et al.*, 1998) therefore concluded that the aperture size is one of the major variables in setting the incoming power.

In the experimental study of (Abanades and Flamant, 2005) different geometries of the nozzle where tested. The results showed that the geometry of the nozzle influences the methane conversion very much. A modified graphite nozzle can cause a larger reaction surface, creating a higher heat exchange area and thus a more efficient radiation absorption.

3.3 Fuel Cell

Fuel cells are very promising in terms of sustainable energy, because they can reach high conversion efficiencies and emit no or less greenhouse gasses than conventional power plants. For simplification we distinguish high temperature fuel cells and low temperature fuel cells. The low temperature fuel cells, such as the Proton Exchange Membrane Fuel Cell (PEMFC) and Alkaline Fuel Cell (AFC), are not in the scope of our research because they cannot be fed with hydrocarbons as they have an intolerance of impurities in the fuel and/or oxidant (Andújar and Segura, 2009). The high temperature fuel cells however, such as the Solid Oxide Fuel Cell (SOFC) and Molten Carbonate Fuel Cell (MCFC) are more tolerant to impurities and can be fed with hydrocarbons as a fuel. Given the fact that we use natural gas as the input fuel for our MSMP energy system, the high temperature fuel cells are favored.

Another fact which favors high temperature fuel cells is that the initial aim of fuel cell development is to achieve a direct conversion of the chemical energy of natural fuels to electrical energy. A high temperature fuel cell has the potential to approximate this goal, by the internal reforming of for instance a hydrocarbon and oxidizing the fuel directly to generate electricity (Andújar and Segura, 2009).

Based on the fact that our input fuel is natural gas and that we want to achieve the highest efficiency we have chosen a high temperature fuel cell for our MSMP energy system. We will present a short overview of the two most common high temperature fuel cell types, the SOFC and MCFC. The DCFC is based on the MCFC, thus is then explained more in detail which will motivate the choice for the DCFC in our MSMP energy system.

3.3.1 High temperature fuel cells

In this subparagraph we will present an overview of the high temperature fuel cells and the basic theory of which the DCFC is based on.

3.3.1.1 SOFC

The SOFC can be operated between 600-1000 °C, which allows fast (electro) chemical reactions and makes spontaneous internal reforming of the fuel possible (Andújar and Segura, 2009). This makes the SOFC flexible in terms of fuel. The SOFC electrolyte conducts oxide ions from the cathode to the anode.

An SOFC can be operated with two geometries: Planar and tubular. The planar geometry is similar to other fuel cells, with two electrodes on both sides of the electrolyte. The tubular geometry, however, is manufactured with an inner and outer tube as the cathode and anode respectively and with an air flow on the inside of the tube. The tubular SOFC is fed with fuel from the outside. This geometry gives the SOFC a higher energy density and is easier to produce (Inal and Deniz, 2020).

The electrolyte is solid, which avoids problems liquid electrolytes have, such as corrosion.

3.3.1.2 MCFC

The MCFC is developed based on the SOFC, but is developed taking into account the limitations of a solid electrolyte (Andújar and Segura, 2009). The MCFC therefore has a liquid electrolyte in the form of molten carbonate salt.

The MCFC operates between 600-700 °C. The high operating temperature is beneficial in terms of cost efficiency, because it minimalizes the need for expensive catalysts and it makes the MCFC flexible with respect to fuels. It can be fed with hydrogen, natural gas or other hydrocarbons.

The electrical efficiency is around 50-60%, however can be increased using a cogeneration system. With such a system, it can reach an efficiency of up to 85%.

3.3.2 DCFC

The DCFC has been developed based on the MCFC. They have the same liquid high temperature electrolyte, however the DCFC can be fed with carbon. The molten carbonate electrolyte has a long term tolerance for CO2, which is present as oxidant at the cathode and is produced at the anode. The molten carbonate has a high ionic conductivity and can catalyze carbon oxidation (Giddey, Badwal, *et al.*, 2012), which makes the DCFC the only fuel cell with a solid as a fuel.

The DCFC offers great thermodynamic advantages over the SOFC and MCFC, because the theoretical electrochemical conversion is almost independent of temperature. The theoretical reversible efficiency can approximate 100% (Cinti and Hemmes, 2011a) for a DCFC oxidizing solid carbon to CO2.

But carbon can also be electrochemically oxidized to carbon monoxide (CO). The entropy change in this reaction is positive, which means that external heat is converted directly into electric power and is not limited by the Carnot efficiency (Hemmes, Cooper, *et al.*, 2013). Here we highlight the exact reason why this thesis focusses on a DCFC and more specifically on carbon oxidation to CO. The enthalpy of the reaction is converted directly into heat, while in a gasifier the enthalpy is converted into heat and the heat is converted into power. With the DCFC we basically skip one conversion step. Theoretically, a DCFC which oxidizes carbon to CO can reach a reversible efficiency >100%. (Hemmes, Cooper, *et al.*, 2013) adds that an efficiency greater than predicted by the Carnot efficiency cannot be accomplished in an isolated process. The positive entropy change is significant and must be compensated in order to stabilize the cell voltage. The cell voltage can be stabilized by a source of thermal energy. In our MSMP energy system, the thermal energy source is presented in the form of the solar reactor.

Another benefit of the DCFC is that the use of solid fuel causes minimal Nernst loss in the fuel cell, while high temperature fuel cells without solid fuel have significant Nernst loss (Cinti and Hemmes, 2011a). The ohmic and polarization losses of a DCFC are similar to an MCFC and SOFC and are in the range of 20%. Consequently, the efficiency of a DCFC is approximately 80% compared to approximately 50% for the MCFC and SOFC.

Moreover solid carbon has a high energy content and the DCFC is mechanically simple, given the fact that it does not need a reformer for the fuel. This allows the DCFC to convert carbon directly to electrical power without combustion (Cinti and Hemmes, 2011a).

The beforementioned advantages of the DCFC contrary to a MCFC and SOFC are the reason why we have chosen for the DCFC in our proposed MSMP energy system.

Now that we have motivated the choice for the type of fuel cell, we will analyze the DCFC more in detail.

3.3.3 Reactions

The reactions taking place in the DCFC have been studied, however still not yet fully understood. The reactions taking place are complex, since many (electro)chemical reactions can take place at the anode. The number of electrons transferred, the possible reactions between the gasses and solids at the anode and the effect of the reverse Boudouard reaction are taking place simultaneously and to understand when and how each reaction takes place and moreover to model and predict the mechanisms is a major challenge for scientists.

Most studies found in literature towards DCFC technology focus on a DCFC with pure CO2 production at the anode side. A pure CO2 anode product is realized when the 4-electron anodic reaction (2) is taken into account (Houwing, Hemmes, *et al.*, 2005). While CO2 is tend to believe as the dominant anode product gas, other studies report a CO/CO2 mixture caused by the Boudouard equilibrium (5) and/or the 2-electron oxidation of reaction (3) (Hemmes, Cooper, *et al.*, 2013). The Boudouard reaction is highly endothermic, indicated by the large positive enthalpy change ($\Delta H = 172\ kJ/mol$). The Boudouard equilibrium shifts towards CO at higher temperature (Houwing, Hemmes, *et al.*, 2005).

The CO produced by the Boudouard reaction can be electrochemically oxidized according to anode reaction (3). Although the reaction kinetics appear to be slow, at $T > 700°C$ the kinetics will accelerate (Chen and Selman, 2017).

Electrochemical reactions

$$C + 2CO_3^{2-} \rightarrow 3CO_2 + 4e \tag{2}$$

$$2C + CO_3^{2-} \rightarrow 3CO + 2e \tag{3}$$

$$CO + CO_3^{2-} \rightarrow 2CO_2 + 2e \tag{4}$$

Chemical reactions

$$CO_2 + C \rightarrow 2CO \quad \text{(Boudouard)} \tag{5}$$

Now that the possible (electro)chemical reactions taking place in the DCFC are known, it is important to understand which reactions take place at what conditions.

In a DCFC under non-equilibrium conditions the anode has an overpotential, a deviation from the equilibrium potential. The sign and magnitude of the overpotential depends on the environmental conditions (Hemmes, Cooper, *et al.*, 2013).

Example T<650 °C (Chen and Selman, 2017)*:* If the atmosphere is 100% CO2 and at T<650 °C, carbon is at a negative overpotential (a negative deviation from the equilibrium potential, Nernst potential). A current flows at the carbon which produces CO, a combination of the two occurring anode reactions, such that the net current at the electrode is cathodic. This is an implication that CO2 will be reduced and the carbon oxidized at the anode undergoes an anodic reaction whereby oxygen and CO2 are evolved as gasses from the carbonate melt.

Example T>650 °C (Chen and Selman, 2017)*:* If the atmosphere is 100% CO2 and at T>650 °C, the anode is at a positive overpotential and an anodic current flows. Carbon will be oxidized at the anode and oxygen and CO2 will be reduced at the cathode. Thus, the DCFC has a normal fuel cell reaction, the negative ΔG chemical reaction corresponding with the two anode reactions.

If both reactions take place at T>650 °*C*, both CO and CO2 are formed anodically, creating the possibility that free or adsorbed CO will electrochemically be converted to CO2:

However, this reaction can only occur if the CO product remains at the anode. For example by chemical or electrochemical adsorption. If CO can escape immediately from the anode, the reaction can only occur with the help of a network of another conducting material in contact with the anode.

If this reaction can occur, any formed CO2 leads to a local concentration of CO2 that can lead to a higher concentration than the equilibrium concentration of the two anodic reactions. When this CO2 comes into contact with electronically isolated carbon particles, it reacts according to the reverse Boudouard reaction, forming CO. Hereby carbon corrosion occurs, lowering the efficiency of the DCFC (Hemmes, Cooper, *et al.*, 2013).

(Chen and Selman, 2017) analyzed the reaction rate distribution of reaction (2), (4) and (5) over the DCFC. This is shown in Figure 10.

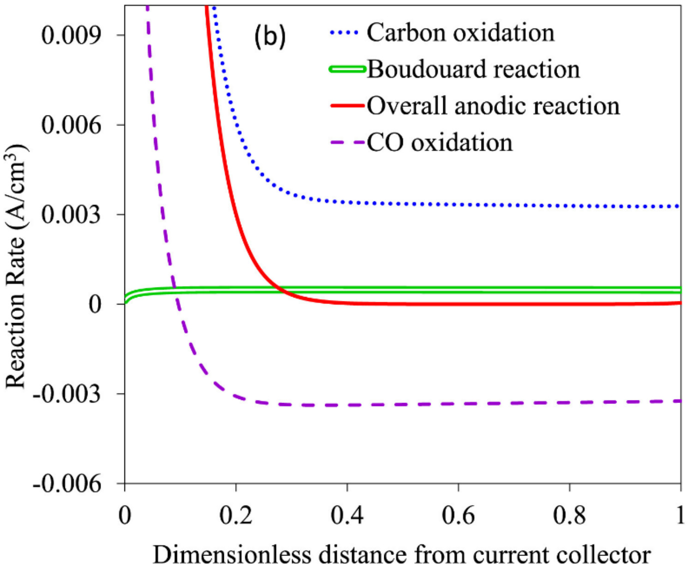

Figure 10: Reaction rate distribution of the reactions taking place at the anode at I= 0.1 A/cm^2 (Chen and Selman, 2017)

As shown in Figure 10, the reaction rate of both electrochemical reaction (2) and (4) drops significantly away from the current collector. (1) remains positive, but (4) becomes negative at around 10% dimensionless distance from the current collector. This means that electrochemical reaction (4) is reversed, so CO2 is reduced to CO instead of CO is oxidized to CO2. However, near the current collector (4) plays an important role in DCFC operation. Since our focus in this thesis is to favor electrochemical reaction (2), the overpotential can be increased in order to lower the reaction rate of (4). In this way, electrochemical oxidation of CO to CO2 can be tempered and more CO will be formed at the anode.

When the composition and flow of the gas into and out of the cell is constant, the DCFC operates at steady state condition. Now the electrochemical reactions (2), (3), (4) and the chemical reaction (5) can take place simultaneously.

When a DCFC has fixed amounts of reactants, temperature and pressure and powering a given load, this will eventually lead to an equilibrium of (electro)chemical reactions (2), (3), (4) and (5). The initial current decays to zero and a steady state open circuit voltage will occur, which only depends on temperature and pressure of the cell (Hemmes, Cooper, *et al.*, 2013).

(Elleuch, Boussetta, *et al.*, 2012a) simplifies the anode reaction mechanism for the 2-electron carbon oxidation process. They combine reaction (4) and (3) to form the simplified anodic reaction (6):

$$C + CO_3^{2-} \rightarrow CO + CO_2 + 2e^- \tag{6}$$

Reaction (6) is later being used in the modelling section of this thesis.

Now that we have analyzed the anode reactions, we will take the cathode into account. The cathode is fed by a gas mixture of CO2 and O2, which can also be in the form of normal air. Since the oxidation of C to CO is a 2-electron process and the oxidation of carbon to CO2 is a 4-electron process, the cathode reaction is different when electrochemically oxidizing carbon to CO or CO2 (Elleuch, Boussetta, *et al.*, 2012b):

$$2CO_2 + O_2 + 4e^- \rightarrow 2CO_3^{2-} \tag{7}$$

$$CO_2 + \frac{1}{2}O_2 + 2e^- \rightarrow CO_3^{2-} \tag{8}$$

For the 4-electron process the overall reaction is:

$$C + O_2 \rightarrow CO_2 \tag{9}$$

And if we take the 2-electron process into account with the simplified anodic reaction (6), (Elleuch, Boussetta, *et al.*, 2012a) assumes that the CO2 produced at the anode will be totally consumed by the cathode electrochemical reaction. Therefore the overall reaction can be considered to produce only CO:

$$C + \frac{1}{2}O_2 \rightarrow CO \tag{10}$$

Now that we have analyzed all reaction mechanisms taking place in the DCFC we will analyze the open circuit voltage of the fuel cell.

3.3.4 Open circuit voltage

The open circuit voltage can be calculated with the Nernst equation:

$$E = E^0 + \frac{RT}{nF}\ln(Q_r) \tag{11}$$

In which Q_r is the reaction quotient of the cell reaction and E^0 is the standard potential:

$$E^0 = \frac{\Delta G^0}{nF} = \frac{\Delta H^0 - T\Delta S^0}{nF} \tag{12}$$

The entropy change of this reaction is nearly independent of temperature, because the entropy change of this reaction is near zero. If we assume ΔH independent of temperature and if we consider the 4-electron electrochemical oxidation of carbon to CO2 as only reaction taking place, the open circuit voltage would be nearly independent on temperature. The open circuit voltage for this reaction is therefore near constant $E^0 = 1.02\ V$.

If we consider the 2-electron electrochemical oxidation of carbon to CO, and assume this is the only reaction taking place, the entropy change of this reaction is positive and the open circuit voltage would increase with increasing temperature. (Cassir and Hemmes, 2004) shows these findings graphically, presented in Figure 11.

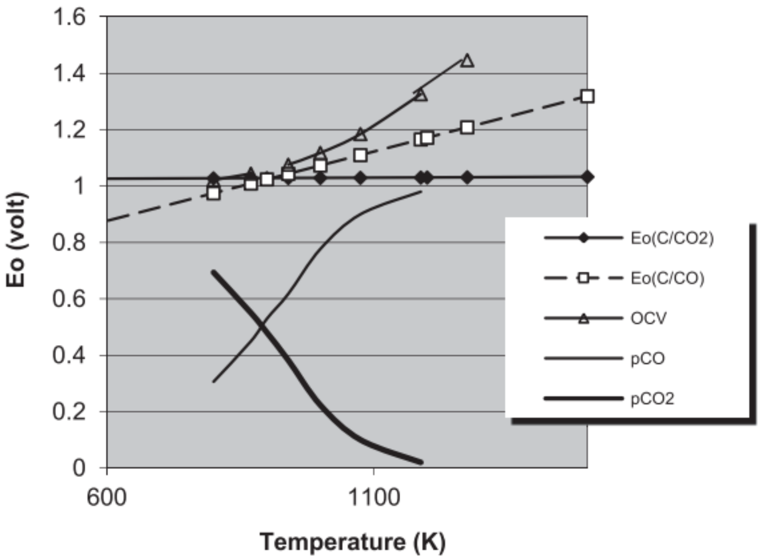

Figure 11: Open circuit voltage for the electrochemical oxidation of C to CO2 and CO (Cassir and Hemmes, 2004)

The simplified 2-electron anode reaction (6), taking into account both CO and CO2 production at the anode is based on the Boudouard equilibrium constant. The CO/CO2 ratio can be determined thermodynamically when their standard potentials E_T° are known. It can also be determined by chemical equilibrium of the Boudouard reaction. The Boudoaurd equilibrium constant K_B is defined as follows (Cassir and Hemmes, 2004):

$$K_B = \frac{P_{CO}^2}{P_{CO_2}} \tag{13}$$

The partial pressures P_{CO} and P_{CO_2} are determined by the Boudouard reaction assuming $P_{CO} + P_{CO_2} = 1\ atm$. Therefore the partial pressures can be determined for given Boudouard equilibrium constant, presented in Table 1.

Table 1: Boudouard equilibrium constant K_B and partial pressures as function of temperature, assuming $P_{CO} + P_{CO_2} = 1$ (Cassir and Hemmes, 2004)

	800 K	870 K	940 K	1000 K	1075 K	1188 K	1275 K
$K_B\ [atm]$	0.14	0.37	1.00	2.718	8.11	49.10	156.00
$\ln(K_B)\ [-]$	-2	-1	0	1	2.09	3.89	5.05
$P_{CO}\ [atm]$	0.31	0.45	0.62	0.78	0.90	0.98	0.99
$P_{CO_2}\ [atm]$	0.69	0.55	0.38	0.22	0.10	0.02	0.01
$OCV\ [V]$	1.02	1.04	1.08	1.12	1.18	1.33	1.45

As can be seen from Table 1 the partial pressure shifts towards CO at increasing temperature, graphically shown in Figure 11. The figure shows clearly that CO production will be dominant at $T > 900\ K$ and at $T > 1200\ K$ CO can be considered as the only produced gas.

If we consider the 2-electron process where CO is produced at the anode of the DCFC, the potential E can be calculated by the Nernst equation, dependent on partial pressure of reactant and oxidant gas:

$$E = E_0^{C/CO} + \frac{RT}{2F}\ln\left(\frac{1}{P_{CO}\cdot P_{CO_2}}\right) \tag{14}$$

$$E_0^{C/CO} = -\frac{\Delta G^\circ}{2F} = \frac{-\Delta H_0^{C/CO} + T\Delta S_0^{C/CO}}{2F} \tag{15}$$

$$E = \frac{-\Delta H_0^{C/CO}}{2F} + \left(\frac{\Delta S_0^{C/CO} + R\,ln\left(\frac{1}{P_{CO}\cdot P_{CO_2}}\right)}{2F}\right)\cdot T \tag{16}$$

For simplicity it is assumed that the partial pressures of O_2 and CO_2 at the cathode are both equal to one, while in reality the partial pressure of O_2 in air is 0.2 (Cassir and Hemmes, 2004). As explained, the standard potential is dependent on the change Gibbs free energy $\Delta G = \Delta H - T\Delta S$. The entropy change is positive, so with increasing temperature the change in Gibbs free energy becomes more negative. This is in contrast with the 4-electron electrochemical reaction, where the standard potential is nearly independent of temperature because the entropy change is near zero.

3.3.5 Losses

Although the DCFC described in this thesis has not been manufactured and tested in practice, literature reports a number of factors which can result in losses. (Giddey, Badwal, *et al.*, 2012) highlights that the factors limiting the performance of a DCFC can be found in the presence of resistive losses caused by the current collectors and electrolyte, losses by the diffusion of gas when it is transported through the electrodes, losses caused by conduction along the electrode surface or through the electrodes and slow reaction kinetics. Just like surface chemistry, carbon crystallinity and crystallite size will affect the reactivity of the fuel and either increase or decrease the number of reactive sites.

The 2-electron process has a standard potential which becomes larger with increasing temperature and the 4-electron process has a near constant standard potential. Therefore, if the polarization losses of the 2-electron process are smaller than the difference in standard potential between the 2- and 4-electron process, the 2-electron process can achieve a higher power density.

3.4 WGS reactor

The last component of our MSMP energy system is the water-gas-shift (WGS) reactor. As described in the previous paragraph, the product gas stream of the anode has a desired content of carbon monoxide.

The WGS reactor is based on the water-gas-shift reaction, where CO reacts with steam to form H2 and CO2.

$$CO + H_2O \leftrightarrow CO_2 + H_2 \qquad \Delta H = -41.16\,kJ/mol \tag{17}$$

The WGS reaction is reversible and is an exothermic reaction. The reaction is temperature dependent, as CO conversion decreases with increasing temperature.

The effect of reaction pressure is not affecting the equilibrium of the WGS reaction, because during the reaction there is no variation in the number of moles.

By increasing the steam to CO ratio above the stoichiometric ratio, the equilibrium moves to the right which improves the CO conversion even more. Figure 12 shows the conversion of CO with varying temperature and steam to CO ratio. It is clear that the best conversion can be achieved at temperatures between 100 °C and 300 °C, at high steam to CO ratio (Reddy and Smirniotis, 2015).

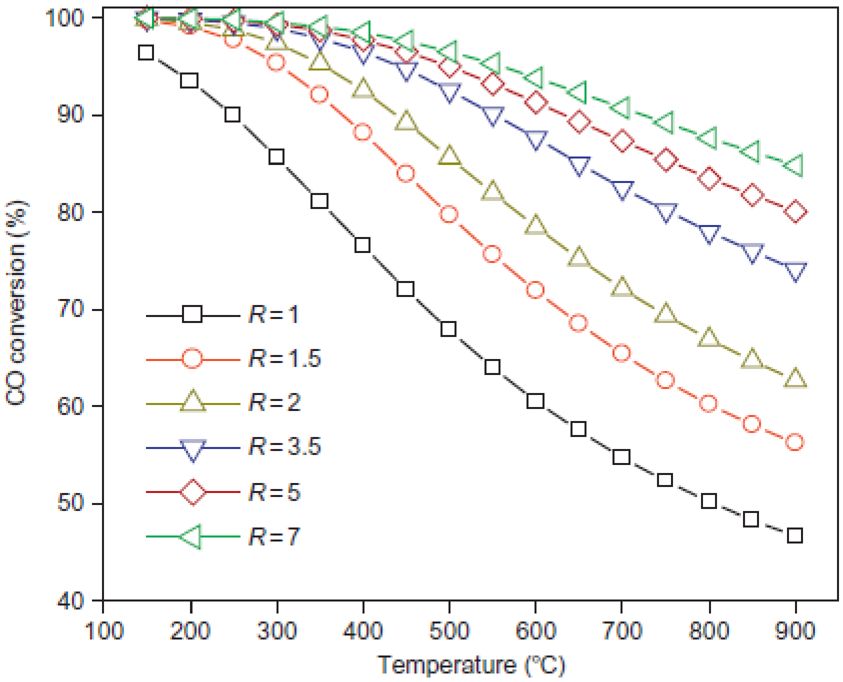

Figure 12: Temperature dependency of CO conversion at different steam to CO ratio (R) (Reddy and Smirniotis, 2015)

3.5 Conclusion

In this chapter we have analyzed the theory related to the main components of the proposed MSMP energy system. We have noticed that in the receiver of the solar reactor, temperatures >1500 K are necessary in order to have a significant methane conversion to hydrogen and carbon particles. This high temperature can be reached by reflecting solar irradiation with heliostat mirrors onto a receiver, where the solar beams are focused. The methane is flowing through the receiver, while carbon particles are heated up and reradiate and conduct the heat to the methane. We have concluded in Chapter 2: Technology that our solar reactor, where methane is thermally decomposed, is not (yet) a mature technology because it has not been tested on an industrial scale. However, there are experimental setups that are able to collect enough solar irradiation and transfer the heat to the methane in order to establish thermal decomposition of methane.

The anode side of the DCFC is a rather complex part of the fuel cell, as multiple (electro)chemical reactions take place simultaneously. We have presented the possible reactions and under what conditions they take place. We have seen that carbon can be oxidized to CO2, which is the common known electrochemical reaction. But we also notice that the carbon can be oxidized to CO and that the formed CO may be oxidized further to CO2. Since both C and CO2 are present at the anode side, we notice that the reverse Boudouard reaction can take place, which chemically converts C and CO2 into CO. With the help of Figure 11, we can determine the temperature dependency of the open circuit voltage of the DCFC. The standard potential of the electrochemical oxidation of C to CO2 is nearly independent of temperature, because the entropy change is near zero. The standard potential of the electrochemical oxidation of C to CO becomes more negative with increasing temperature.

Of the three main components of the MSMP energy system, the WGS reactor is the only mature technology. Here the CO formed at the anode of the DCFC is mixed with steam to form H2 and CO2. We noticed that the WGS reaction has too low kinetics to establish the reaction at lower temperatures, that the conversion efficiency is decreasing with increasing temperature and is dependent of the steam to CO ratio. A high steam to CO ratio provides a higher conversion efficiency. Temperatures between 200 – 400 °C with a steam to CO ratio between 2-5 are desired to establish conversion efficiency > 90%.

We have presented the technology status in Chapter 2 and the detailed theory in Chapter 3. In the following chapter we will present our modelling efforts in which we will simulate the MSMP energy system and where we will analyze the results.

4 Modelling

In this chapter we will present the Cycle-Tempo model of the MSMP energy system and we will present and analyze the modelling results.

4.1 Introduction

In the previous chapters we have presented the current state of relevant technology and the detailed theory of the three main components of the fuel cell; the solar reactor, DCFC and WGS reactor. As described both the solar reactor and the DCFC are immature technologies and especially the DCFC has a lack of experimental results. In this chapter we present a model that simulates the MSMP energy system. The system is modelled in the flow sheeting computer program Cycle Tempo, which is capable of calculating the energy balance, mass flows and efficiencies of the system.

We will analyze the Cycle Tempo modelling results to see if it matches our expectations based on the theory. Furthermore we will use the modelling results for the technical, economic and social feasibility studies. For the technical feasibility we will analyze whether and mass flows calculated with Cycle Tempo can be realized in practice and if the temperatures at which the solar reactor and fuel cell operates can be handled. For the economic feasibility we will use the mass flows calculated in Cycle Tempo to calculate the costs and revenues of the sources and products in the system. For the social feasibility we will compare the CO2 emission calculated with Cycle Tempo with competing technologies to determine the sustainable contribution of the MSMP energy system.

With the help of Cycle Tempo we have also performed an exergy analysis, which indicates where exergy losses occur in the model. This gives us insight where our model could be optimized, which can be used for further research.

In this chapter, we will first explain how Cycle Tempo works and what challenges we faced and what adaptations we had to do in order to be able to simulate our system. Then we will present the Cycle Tempo model, as we describe how we modelled all parts of the MSMP energy system. This is followed by the modelling results and exergy analysis, which will both be discussed.

4.2 Cycle-Tempo

The DCFC is modelled in Cycle Tempo, a flow sheeting computer program developed by TU Delft and TNO. It is a program for thermodynamic modelling and optimizations of systems for the production of electricity, heat and refrigeration. It assumes thermodynamic equilibrium.

The computer program has various interconnected cycles, each containing many different apparatuses. An apparatus is the term Cycle Tempo uses for a specific component in the model. Examples of apparatuses are a fuel cell, gasifier, heat exchanger, pump, valve, separator, etc. These apparatuses form a network of mass and energy flows, since the apparatuses are connected by pipes. Cycle Tempo has the capacity of handling complex modelling of a complete power plant.

The basic modelling structure is relatively simple. Cycle Tempo offers different apparatuses, such as a gasifier, compressor, fuel cell, valve, etc. For each apparatus certain fixed variables are demanded and by interconnecting the apparatuses via pipes Cycle Tempo can calculate the mass and energy flows in the system.

Although Cycle Tempo has many types of apparatuses, there were two limitations for our model. The first is the limitation that Cycle Tempo does not have a solar reactor apparatus. Houwing et al. presents a solution, by modelling the solar reactor as a gasifier with a 0,0 kg/s air input (Houwing, Hemmes, *et al.*, 2005). The input methane combined with a thermal source makes the gasifier behave like a solar reactor, because Cycle Tempo calculates thermodynamic equilibrium of the species in the gasifier (solar reactor). A schematic view of the Cycle Tempo model by (Houwing, Hemmes, *et al.*, 2005) is shown in Figure 13, where the gasifier is indicated by the orange dotted square.

The second limitation is that the DCFC apparatus is programmed as the 4-electron process, thus at the anode only CO2 is produced independent of temperature. It turned out that we had to adjust the DCFC's FORTRAN subroutine, since we also desire to study the 2-electron process where both CO2 and CO is produced at the anode.

With the help of Teus van der Stelt of Asymptote, the company that developed Cycle Tempo, we were able to rewrite the subroutine of the DCFC. The most important rewritten part was changing the 4-electron anode and cathode electrochemical reaction to the 2-electron electrochemical reaction (3) and (4) and the Nernst equation (16). A basic overview of the subroutine changes is shown in Appendix 12.1.

As described in Chapter 3: Theory, both the 2-electron and the 4-electron process take place in the DCFC. Unfortunately it was too complex to rewrite the subroutine in such a way that both processes can run simultaneously. The subroutine for this component can only run either the 2-electron DCFC or the 4-electron DCFC. This was a major limitation for our Cycle Tempo model, because now we had to assume the ratio between the 2- and 4-electron process. Running the model became also very time consuming, since we had to close Cycle Tempo and install the other subroutine in order to run the other process (and vice versa). We modelled the 2-electron and 4-electron DCFC in parallel by running them separately and combining the results. So the gas composition and conditions of the anode output of both individual modelled DCFC's is noted and given as input variables for the two combined inputs for the Boudouard reactor, shown in Figure 16.

Besides the electrochemical reactions, also the Boudouard reaction takes place at the anode. Although the Boudouard reaction is integrated in Cycle Tempo, it is not integrated in the DCFC. Therefore we had to implement an extra Boudouard reactor after the anode of the DCFC to have the Boudouard reaction present.

In this section we have briefly explained how Cycle Tempo works and what limitations there are for our model. In the following paragraph we will present the Cycle Tempo model.

4.3 Model

In this paragraph we will analyze our proposed Cycle Tempo model. The model is based on the Cycle Tempo model used in the study towards a CO2 producing DCFC performed by (Houwing, Hemmes, *et al.*, 2005), shown in Figure 13. The purpose of this model was to design a MSMP energy system for an alternative use of natural gas to generate power with a DCFC operating around 700°C. At this temperature, mainly CO2 is formed at the anode. As described above we want to analyze the DCFC at higher temperatures, where also CO is formed at the anode. Therefore the model of (Houwing, Hemmes, *et al.*, 2005) is rebuilt to a MSMP system with a DCFC where also CO is formed at the anode.

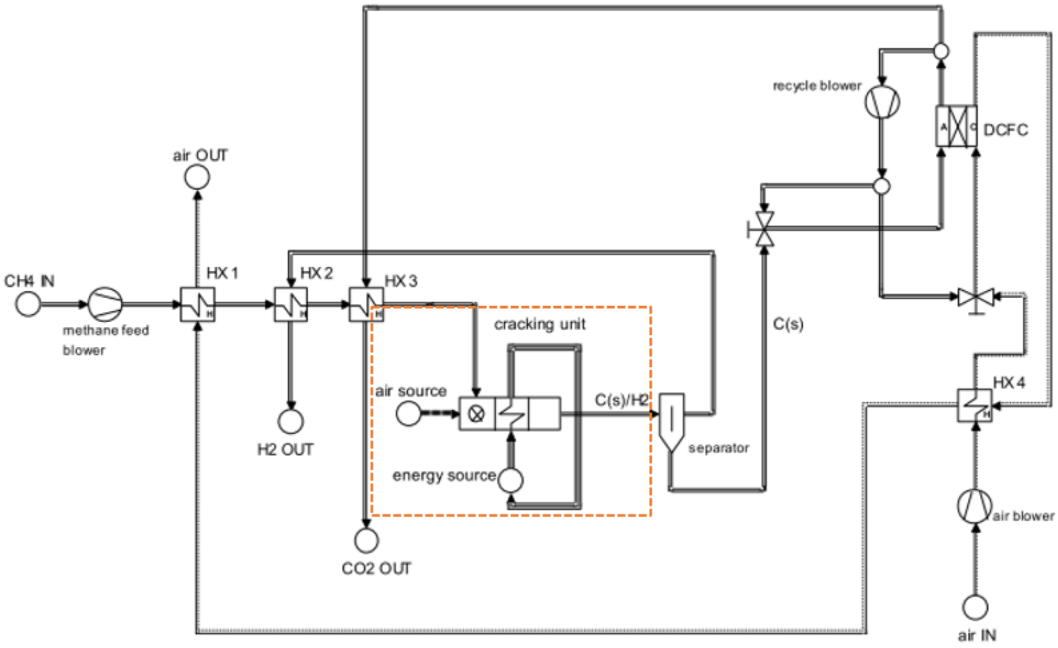

Figure 13: MSMP system - methane fueled CO2 producing DCFC modelled in Cycle Tempo by (Houwing, Hemmes, *et al.*, 2005)

Due to the limitations of the software the model cannot run the DCFC 2- and 4-electron process simultaneously. We had to rewrite the fuel cell subroutine to implement the 2-electron process, but it seemed too complex to implement both processes in the subroutine. This caused us to model the MSMP energy system in separate parts which run individually: The solar reactor, DCFC-4 electron, DCFC-2 electron, Boudouard reactor and WGS reactor.

As explained, Cycle Tempo has no solar reactor apparatus, so following Houwing we used a gasifier as solar reactor. A hot artificial gas stream simulates solar heat, as shown in Figure 14. The hot gas transfers its heat to the gasifier, where the heat is used for the methane cracking process to split CH4 molecules into solid carbon particles and hydrogen gas. The hot gas enters the system at node 17 and leaves at node 2. Figure 14 shows via pipe 14 that also air is connected to the gasifier. Cycle Tempo will not run without a connected air stream, but the air stream is set with mass flow of 0,0 kg/s. Therefore this airstream can be neglected. A separator (apparatus 15) is used to separate the produced hydrogen and carbon particles.

The artificial hot gas enters the gasifier at T = 1500 °C with $T_{in} - T_{out} = 100\ °C$. Cycle Tempo calculates the mass flow of the hot gas automatically in order to provide the necessary heat for the thermal decomposition of methane.

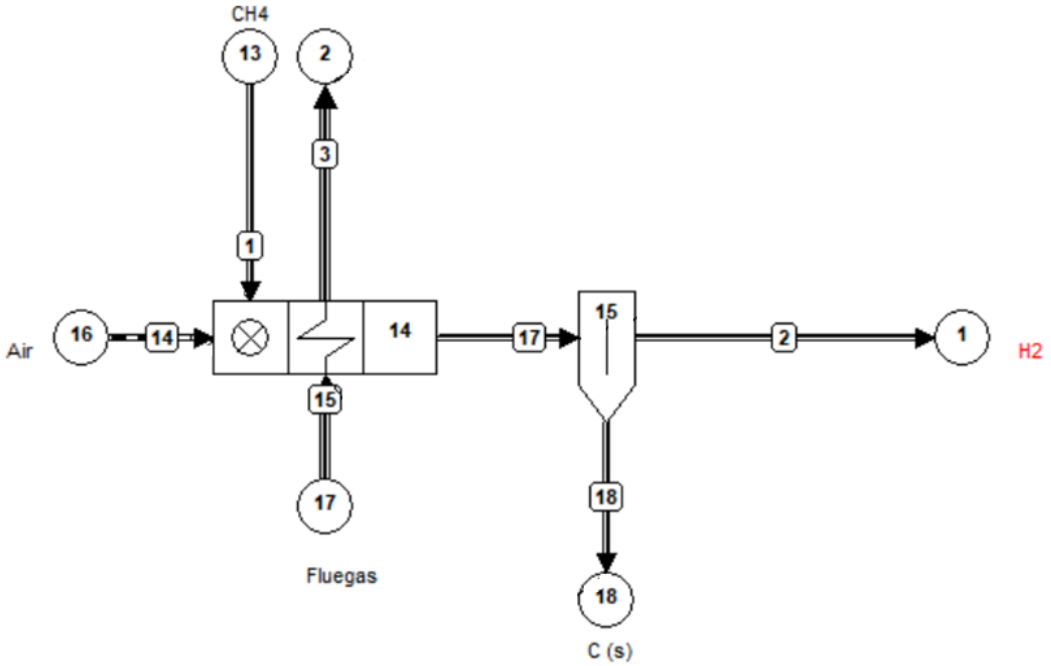

Figure 14: Cycle Tempo model of the Solar Reactor

The carbon produced in the solar reactor is fed to the anode of the DCFC, which is shown in Figure 15. Because of the above mentioned limitation, we cannot model a DCFC where both the 2-electron and the 4-electron process takes place simultaneously. Therefore we have chosen to model two parallel DCFC's, independently. This means that 50% of the carbon produced at the solar reactor is fed to the 2-electron DCFC and the other 50% is fed to the 4-electron DCFC. We have to take into account that in reality the ratio of which process is favored depends on operating conditions. As explained in the Chapter 3: Theory, it is expected that more CO is formed with increasing temperature but unfortunately this was too complex to implement in our model.

The cathode is fed by a CO2/O2 gas mixture at a stoichiometric molar ratio of 2/1. In reality the cathode input would be air combined with the recycled CO2 produced at the anode, or an artificial source of CO2/O2. For simplification we took a CO2/O2 mixture, without recycling of the CO2 produced at the anode.

The anode input is fixed and the cathode input mass flow depends on the anode mass flow and heat demand for the fuel cell, because in our model the mass flow over the cathode is also the thermal source for the fuel cell. For the 2-electron DCFC the electrochemical reaction at the anode is endotherm, thus an external thermal source is desired. At the cathode, we modelled a larger CO2/O2 mass flow than necessary for the electrochemical reaction. This extra mass flow enters and leaves at the cathode, but with $\Delta T = 100°C$. In this way, the 'extra' cathode mass flow provides the heat necessary for the endothermic reaction in the DCFC thus acts as the thermal source for the fuel cell.

In reality, the heat is provided directly to the fuel cell by the ('waste') heat of the solar reactor. Therefore in the overall analysis of this MSMP energy system, we assume that the transferred heat from the cathode mass flow to the fuel cell equals the heat which in reality would be provided by the solar reactor.

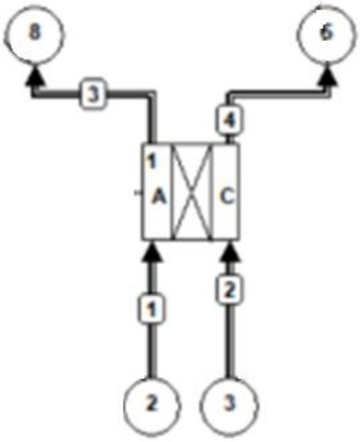

Figure 15: Cycle Tempo model of the DCFC

For the 2-electron DCFC, the molar ratio of the output gas mix at the anode is 1:1 CO/CO2, independent of temperature. In reality this would be dependent of temperature, but it was too complex to implement this in the rewritten subroutine of Cycle Tempo.

In Figure 16 the Boudouard reactor is shown. Here, the anode outputs of the 2- and 4-electron DCFC's are combined before they enter the Boudouard reactor via pipe 6. Normally, the Boudouard reaction(s) takes place at the anode, but this reaction is not implemented in Cycle Tempo for the DCFC. This caused us to set the fuel cell utilization to 0.8, in order to have carbon particles available at the Boudouard reactor. With a fuel cell utilization of 0.8 all carbon particles left in the anode output are converted in the Boudouard reactor.

Boudouard is implemented in the gasifier, so we lead the combined anode outputs to the gasifier. The gasifier is fed by a flue gas stream (pipe 4). Similar to the solar reactor, the flue gas provides the necessary heat to establish Boudouard equilibrium. The heat provided by the flue gas to the Boudouard reactor simulates the heat provided by the solar reactor to the Boudouard reactor.

We will analyze methods of heat transfer from the solar reactor to the fuel cell in Chapter 5: Technical Feasibility.

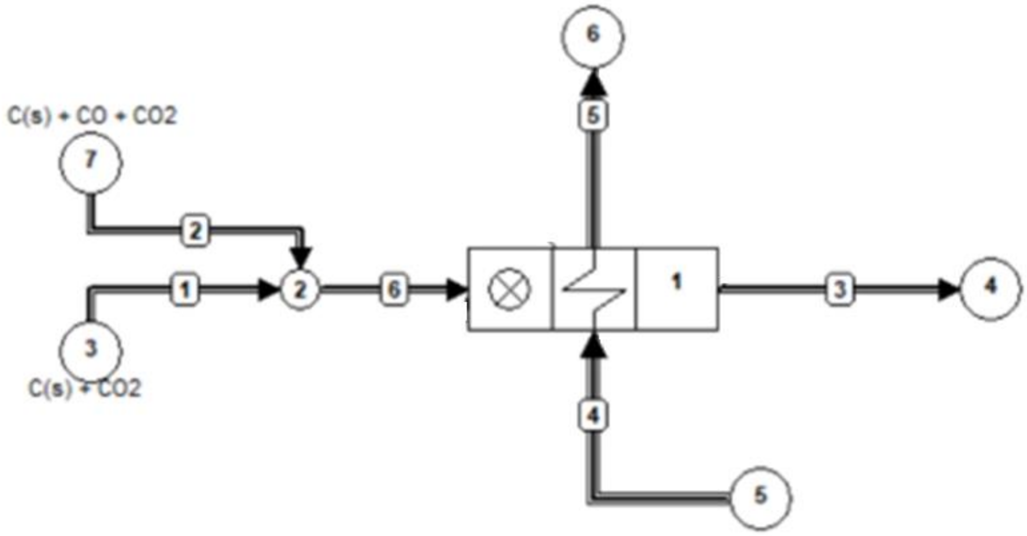

Figure 16: Cycle Tempo model of the Boudouard reactor which in reality is part of the fuel cell

Ultimately, pipe 3 in Figure 16 is the real anode outlet of the combined parallel DCFC. The gas mixture in pipe 3 contains the calculated CO2, CO and C concentrations, taking into account the 2- and 4-electron electrochemical reactions, the fuel utilization of the DCFC and the Boudouard reaction.

Figure 17 shows the last part of our MSMP energy system, the WGS-reactor. The apparatus used for this part is a chemical reactor. The output gas mix from the anode, pipe 3 in Figure 16, is mixed with steam in valve 2. The gas mixture leaving the Boudouard reactor has a higher temperature then necessary for the WGS reaction, so the heat is used for preheating the water/steam. The valve mixes the steam and CO/CO2 mixture with a fixed steam-to-CO ratio of 2:1. With this ratio the CO concentration in the product stream leaving the WGS reactor (pipe 3) is < 1%. We could increase the steam-to-CO ratio to establish an even lower concentration of CO, but the water needs to be converted into steam too which will cost significant energy.

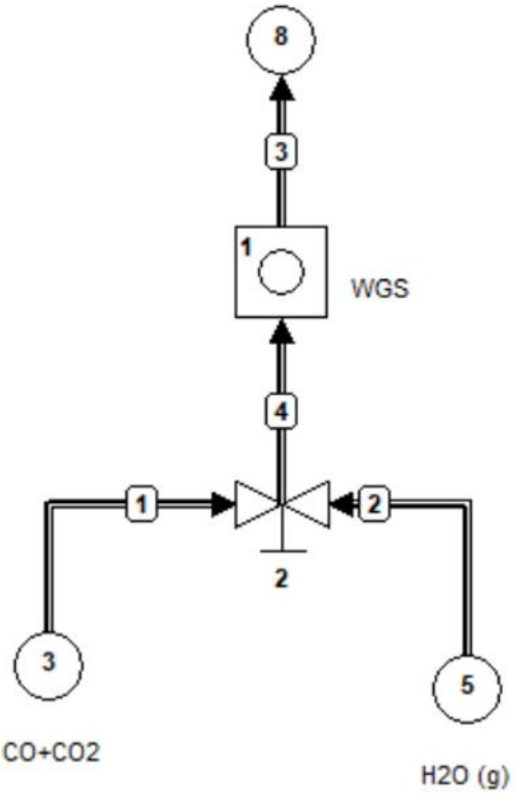

Figure 17: Cycle Tempo model of the WGS-reactor

Important to notice is the lack of heat exchangers present in our system. Every process requires its own reaction temperature, thus a number of streams with waste heat from the solar reactor or necessary preheating are expected. For example, the produced hydrogen leaving the solar reactor has a temperature of approximately 600 °C. In our Cycle Tempo model we have not modelled heat exchange of this stream, but in our overall analysis we assume that the hydrogen is cooled down to 25 °C and that its heat is used to preheat the cathode input stream. We assume a 100% heat exchange.

For simplification pumps and blowers, needed for the transportation of the different mass flows, have not been modelled in our system. Also heat exchangers are not present in our model. However, we assume that every mass flow leaving the system is cooled down to room temperature (25 °C) and exchanges its heat to the system. For example, the hydrogen produced at the solar reactor has a temperature of 750 °C. We assume that, before it exits the system, it exchanges its heat to the water/steam entering WGS reactor without heat exchange losses.

Below a list of the most important assumptions and modelling design choices are presented:

- A gasifier is used to simulate the solar reactor.
- The carbon produced at the solar reactor is fed 1:1 mass ratio to the 2- and 4-electron DCFC.
- Both DCFC's are modelled with a fuel utilization of 0.8 in order to have carbon particles available at the Boudouard reactor.
- We assume fixed power densities for the fuel cells at the values presented in Table 2.
- The CO/CO2 gas mixture produced at the anode of the 2-electron DCFC has a fixed molar ratio of 1:1, independent of temperature.
- The necessary heat for the DCFC is provided at the cathode.

- The cathode inlet composition is fixed at 1:2 O_2/CO_2 molar ratio.
- All gas/product streams leaving the system are cooled down to 25°C and are assumed to exchange their heat tot the system with 100% efficiency.

We have presented our model and explained what assumptions and design choices we have made because of limitations in Cycle Tempo and for simplification of our model. In the next paragraph we present and analyze the modelling results.

4.4 Results

In this paragraph we will present and analyze the modelling results. First we will focus on the individual results of the modelled DCFC's. We will analyze the open circuit voltage (OCV) of the DCFC, which we will compare with experimental and literature results. With this comparison we try to analyze whether our modelling results match the findings of other researches and experiments.

Once the modelling results of the individual DCFC's are analyzed we will analyze the overall modelling results, which includes all sub systems of the MSMP energy system.

4.4.1 DCFC results

We will now present the modelling results of the 2-electron and 4-electron DCFC and we will compare the results with literature and experimental results. We will determine the OCV with Cycle Tempo and compare this with literature and experimental results as a measure of reliability of the DCFC models. If our modelling results match literature and experimental results we consider the models as reliable and we will determine the maximum power density.

Figure 18 shows the I-V curve of the 4- electron DCFC modelled in Cycle-Tempo, while increasing the temperature and varying the cell resistance. The I-V curve is a measure of the current density (I) and voltage (V) of the fuel cell. It is important to notice that Cycle-Tempo will not compile at $I<100$ A/m2. Therefore we have to determine the OCV manually.

In Figure 18 linearity is assumed for the cell voltage at $I<100$ A/m2. The OCV would be where the dotted line crosses the Y-axis, in Figure 18 indicated by the dotted line. Figure 18 shows that a change in cell resistance does not affect the point where the graph crosses the Y-axis, the OCV. Increasing the cell resistance results in a faster decrease of the cell voltage with increasing current density.

Figure 18 also shows that the OCV decreases with increasing temperature, which is in contrast with theory. As explained in Chapter 3: Theory and shown in Figure 11, the electrochemical oxidation of C to CO_2 is nearly independent of temperature, so the OCV is expected to be approximately 1.02 V independent of temperature.

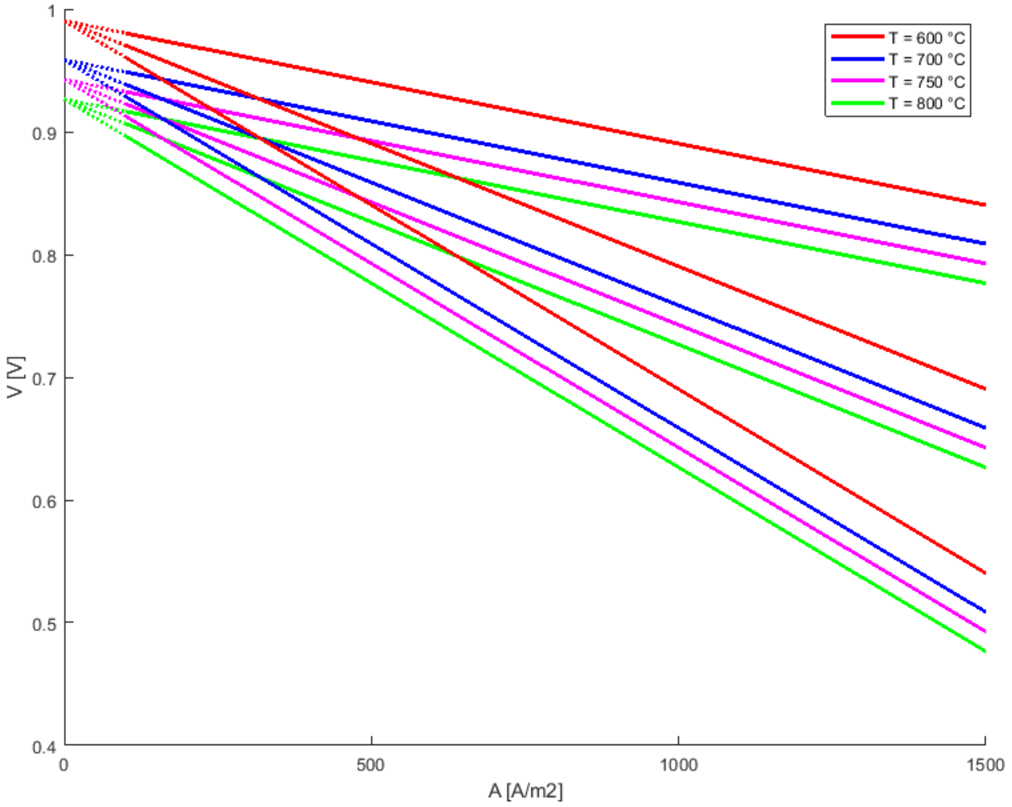

Figure 18: Cycle Tempo simulation of the 4-electron DCFC at different operation temperatures and cell resistance. The dotted line crossed with the y-axis marks the OCV if we assume linear activation polarization

We have tried to analyze how the OCV is calculated in Cycle Tempo, but unfortunately this is calculated in a separate subroutine. We have asked Teus Van Der Stelt (Asymptote/ Cycle Tempo) if there was an explanation, but he answered that OCV calculation in Cycle Tempo is a complex subroutine and it would be time consuming to analyze it. Therefore this aspect will be one of our recommendations for further research.

In Figure 19, the I-V curve of the 2-electron DCFC is presented with changing internal resistance and temperature. Similar to the 4-electron DCFC, Cycle Tempo did not compile at I<100 A/m2. So again we had to assume the OCV.

In Figure 19, again linearity is assumed in the low current density region. Although the graph shows that the OCV is higher at T = 800 °C (green) than the OCV at T = 600 °C (red), the difference in OCV was expected to be more significant based on the theoretical OCV presented by (Cassir and Hemmes, 2004) in Figure 11.

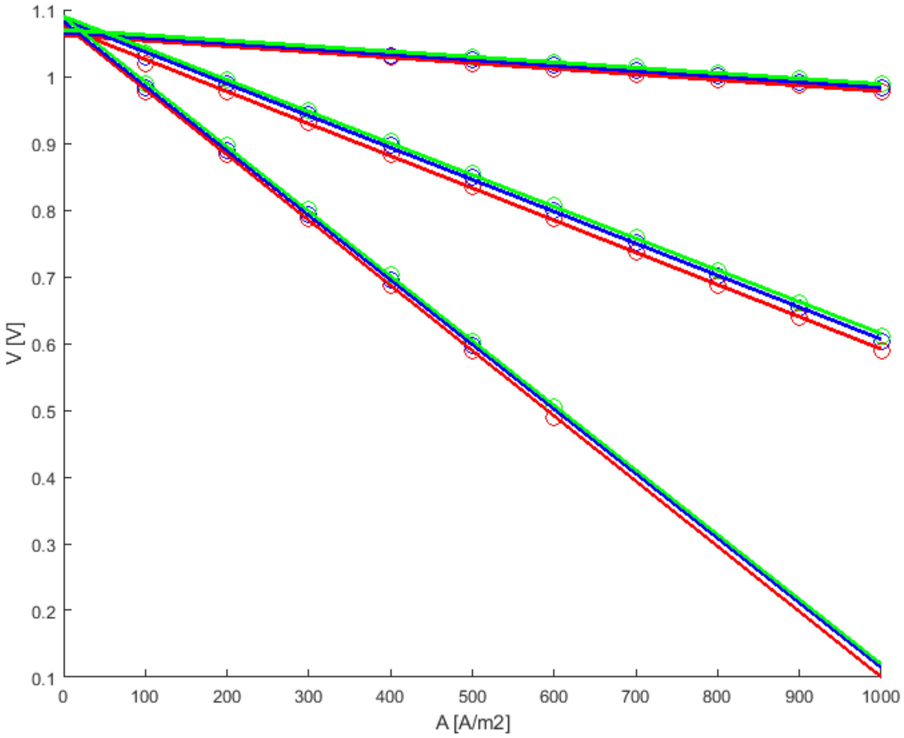

Figure 19: I-V curve of the 2-electron DCFC with assumed linearity in the low current density region. T=600°C (blue), T=700°C (red), T=800°C (green)

Our aim was to tune the internal resistance and current density of the DCFC's in such a way, that the OCV and I-V curve of the Cycle Tempo model would match what was explained in Chapter 3: Theory. With a proper tuned DCFC, we would be able to determine the maximum power density of the 2- and 4-electron DCFC.

Since both the OCV of the 4-electron and the 2-electron DCFC respectively show an unexpected temperature (in)dependency compared with theory and the fact that we were unable to explain or to solve this unexpected behavior, we cannot consider the OCV and the I-V curve of the modelled DCFC's as reliable.

Therefore we have chosen to determine the maximum power density based on literature. We will tune the internal resistance and current density in Cycle Tempo in such a way that our DCFC operates at the determined maximum power density.

Figure 20 shows experimental results found in literature for maximum power density at different temperatures.

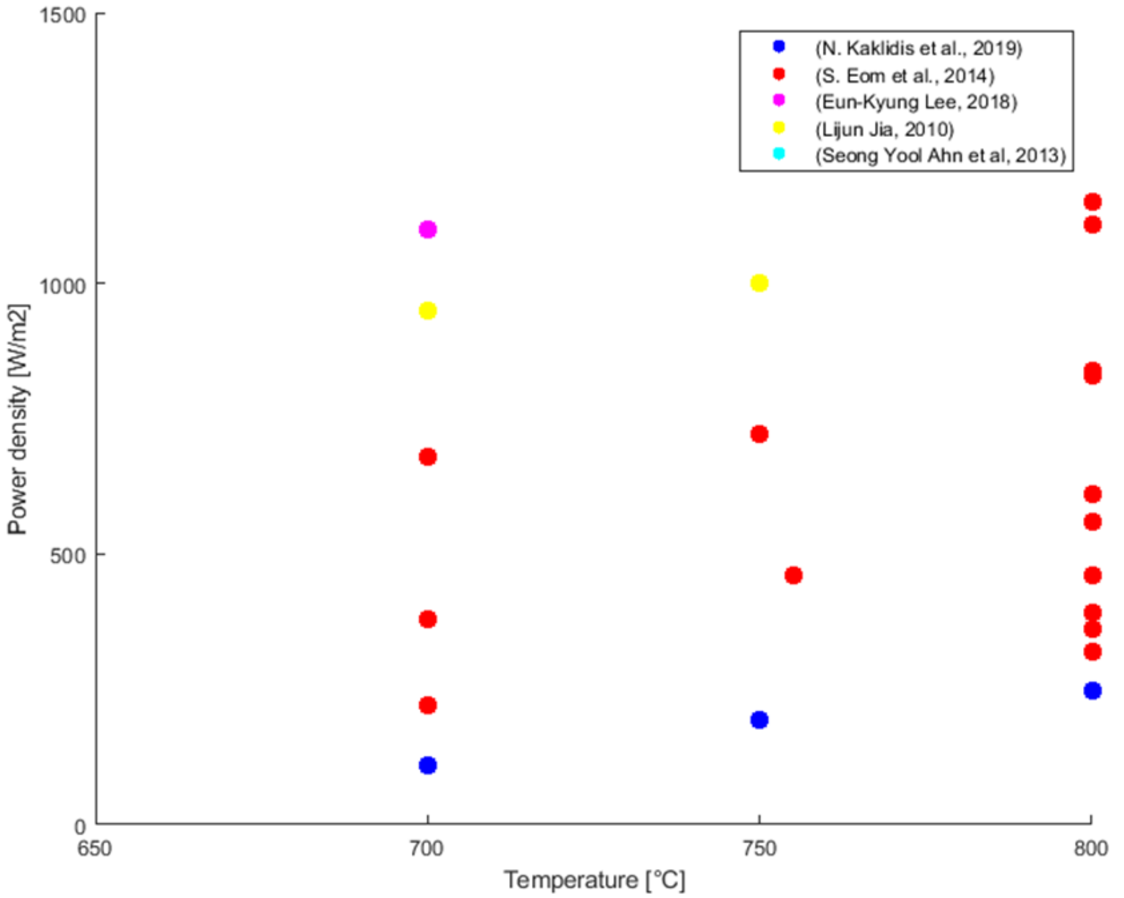

Figure 20: Maximum power density found in literature which are determined in practical experiments.

Figure 20 shows that the maximum power density values found in literature are not very consistent. Therefore we still have to assume the maximum power density, which is presented in Table 2.

Table 2: Input parameters for the DCFC's to operate at the maximum power density determined by literature

Temperature DCFC	Current density	Internal resistance	Max power density
700 °C	1100 A/m2	12.8 E^{-5} Ω/m2	900 W/m2
750 °C	1250 A/m2	11.4 E^{-5} Ω/m2	1000 W/m2
800 °C	1300 A/m2	6.18 E^{-5} Ω/m2	1100 W/m2

We will use the input parameters temperature, current density and internal resistance presented in Table 2 for further simulations, so the DCFC's operate at the determined maximum power density.

Now that we have determined the input variables where our DCFC operate at maximum power density, we will compare our proposed DCFC (2-electron and 4-electron electrochemical reaction and the Boudouard reaction) with the common DCFC (4-electron electrochemical reaction). We will compare both DCFC's by considering equation (18):

$$\eta = \frac{P_{DCFC} + HHV_{an_{out}}}{HHV_{C_{in}} + Q_{in}} \tag{18}$$

Table 3: DCFC efficiency of proposed and common DCFC according to equation (17)

	Our proposed DCFC	Common 4-electron DCFC
	$\eta\ [-]$	$\eta\ [-]$
700 °C	0.969	0.842
750 °C	0.911	0.709
800 °C	0.942	0.784

Table 3 shows that the efficiency according to equation (18) of the proposed DCFC is significantly higher than for the common 4-electron DCFC. Considering the fact that our proposed DCFC converts heat directly into power and that at the anode CO is produced, the higher efficiency according to equation (18) was expected.

4.4.2 MSMP energy system results

Now that we have determined the fuel cell input variables, we can analyze the modelling results if we combine all components of the MSMP energy system. As explained in this chapter we model and run the components individually because of software limitations. So the modelling results analyzed in this chapter are based on the combination of the individual modelled solar reactor, 2-electron DCFC, 4-electron DCFC, Boudouard reactor and WGS-reactor.

The input variables presented in Table 2 are used for both the 2-electron and 4-electron DCFC. Cycle Tempo calculates the mass flow of carbon as fuel input, which is taken as an input variable for the solar reactor. Based on the mass flow and temperature of carbon, the input methane mass flow and heat at the solar reactor is calculated.

Based on the mass flow and molar fraction of the product stream at the DCFC anode, the heat necessary for the Boudouard reactor is calculated and based on the molar content of CO at the output stream of the Boudouard reactor the mass flow of steam is calculated for the WGS-reactor.

By combining all results we can present the overall modelling results of the MSMP energy system, which is presented in Table 4.

Although the results in Table 4 show a very high efficiency of the system, we to take into account that we neglect certain losses in the system. Losses by heat exchange, pumps, valves and blowers are not present in the system. The effect of these losses will be discussed in Chapter 8: Discussion.

In Table 4, Q_{sun} is all heat necessary in the system, in practice heat from the sun. So Q_{sun} is the heat necessary for thermal decomposition at the solar reactor (Figure 14), for the endothermic electrochemical reactions at the DCFC (Figure 15), for the endothermic chemical reaction at the Boudouard reactor (Figure 16) and for the conversion of water to steam at the WGS-reactor (Figure 17). We calculate manually the waste heat leaving the system, by assuming that every mass flow leaving the system is cooled down to 25 °C and exchanges its heat to the system at 100% efficiency. The summation of all heat necessary at the individual modelled components is subtracted by the heat exchanged from the leaving mass flows to the system. In this way Q_{sun} is the total heat from the sun demanded by the system.

E_{CH4} is the higher heating value (HHV) of the methane entering the solar reactor. The HHV is a measure of the amount of heat released during combustion of the fuel. P_{DCFC} is the electricity produced at both fuel cells combined. E_{H2} is the HHV of hydrogen produced at the solar reactor and at the WGS reactor. M_{CO2} is the net mass flow of CO2, leaving the system. Here the outputs at the DCFC's and at the WGS reactor are combined.

We define equation (19) as the energy efficiency, which is a ratio of the input energy to the system and output energy from the system. As input we have solar power Q_{sun} and methane E_{CH4} and as output energy we have the power produced by the DCFC P_{DCFC} and the produced hydrogen E_{H2}.

$$\eta = \frac{P_{DCFC} + E_{H2}}{Q_{sun} + E_{CH4}} \tag{19}$$

Table 4: modelling results of MSMP energy system modelled in Cycle Tempo

DCFC Temperature		**700 °C**	**750 °C**	**800 °C**
In				
Q_{sun}	MW	16.0	17.6	19.0
E_{CH4} (HHV)	MW	65.3	74.2	77.2
Out				
P_{DCFC}	MW	20.5	20.7	24.1
E_{H2} (HHV)	MW	58.1	66.0	68.5
M_{CO2}	kg/s	3.39	3.86	3.95
η	-	0.963	0.944	0.963
CO2 emission	kg_{co2}/kWh	0.155	0.160	0.153

In Table 4 we present the CO2 emission in the system per produced kWh. CO2 is produced at the anode of the DCFC, but then reacts with carbon by the Boudouard reaction (in the Cycle Tempo model this process is modelled as a separate Boudouard reactor). The gas mix leaving the Boudouard reactor is fed to the WGS reactor where the present CO reacts with steam to form H2 and CO2. We take the CO2 content leaving the WGS reactor as the CO2 produced by the whole MSMP energy system. The CO2 fed to the cathode of the DCFC is subtracted from the CO2 leaving the WGS reactor. In this way we can calculate the net CO2 production by the system.

CO2 emission is defined as emission per kWh produced. We calculate the produced kWh by combining the power produced by the DCFC and the hydrogen (HHV) produced at the solar reactor and WGS reactor. By calculating the time our MSMP energy system needs in order to produce 1 kWh of electricity + hydrogen, we can calculate how much kg of CO2 is produced in this time.

Both the energy efficiency (19) and the CO2 emission will be later in this thesis used in the feasibility studies.

As explained in paragraph 4.3 we have based our model on the Cycle Tempo model of Houwing et al. Their model was shown in Figure 13 and we explained that their model did not include the WGS reactor, because their DCFC only included the 4-electron electrochemical oxidation of C to CO2 so no CO is produced in their system. The solar reactors of both models are equal.

We will compare our Cycle Tempo modelling results with the Cycle Tempo results of Houwing et al. The results are presented in Table 5.

Table 5: Comparison between the modelling results of our model and the model of (Houwing, Hemmes, *et al.*, 2005)

	Houwing at DCFC = 775°C	Ours at DCFC = 700 °C	Ours at DCFC = 750 °C	Ours at DCFC = 800 °C
DCFC eff [-]	0.78	0.90	0.93	0.99
Electr eff [-]	0.27	0.09	0.06	0.10

Hydrogen eff [-]	0.66	0.88	0.88	0.87
Total system thermal eff [-]	0.92	0.95	0.92	0.95

Houwing et al. calculates the DCFC efficiency as the produced power divided by the LHV of the carbon fuel. If we would calculate the DCFC efficiency accordingly, our DCFC efficiency would be lower than for Houwing et al. because their method does not take the heat added to the DCFC and the energy content of the produced CO into account. Therefore we use equation (17) for the DCFC efficiency.

We notice a difference in DCFC efficiency between the values in Table 4 and Table 5, which can be explained by the fact that the DCFC efficiency in Table 4 only includes the modelled 2-electron DCFC (Figure 15) and Table 5 includes also the Boudouard reactor (Figure 15 + Figure 16). So in Table 5 the parallel 2-electron and 4-electron DCFC and the Boudouard reactor are taken into account, resulting in a higher CO content at the anode (because of the Boudouard reaction) and additional heat to the Boudouard reactor.

Table 5 shows that our DCFC efficiency is higher than for Houwing et al, which we expected based on the theory presented in Chapter 3. We also notice an increase in DCFC efficiency with increasing DCFC temperature. This can be explained by the fact that at higher DCFC temperature, less heat is needed for the Boudouard reactor. This results in an increase in DCFC efficiency, according to equation (18).

The electric efficiency and hydrogen efficiency are calculated by equation (20) and (21):

$$\eta_{electric} = \frac{P_{DCFC} - Q_{sun}}{LHV_{CH4}} \tag{20}$$

$$\eta_{H2} = \frac{LHV_{H2}}{LHV_{CH4}} \tag{21}$$

Table 5 shows that the electric efficiency of Houwing et al. is significantly higher than our model, but that the hydrogen efficiency is much higher for our model. This can be explained by the fact that in our system CO is produced at the anode of the DCFC, which is used in the WGS reactor to produce hydrogen. So more heat is necessary for the fuel cell and WGS reactor, which decreases the electric efficiency. But more hydrogen is produced in the system compared to Houwing et al, which explains the increased hydrogen efficiency.

Houwing et al. defines the total system thermal efficiency as (22):

$$\eta_{th_{system}} = \frac{LHV_{H2} + P_{DCFC} - Q_{sun}}{LHV_{CH4}} \tag{22}$$

We notice that our total system thermal efficiency increases a little compared to Houwing et al. This highlights again the potential of our proposed MSMP energy system.

4.5 Exergy

In this paragraph we will perform an exergy analysis of the Cycle Tempo model. With the exergy analysis we are trying to get better insight in where exergy losses occur and with what magnitude.

Exergy is defined as the maximum obtainable work the MSMP energy system can yield when brought reversibly to equilibrium with the environment (Asimptote, 2018). The second law of thermodynamics and the concept of irreversible entropy is the base for our method of exergy analysis. Exergy analysis determines how efficient the work generated from the energy resources is used and indicates where the true losses occur in the system. In every thermodynamic process exergy losses occur in the form of internal irreversibility's and external losses to the surroundings. Determining the magnitude of these losses tells us how much the system differs from an ideal reversible process (Houwing, 2003).

Once the environmental conditions are given manually, Cycle Tempo calculates automatically for all process streams the exergy values. Combined with calculation of power and heat taken or released for each component in the MSMP energy system, the exergy losses are calculated. If all values are known, Cycle Tempo can calculate the exergy efficiency of the components.

The exergy analysis of our MSMP energy system shows exactly where the losses occur in our system and what losses are significant. In this way it is possible to focus on certain losses for further research and for further optimization of our MSMP energy system. If we analyze the exergy efficiency, we can compare the loss with the total exergy loss in the system or component, giving a better insight in the significance of the exergy loss (Houwing, Hemmes, *et al.*, 2005). Cycle Tempo calculates the functional exergy efficiency for the various parts in our system (Stelt, 2018):

$$\eta_{ex_f} = \frac{\sum Ex_{product}}{\sum Ex_{source}} \tag{23}$$

Where $\sum Ex_{product}$ is the sum of all exergy values of the output products and $\sum Ex_{source}$ is the sum of all exergy values of the input products.

If only a part of an exergy flow is part of a source or product flow, an active (source and product) and passive (ballast) part is required. Distinction can be made between thermo-mechanical exergy and chemical exergy:

Thermomechanical exergy is power produced when a flow is brought into thermomechanical equilibrium with the environment, while the chemical composition does not change. Chemical exergy is power produced when a flow is brought into chemical equilibrium with the environment. This means that the components in the input flow are converted to environmental components and contribute to the partial pressure of the environmental components (Houwing, 2003).

We quantify three different functional exergy efficiencies in our total MSMP energy system (Stelt, 2018):

Fuel cell
In the fuel cell the input fuel reacts with the oxidant, generating electricity and heat. In practice, other components than the reacting fuel and oxidant are present in the in- and output streams. For example, in practice air is fed to the cathode. For simplification, we have modelled our fuel cell being fed by only reacting products. Only at the cathode, an excess CO2/O2 mixture is being fed to provide the necessary heat at the fuel cell. The electrical energy, in the form of direct current, is the exergy product of the fuel cell. The change in chemical exergy of both fuel and oxidant is the exergy source of the fuel cell.

$$\eta_{ex_f} = \frac{P_{electric}}{\left(Ex_{C_{in}} - Ex_{C_{out}} - Ex_{CO_{2_{out}}} - Ex_{CO_{out}}\right) + \left(Ex_{CO_{2_{in}}} + Ex_{O_{2_{in}}} - Ex_{CO_{2_{out}}} - Ex_{O_{2_{out}}}\right)} \tag{24}$$

Solar Reactor (Gasifier)

In our proposed Cycle Tempo model, the gasifier simulates a solar reactor given the fact that Cycle Tempo does not have an available solar reactor apparatus. In the gasifier the fuel (CH4) is converted into carbon particles and hydrogen by thermal decomposition. Normally the gasification takes place using an oxidizer, but in our model flue gas is fed to the gasifier. It does not react with the natural gas, but only provides the necessary heat imitating the heat from the solar reactor.

$$\eta_{ex_f} = \frac{Ex_{H_2} + Ex_C}{Ex_{CH_4} + Ex_{fluegas_{in}} - Ex_{fluegas_{out}}} \tag{25}$$

Boudouard reactor (Gasifier)

The Boudouard reactor is in practice part of the fuel cell, since this reaction mechanism occurs at the anode. However, this is not implemented in Cycle Tempo for this type of fuel cell. Therefore we have chosen to model a gasifier fed by both the anode output gas mixtures of the CO2-DCFC and CO2-CO-DCFC, respectively. The functional exergy efficiency is formulated as follows:

$$\eta_{ex_f} = \frac{Ex_{CO_{out}} + Ex_{CO_{2_{out}}} + Ex_{C_{out}}}{Ex_{CO_{in}} + Ex_{CO_{2_{in}}} + Ex_{C_{in}} + \left(Ex_{fluegas_{in}} - Ex_{fluegas_{out}}\right)} \tag{26}$$

WGS reactor

Cycle Tempo does not calculate a functional exergy efficiency. For specific designs of reactors the specifications can vary strongly. For the specifications given, Cycle Tempo distinguishes how heat is fed to the process and how the outgoing process flow is used for chemical and thermo mechanical purposes. Therefore, Cycle Tempo cannot define a generally functional efficiency.

Table 6 shows the functional exergy efficiency of all components in our MSMP energy system. Important to notice is that the exergy loss of the valve at the entrance of the WGS-reactor is neglected in this overview. Table 6 shows that for the 2-electron DCFC the exergy loss is negative, indicating an exergy gain in the fuel cell. Theoretically it is impossible to gain exergy in a process, so we have to find an explanation how this outcome is possible.

Table 6: Exergy analysis of all components in the Cycle Tempo model

DCFC temperature		Functional exergy efficiency η_{ex_f} [%]	Exergy loss [kW]	Relative exergy loss to total loss [%]	Relative exergy loss to fuel [%]
700°C	4-electron DCFC	93.3 %	643 kW	14 %	1 %
	2-electron DCFC	115.1 %	-1377 kW	-30 %	-2.4 %
	SolarReactor	96.7 %	2006 kW	44 %	3.3 %
	Boudouard reactor	99.7 %	67.6 kW	1.5 %	0.1 %
	WGS-reactor	-	487.2 kW	10.6 %	0.8 %
	Total		**1826 kW**		**2.8 %**
750°C	4-electron DCFC	92.9 %	758 kW	15 %	1.1 %
	2-electron DCFC	113.7 %	-1432 kW	-28 %	-2.1 %
	SolarReactor	96.6 %	2320 kW	45 %	3.3 %
	Boudouard reactor	99.6 %	94.3 kW	2 %	0.1 %
	WGS-reactor	-	553.7 kW	11 %	0.8 %
	Total		**2294 kW**		**3.2 %**
800°C	4-electron DCFC	94.7 %	611 kW	12 %	0.9 %
	2-electron DCFC	113.5 %	-1561 kW	-29 %	-2.0 %
	SolarReactor	96.6 %	2452 kW	46 %	3.3 %
	Boudouard reactor	99.5 %	114.8 kW	2 %	0.2 %
	WGS-reactor	-	571.7 kW	11 %	0.8 %
	Total		**2188 kW**		**3.4 %**

As explained in the modelling chapter of this thesis, the software is adapted in order to establish a CO-CO2 producing DCFC. Therefore the anode and cathode reactions, the overall reaction and the Nernst equation has been changed. Cycle Tempo uses FORTRAN subroutines to calculate the different values. The subroutine for exergy calculations has not been rewritten for the fuel cell, because this seemed too complex.

We have contacted Cycle Tempo founder Teus van der Stelt and asked if he can tell us why the 2-electron DCFC shows a negative exergy loss. Unfortunately he told us that the case was too complex to solve pro deo. Therefore we have to find a possible explanation ourselves.

For the 4-electron DCFC the process is exotherm, where temperature increases over the fuel cell. For the 2-electron DCFC the process is endotherm, where the temperature decreases over the fuel cell. It is plausible that this difference causes the negative exergy loss for the 2-electron DCFC, since the it Cycle Tempo runs the exergy subroutine based on the 4-electron DCFC. A hypothesis can be that the negative loss is actually a normal loss, but that the minus sign is because of the endotherm reaction of the DCFC, while Cycle Tempo calculates this as an exotherm reaction.

If we assume that this hypothesis is valid, we can analyze the exergy of the MSMP energy system.

If we analyze the functional exergy efficiency of the subsystems, two parts are highlighted in terms of functional exergy efficiency magnitude and absolute value: The 2-electron DCFC and the solar reactor. They show the biggest exergy losses present in the MSMP energy system. In fact, the magnitude of the 2-electron DCFC is more than double the magnitude of the 4-electron DCFC. This can be explained by the difference in cathode exergy in- and output flow. Given the fact that the 2-electron DCFC is endothermic and takes heat from the cathode stream, the mass flow at the cathode is approximately a factor 4 higher than the cathode mass flow of the 4-electron DCFC. Therefore the exergy difference over the cathode is more significant for the 2-electron DCFC, which decreases the functional exergy efficiency. Table 6 shows that the functional exergy efficiency increases with increasing temperature for both DCFC's, possibly because of better reaction kinetics at higher temperature.

The main contributor to the total exergy loss of all MSMP components is the solar reactor, where the methane is thermally decomposed at high temperature. The total loss relative to the exergy of the input fuel (CH4) is around 7.5 %, decreasing slightly with increasing temperature.

A more detailed analysis of the exergy in our MSMP energy system falls beyond our scope and will be given as a recommendation for further research. The components neglected in our system (valves, pumps, etc) need to be implemented to simulate a more realistic model and especially the 2-electron DCFC need to be remodeled in order to verify whether our hypothesis of the negative exergy loss is valid or not.

4.6 Discussion

In this chapter we have presented a Cycle Tempo model and the modelling results. The goal of our model was to simulate our MSMP energy system and see if the modelling results showed what was expected based on the theory. This will be used as a measure of reliability, as we will use the modelling results later in this thesis for the technical, economic and social feasibility.

The model design involved some limitations. There was no solar reactor apparatus integrated in Cycle Tempo, but with the solution presented by (Houwing, Hemmes, *et al.*, 2005) we modelled a gasifier that behaves like the desired solar reactor.

Another limitation was the fact that the DCFC apparatus in Cycle Tempo was only programmed with the 4-electron process, thus only taking into account the electrochemical oxidation of C to CO2. Therefore we had to rewrite the DCFC Cycle Tempo subroutine in order to implement the desired electrochemical reactions and Nernst equation. This limited the possibility to model the MSMP energy system as one, because the 4- and 2-electron DCFC could not run simultaneously. Since the Boudouard reaction is not integrated in the DCFC, we also modelled a separate Boudouard reactor which was fed by the anode output stream. We ran the DCFC's separately and combined the anodic products, which was fed to the Boudouard reactor. This caused that the carbon produced at the solar reactor was fed 1:1 mass ratio to both DCFC's and that the anode output molar ratio of the 2-electron DCFC is always 1:1 CO/CO2, while in reality CO is favored more when the DCFC temperature increases.

Because we had to model the main components separately, modelling became quite complex. Therefore we chose to not implement pumps, valves, blowers and heat exchangers for simplification of the model. Consequently, losses by these components are neglected in the modelling results.

First we tried to tune the input variables of the DCFC (current density and internal resistance) in such a way, that the I-V curve showed similar behavior as literature and experimental results. In this way we could determine the maximum power density, which we wanted to use for further calculations. Unfortunately the results showed not what was expected and we were unable to explain the cause of it. Therefore we chose to determine the maximum power density based on literature and we fixed the current density and internal resistance at values where this maximum power density was reached.

With the assumed maximum power density, the DCFC efficiency of the 2-electron DCFC was significantly higher than for the 4-electron DCFC. This matched with what was expected based on the theory, so we conclude that both modelled DCFC's show realistic behavior with fixed input variables at the assumed maximum power density.

The energy efficiency according to equation (19) of the MSMP energy system was for all temperatures > 90%, which shows the potential of the proposed MSMP energy system. However, we have to take into account that we assume 100% heat exchange in the system and we neglect losses by pumps, valves and blowers. In practice, these components will contribute to the system losses.

Since our model is based on the model of Houwing et al. and our research adds CO production at the anode and a WGS reactor, we compared our modelling results with theirs. As expected our model showed an increased DCFC efficiency. Another difference was to be found in the electric and hydrogen efficiency. Where our model had significantly higher hydrogen efficiency, Houwing et al. had a significantly higher electric efficiency. The system total thermal efficiency was just a little higher for our MSMP energy system. Especially the difference in hydrogen- and electric efficiency was interesting, indicating that hydrogen is a more important product for our MSMP energy system than for Houwing et al.

Lastly we performed an exergy analysis with Cycle Tempo. The exergy loss was negative for the 2-electron DCFC, which is physically impossible. A valid explanation was not possible to have, but our hypothesis is that an explanation can be found in the fact that we have rewritten the DCFC subroutine without rewriting the exergy subroutine. Since the 2-electron DCFC is endotherm and the 4-electron DCFC is exotherm, it is possible that Cycle Tempo therefore calculates negative exergy losses. Nevertheless, the solar reactor showed the highest contribution to the total exergy loss of the system. This implies that in this part the most significant improvements are to be found.

Ultimately, the modelled DCFC's showed expected behavior when we fixed the input variables to operate at the assumed maximum power density. The various efficiencies showed the expected potential in terms of energy efficient electricity generation and hydrogen production. Because our model showed expected results, we can conclude that the model is a proper simulation of reality. Therefore we can use the modelling results in the following technical, economic and social feasibility studies.

5 Technical feasibility

This chapter analyzes the technical barriers and how to overcome them, in order to determine the technical feasibility of the MSMP energy system.

5.1 Introduction

In the technical feasibility we try to determine whether it is realistic if our proposed MSMP energy system can be manufactured or not. In the previous chapters the relevant technology status and detailed theory are presented, so are the Cycle Tempo model and the modelling results. In this chapter we will use this information in order to answer the first sub-question of this thesis:

1. Is the MSMP energy system technically feasible?

The technical feasibility is all about the practical side of the proposed concept. For example, if the theory and modelling results tell us that the DCFC operation temperature needs to be 800 °C this need to be technically feasible. The DCFC needs to be manufactured from a material that can withstand this kind of temperature. If such a material would not exist, the DCFC cannot be manufactured and the concept would be theoretically fantastic, but technically not feasible.

First we will analyze the technical feasibility in terms of heat in the system. Both the solar reactor and the DCFC have high operating temperature, which is a challenge for materials to handle. Also heat transport and heat exchange between the different components in the system are analyzed. Then we will analyze the different mass flows in the system and how to establish them.

5.2 Heat

In the MSMP energy system both the solar reactor and the DCFC have a high operating temperature. The challenge for the materials of which the components are made of is to withstand these temperatures. Preferably we desire materials that can withstand these temperatures on the long term, to prevent frequent maintenance. There is also heat exchange between several in- and output streams. In our Cycle Tempo model we assume 100% heat exchange, however this is fairly impossible in practice. We will analyze possibilities for heat exchange in the system and the effect on the overall losses.

First we will analyze what challenges there are in handling high temperatures, then we will analyze heat exchanging possibilities and we also focus on heat transportation.

5.2.1 Thermal resistance

If we consider the operating temperature of the solar reactor, Figure 7 shows that a temperature of approximately 1500 K is desired. This temperature is necessary to have a proper conversion of methane to carbon and hydrogen. In Chapter 2: Technology, and in more detail in Chapter 3: Theory it became clear that the solar reactor is not yet a mature technology. But there are experimental setups with promising results. (Dahl, Buechler, *et al.*, 2004) made their fluid-wall aerosol flow reactor from graphite and quartz tubes, shown in Figure 8. The center tube, where the methane is entering the reactor, is made of solid graphite. The middle tube is made of porous graphite and the outer tube from quartz. The concentrator is also made from solid graphite. These materials have excellent thermal properties and (Dahl, Buechler, *et al.*, 2004) reports that there was no evidence of corrosion or erosion of the reactor tubes. (Hirsch and Steinfeld, 2004) made a vortex solar reactor. This was also made of graphite and quartz elements, but their cavity body was made of a heat resistant steel alloy. Similarly they did not report any evidence of corrosion or erosion of the materials.

Although we have to take into account that both solar reactors were experimental setups, the materials of which the solar reactor was made of showed a promising temperature resistance.

Similar to the solar reactor, the DCFC is not a mature technology. There are limited experimental setups of the DCFC and they are all focused on the 4-electron process. Our fuel cell operates at higher temperatures, which has consequences for the materials. One of the most described DCFC in literature is the experimental setup of LLNL (Giddey, Badwal, *et al.*, 2012). They made both the anode and the cathode out of nickel and they were separated by a zirconia layer. Nickel was also used for the DCFC in the experimental setup of Lee et al., although the anode was made from a nickel-alumina alloy. (Giddey, Badwal, *et al.*, 2012) reports that both DCFC's showed a number of material degradation in the early stages of testing, but over the past decade there are some improvements reported. Especially the electrolyte melt showed more stability, which improved the lifetime of the DCFC.

The operation temperature of the WGS reactor is approximately 200 °C, significantly lower than the other two components. Temperature handling is therefore less challenging and taking into account that the WGS reactor is a mature technology and is applied on an industrial scale, we can say that temperature handling is technically feasible.

5.2.2 Heat exchange

As described in the modelling chapter, we assume that all mass flows exiting the system transfer their heat back to the system at 100% efficiency. This involves the hydrogen produced at the solar reactor, which leaves the reactor at a temperature of 700 - 800 °C. The hydrogen stream can be cooled down in order to transfer its heat to for example the cathode input gas stream which needs to be heated up to the fuel cell operation temperature. There is also a difference in operation temperature between the fuel cell (700 – 800 °C) and the WGS reactor (200 °C). Therefore the gas streams leaving the anode and cathode of the fuel cell can transfer their heat to the system, similar to the hydrogen leaving the solar reactor.

The challenge for the heat exchange equipment is to withstand temperatures of 700 – 800 °C and to have such a heat transfer coefficient to establish a workable heat transfer efficiency. Solutions are available in the process industry, for example heat recovery from waste gas in an oil refinery. Conventional high temperature heat exchangers are made from metal. Although ceramic heat exchangers are also technically feasible, the application in the process industry is more expensive than the metal heat exchangers. Therefore metal is a more common used material (Stehlík, 2011).

Heat exchangers exist in different forms. There are plate heat exchangers, shell and tube heat exchangers, plate fin heat exchangers, adiabatic wheel heat exchangers and many more types. The type depends on the temperature, medium and size of the heat exchanger. If the temperature is more than 500 °C it is better to use plain heat transfer surfaces (Kilkovsky, Stehlik, *et al.*, 2014). At lower temperatures more enhanced heat exchangers are beneficial and especially tubular heat exchangers with plain tubes are widely used in the process industry.

If we consider our MSMP energy system, we desire heat exchange between hydrogen at 700 °C and air for the cathode at 25 °C. In this case, multiple heat exchangers would be beneficial.

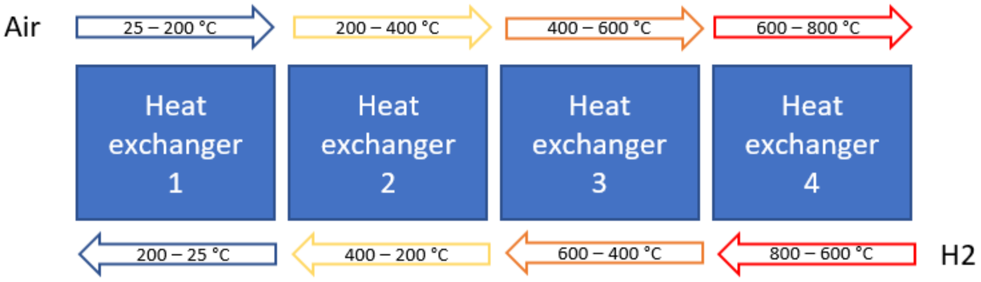

Figure 21: schematic view of multiple heat exchangers in the MSMP energy system

Figure 21 shows a schematic view of a possible heat exchange setup. Heat exchanger 1 and 2 would be of the tubular type, because it operates in the lower temperature region. Heat exchanger 3 and 4 would be plate heat exchangers because higher temperatures are present.

Given the fact that heat exchanging equipment is a mature technology and is used in many industries, we can say that heat exchanging is technically feasible for our MSMP energy system.

5.2.3 Heat transfer

At the anode of the DCFC, both the electrochemical 2-electron and the Boudouard reaction are endothermic, thus the fuel cell demands heat for these reactions. In Chapter 2: Theory we have described that the solar reactor will provide the heat necessary to stabilize the anodic reactions. In the Cycle Tempo model it was not possible to simulate the solar reactor as a thermal source for the DCFC, so alternatively we increased the preheated cathode mass flow. The increased cathodic mass flow provided the heat for the DCFC.

Although the increased mass flow as thermal source worked for the Cycle Tempo model, in reality this is not desired. In our Cycle Tempo model the cathodic mass flow is a CO2/O2 mixture, but in reality it would be an air flow. Since air is a bad thermal conductor, it would be energy inefficient to use air as the thermal source for the fuel cell. A better solution can be found in the electrolyte of the DCFC. The electrolyte is made of molten carbonate, which has a far better thermal conductivity than the air which was used in the Cycle Tempo model. The thermal conductivity of air is around 0.4 - 0.6 W/mK and for molten carbonate it is around 1.0 W/mK (Gheribi, Torres, *et al.*, 2014).

A possible solution is shown schematically in Figure 22. The molten carbonate is flowing in a repeating cycle, where it is heated by the solar reactor, then flows to the fuel cell where it functions as the electrolyte and provides the necessary heat, than flows back to the solar reactor and is heated again. In this way the molten carbonate functions both as the electrolyte and as the thermal source for the DCFC.

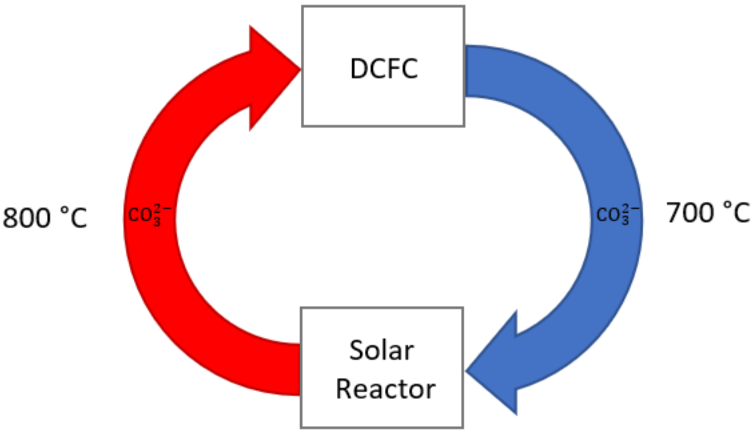

Figure 22: Schematic view of electrolyte functioning as thermal source for the DCFC

In this paragraph we analyzed the technical feasibility in terms of temperature handling of materials, heat exchange and heat transfer. Both for temperature handling and heat exchange we can fairly say that there are viable technical solutions available, especially in the process industry. For the heat transfer to the DCFC we do not have a practical example of a solution, but the solution presented in Figure 22 seems like a logical and relatively easy technical possibility to function as the thermal source for the DCFC. Based on our findings regarding heat challenges we determine that the MSMP energy system is technically feasible to build.

5.3 Mass transfer

Our proposed system has multiple sources and multiple products, all with their own mass flow. We have a mass flow of methane entering the solar reactor, hydrogen leaving the solar reactor, carbon particles leaving the solar reactor and entering the anode of the DCFC, air entering the cathode, a CO/CO2 gas mixture leaving the anode of the DCFC and entering the WGS reactor, water/steam entering the WGS reactor and a CO2/H2/steam gas mixture leaving the WGS reactor.

The Cycle Tempo model neglected mass transferring components, such as recycle blowers and pumps. In this paragraph we will analyze what kind of equipment can establish the mass flows and if this is technically feasible.

At the solar reactor as mass transfer of methane (or natural gas) is present. There is a global infrastructure of gas pipelines, so we can say that the mass transfer of methane is technically feasible. We are only bounded by limitations in capacity of mass transfer. (Wang, Zhang, *et al.*, 2020) analyzed a number of Chinese gas pipelines and reports mass flows between 30 and 152 kg/s. The modelling results in the Cycle Tempo model showed that we produce an electric power of around 20 MW with a CH4 mass flow of 1.3 kg/s. The biggest gas fired power plant in the world, the Surgut-2, produces around 5.6 GW of electric power (Energy, 2019), so it is fair to say that gas distribution to our MSMP energy system will be technically feasible.

We can say the same about the mass flows of hydrogen leaving the solar reactor. Mass transfer can be established similarly, although we have to take the high temperature of hydrogen into account. A centrifugal compressor, commonly used for gas transportation, can process temperatures of up to 150 °C. Therefore it will be best to install the compressor for hydrogen transportation after the heat exchangers. In this way the hydrogen is cooled down before it enters the compressor, so there will be no challenge in temperature handling.

More challenging is the mass transfer of the carbon particles from the solar reactor to the DCFC. First, the carbon particles need to be separated from the hydrogen/carbon mixture and then need to be fed at 700 – 800 °C to the DCFC. (Houwing, Hemmes, *et al.*, 2005) modelled their Cycle Tempo model with a recycle blower. The CO2 produced at the anode was recycled and partly being fed to the anode. Before entering the DCFC it was mixed with the carbon particles and with a recycle blower the mix of CO2 and carbon particles were fed to the anode. In industrial processes, high temperature blowers are widely applied. For example, industrial blower manufacturer Daniels Fans constructs blowers with a capacity of up to 210 m3/s. Their blowers are capable of handling an operation temperature of 1200 °C (Daniels-Fans, 2021).

Another solution would be to use the molten carbonate electrolyte for the transport of carbon to the fuel cell. The carbon particles produced at the solar reactor can be fed to the carbonate slurry and when the carbonate is transferred to the fuel cell it already has the carbon particles present. If we combine this with the heat transfer suggestion showed in Figure 22, the carbonate slurry functions as the electrolyte, as the thermal source for the DCFC and transfers the carbon particles to the fuel cell. The challenge is to transport the fluidic molten carbonate to the fuel cell. If we consider literature, we notice that very little research has been done towards the transport of molten salts. Molten salt is applied on an industrial scale, however mostly in stationary applications such as in a CSP plant where the molten salt is used for thermal storage.

We did find some experimental setups, where different transport technologies were tested for molten salts. The highest reported mass flow of molten salt was in a centrifugal pump. Here a mass flow of 0.36 kg/s was established (Hijikata, Kionoshita, *et al.*, 2013). If we consider the same electrical power output of our Cycle Tempo model (+/- 20 MW), with a temperature drop of 100 K over the fuel cell, a mass flow of approximately 30 kg/s is desired for the carbonate slurry in order to provide the necessary heat for the fuel cell.

The suggestion of a multi functioning carbonate slurry is potentially a good solution for carbon and heat transportation to the fuel cell, but is not (yet) technically feasible. The experimental setup shows that it is possible to transport molten salts, but on an industrial scale there are no practical results available.

5.4 Discussion

In this chapter we have analyzed the technical aspects of the proposed MSMP energy system. Based on earlier chapters we explored if the concept is technically feasible. The technical feasibility answers the first sub question of this thesis and basically tells us if the concept can be manufactured and operated in practice. The technical feasibility is explored with the help of the earlier presented theory and modelling, literature research and common sense. We determined that two practical challenges were most significant: Temperature handling and mass transfer.

Both the solar reactor (> 1200 °C) and the DCFC (700 – 800 °C) have a high operation temperature. A proper thermal resistance of the materials of which they are made of is therefore a must. The solar reactor is not a mature technology, but there are experimental setups with receivers made of graphite, stainless steel alloys and/or quartz. Proper thermal decomposition of methane was achieved without evidence of corrosion or erosion of the materials.

Similarly, the DCFC is not a mature technology but is tested in a few experimental setups. Material degradation in the fuel cell was reported, but showed improvements over the years. Important is that the technology was successfully tested in practice.

Heat exchange is important for our proposed MSMP energy system, because without heat exchange between source- and product mass flows, the efficiency would drop significantly because of heat loss. We noticed that heat exchange of high temperature and large mass flows is applied on an industrial scale in the process industry. There are multiple types of heat exchangers and it seemed that heat exchange is more efficient if we do this stepwise, as showed in Figure 21. In the lower temperature zone a different heat exchanger is more efficient than at higher temperatures.

Another challenge in heat is the thermal source for the DCFC. As described in the theory, at the anode the endothermic electrochemical oxidation of carbon to CO and the endothermic Boudouard reaction take place. Therefore the DCFC demands an external thermal source. In our MSMP energy system the thermal source is the solar reactor and we analyzed how the solar reactor can transfer its heat to the DCFC. Our proposed solution is presented in Figure 22, where we use the molten carbonate electrolyte as medium to transport the heat. The molten carbonate slurry is heated at the solar reactor, flows to the DCFC where it functions as the electrolyte and provides the heat for the occurring endothermic reactions and flows back to the solar reactor to be heated again.

Although our MSMP energy system has not been tested in practice, the technical feasibility study showed that technology related to heat handling can is available in the process industry. We did find available solutions to heat exchange and temperature handling. We did not find an available method for transferring the heat from the solar reactor to the DCFC. However, we proposed a solution where the molten carbonate functioned as the heat transferring medium.

The other technical challenge is mass transfer of the different sources and products in the MSMP energy system. For the input methane, output hydrogen and input air we can fairly say that the desired mass flow is technically feasible, because high mass flows of certain media are present in the process industry. More challenging is the mass transfer of the carbon particles from the solar reactor to the DCFC. We could use a blower that uses part of the produced CO2 to blow the carbon particles present in the CO2 stream to the anode. We could also use the electrolyte, if we consider the proposed setup shown in Figure 22. Here carbon particles are fed to the molten carbonate and transported to the fuel cell. In this way, the molten carbonate is multifunctional by functioning as the electrolyte, transporting the carbon particles to the anode and functions as the necessary thermal source. Mass transfer of molten carbonate is not yet to be found at an industrial scale, but experiments showed that it is possible with a centrifugal pump to establish a mass flow of molten carbonate on a small scale.

In this technical feasibility were able to find a technical solutions in the process industry and for the challenges without an available solution we proposed our own method to overcome the problem, supported by experiments and literature. Given the fact that we were able to find logical solutions for the possible challenges we can say that our MSMP energy system has high potential to be technically feasible.

6 Economic feasibility

In this chapter we focus on the economic aspect of our proposed MSMP energy system. We will analyze the economic potential and try to answer the second sub question.

6.1 Introduction

Earlier in this thesis we presented the modelling results. We have to take into account that our model is not fully representative to practice, because we have made some design choices and assumptions for simplification. Taking this into account we will use the modelling results to analyze the economic potential of our MSMP energy system. The economic potential is important to explore if the MSMP is suited for commercial use. The system can be very interesting in terms of state-of-the art technology and sustainable hydrogen production, but if it is significantly more expensive than competing technologies it will not have commercial value.

Our proposed MSMP energy system is not present in practice and our desired DCFC has not even been tested experimentally. Therefore developing, manufacturing, operation and maintenance costs are hard to determine. We will therefore try to determine what these costs approximately need to be in order to be competitive with competing technologies. Based on the presented modelling results, we will value the in- and output products. Since the WGS reactor is a mature technology, we can determine the cost of this component. For the DCFC and solar reactor we will analyze the cost of referent technologies, in order to estimate what the costs of these components will be. Then we will present the economics of competing technologies in order to determine the maximum other costs of our MSMP energy system. This will help answer the second sub question:

2. Is the MSMP energy system economically feasible?

First we will value the sources and products of our MSMP energy system. We will determine the cost of the technologies of which the solar reactor and DCFC are based on. Then we will analyze competing technologies of hydrogen production and electricity generation. Based on these two analysis we will determine the economic feasibility.

6.2 Costs and revenue

We cannot determine the developing, manufacturing and operation and maintenance costs for the system, since the system does not exist in practice. However, we can determine the value of the sources and products of our system. As a source with value we have methane entering the solar reactor and water necessary for the WGS reactor. We also have air as a source for the cathode, but given the fact that air is freely available we assume that air has no economic value.

As products with economic value we have the hydrogen produced both at the solar reactor and WGS reactor, the electricity generated at the DCFC and the water (steam) produced at the WGS reactor. The CO2 produced at the WGS reactor is assumed to have no economic value.

We use the modelling results presented in detail in Appendix 12.3 to determine the mass flows of the sources and products. The price of the source or product is found in literature.

First we will determine the price of methane, hydrogen and electricity. These prices are dependent of the country where the MSMP energy system operates. The countries with highest potential of applicability are explored in Chapter 7, where we will analyze the social feasibility. Based on these findings we conclude that Algeria and Tunisia are favored. Therefore we will take the prices in these countries into account.

Natural gas in Algeria is relatively cheap, possibly because of the abundancy of gas in this country. Although the price is fluctuating every day, we can take the average of the last ten years. The average cost of gas in Algeria is 4.37 €/MWh (HHV) (Globalpetrolprices.com, 2020).

The hydrogen price depends on the production method. Our price is therefore based on the hydrogen study of (Hydrogen Council, 2020), where an overview is presented of hydrogen production costs for different production methods and hydrogen use. For the use of hydrogen for industrial heat and power they conclude that break-even hydrogen costs are between 1 and 6 €/kg. (Kayfeci, Keçebaş, *et al.*, 2019) reports for a variety of hydrogen production methods lower costs, in the range 1 to 3 €/kg. The hydrogen produced in our MSMP energy system needs to be sold to the hydrogen market, so the price needs to be competitive. Based on hydrogen production costs presented by (Hydrogen Council, 2020) and (Kayfeci, Keçebaş, *et al.*, 2019), we set the price at 1.5 €/kg for the hydrogen produced in our MSMP energy system.

If we take into account the electricity price, we could analyze the current electricity price in Algeria. But we can also analyze the feed-in tariff at which renewable energy is sold to the Algerian grid. Algeria has the desire to increase the share of renewable energy, so is willing to pay more for renewable energy than for fossil fueled energy. In 2019 an Algerian 500 MW PV project sold its electricity for 0.056 €/kWh to the grid (Bellini, 2019). In Tunisia, solar electricity is sold at a price of 0.020 €/kWh to the grid (Bellini, 2019). Based on these findings we will set our electricity price at 38 €/MWh.

Lastly, we have to determine the cost of water. In Algeria in 2011, the cost of water was 0.18 €/m^3 (Boukhari, Djebbar, *et al.*, 2011) and in 2018 the cost of water was 0.15 €/m^3 (OBG, 2018). Based on the mass flow of water entering the WGS reactor, shown in Appendix 12.3, the cost of water in our system would be € 0.000052 per produced MWh of electricity and hydrogen. This is less than 1% of the cost of methane, so it is not contributing significantly to the cost of sources. Therefore we will neglect the cost of water for further calculations.

Now that we have determined the prices of our sources and products, we can determine the costs and revenue per produced MWh. Because our system produces both hydrogen and electricity, the produced MWh takes both into account. For every 1 MWh$_p$, 0.0022 MWh H2 (HHV) is produced and 0.99 MWh electricity is generated. In Table 7 the costs and revenue are presented, based on the modelling results.

Table 7: Costs and revenue per produced MWh of the MSMP energy systems

	DCFC = 700 °C	DCFC = 750 °C	DCFC = 800 °C
Costs			
Methane [€/MWh$_p$*]	0.014	0.016	0.014
Revenue			
Hydrogen [€/MWh$_p$]	0.11	0.13	0.11
Electricity [€/MWh$_p$]	37.9	37.9	37.9
Balance [€/MWh$_p$]	38.0	38.0	38.0

*MWh$_p$ is the energy of both the produced H2 and generated electricity in the MSMP energy system

The results presented in Table 7 show that the margin is 38.0 €/ MWh$_p$ for the system. This means that the MSMP energy system is profitable if the developing, manufacturing and operation and maintenance costs are lower than 38.0 €/ MWh$_p$.

Although we cannot determine all other costs, we can determine the costs of the WGS reactor since many WGS reactors are operational in the process industry. (Moraes, Cozendey da Silva, *et al.*, 2019) calculated the costs of hydrogen production in a compact fuel processor. Here ethanol is reformed in a steam reformer, which is then fed to a WGS reactor. They determined that the costs of the individual WGS reactor was 0.69 €/kg_{H2}.

For the solar reactor we cannot determine the costs very specifically, since no solar reactors are operational. However, since the solar reactor is based on CSP technology we can determine the costs of components shared by the solar reactor and CSP plants. (Abaza, El-Maghlany, *et al.*, 2020) performed a techno-economic analysis of a 10 MW CSP plant. They calculated that the manufacturing costs of the heliostat mirrors of the solar tower configuration cost 1.1 M€/MW. (Vallentin and Viebahn, 2010) calculated that the costs of the whole collector field (thus the mirrors tower and receiver) are 2.7 M€/MW, but they determined that the price would decrease to approximately 1.0 M€/MW in 2025 because of technological development. (Pizzolato, Donato, *et al.*, 2017) studied the solar field labor, which is for example mirror cleaning, and they calculated that O&M costs of the mirrors is 15.5 k€/MW/y.

For our estimation of the solar reactor costs, we will use manufacturing costs of 1.0 M€/MW for the heliostat mirrors and tower construction. For O&M costs of the mirrors we use 15.5 k€/MW/y. So manufacturing and O&M costs of the solar reactors receiver is unknown.

As explained in Chapter 3: Theory, the DCFC is based on the MCFC because they have the same electrolyte (molten carbonate). (Slater, Chronopoulos, *et al.*, 2019) calculated that the manufacturing costs of an MCFC is 3.5 M€/MW and (Verda and Nicolin, 2010) presented 1.0 M€/MW as the manufacturing costs of an MCFC. We will take the costs of Verda and Nicolin (1.0 M€/MW) for our calculations, taking into account that the costs of the fuel cell will decrease in time by technological development.

Now that we have determined the value of the sources and products and the known costs of the components in the MSMP energy system, we can determine what all unknown costs need to be to stay profitable. This depends on the lifetime of the system. We assume that the DCFC needs to be replaced every five years (Verda and Nicolin, 2010). The balance taking into account the abovementioned costs is presented in Table 8.

Table 8: Calculated balance for the unknown costs of the MSMP energy system

Lifetime [y]	**10**	**15**	**20**	**25**
Annual sun hours [h/y]	3000	3000	3000	3000
MWh_p [MWh]	6.2 E^8	9.2 E^8	12.3 E^8	15.4 E^8
Hydrogen production [kg]	4.6 E^7	7.0 E^7	9.3 E^7	11.6 E^7
DCFC [€/MWh_p]	0.078	0.078	0.078	0.078
Solar Reactor [€/MWh_p]	0.031	0.021	0.016	0.013
WGS reactor [€/MWh_p]	0.052	0.052	0.052	0.052
Balance [€/MWh_p]	37.8	37.8	37.9	37.9

Table 8 shows that the unknown costs need to be lower than 37.8 €/MWh_p for the MSMP energy system in order to be profitable and commercially interesting. Part of the unknown costs are the developing costs, the manufacturing cost of the solar reactors receiver, the extra manufacturing costs of a DCFC compared to an MCFC, pumps, valves, blowers, pipes, O&M costs of the system and possible costs or revenue by increase/decrease of methane, hydrogen or electricity price.

6.3 Competing technologies

Now that we know what the limit is for the total costs in order to be profitable commercially, we can compare our MSMP energy system with competing technologies economically. We desire economic competitiveness, thus we want to know what the costs need to be in order to compete with other technologies of hydrogen production and electricity generation.

Our system produces both hydrogen and electricity. Therefore we have to analyze competing technologies for hydrogen production and electricity generation.

If we consider competing hydrogen production methods, we have pyrolysis, gasification, steam reforming of natural gas and electrolysis of water. The production costs of H2 by these technologies are presented in Table 9, which are taken from a techno-economic analysis towards multiple hydrogen production methods performed by (Yukesh Kannah, Kavitha, *et al.*, 2021). Although pyrolysis and gasification are common H2 production methods, these technologies are not sustainable as they both produce significant higher amounts of CO2 than steam reforming, electrolysis and our MSMP energy system. Therefore it is arguable to say that pyrolysis and gasification are no competing technologies, however we do take them into account to compare our method with non-sustainable methods since commercial parties are not always aiming for the most sustainable production methods.

Table 9: Cost of H2 production for various competing technologies (Yukesh Kannah, Kavitha, *et al.*, 2021)

H2 production method	**Cost of H2 production [€/MWh]**
Pyrolysis	28.1
Gasification	20.8
Steam reforming	29.9
Electrolysis	92.4

Table 9 shows that gasification is the cheapest method of H2 production and electrolysis the most expensive. In our system, if we want to produce one MWh of hydrogen, the cost of methane would be around € 42.-. Without all other costs, this is much higher than competing technologies. This is logical, since our system also produces electricity which is not taken into account in the calculation. Therefore we combine the electricity and the hydrogen (MWh_p) for comparison with other technologies.

Table 7 and Table 9 show, that for every MWh of hydrogen produced and electricity generated, the unknown costs need to be lower than 27.9 €/MWh_p to be competitive with pyrolysis H2 production, 20.6 €/MWh_p for gasification, 29.8 €/MWh_p for steam reforming and lower than 92.2 €/MWh_p to be competitive with electrolysis H2 production.

If we consider electricity generation, there are various methods. We will not compare every technology with our MSMP energy system, because some electricity generation methods are not fair to compare. For example hydro power is not fair to compare, since it depends on completely other environmental conditions. Our system is highly dependent on solar power and is therefore desired to be installed in a high solar density area. In most cases these areas lack water availability, therefore hydro power cannot be applied.

Most fair is to compare our system with conventional gas fed power plants, since they also use gas as source. Table 10 shows the costs for a number of gas fired power plants. We take gas power plants at different locations around the world into account, to make a proper overview of the average costs and revenue. The efficiency and costs of a gas power plant can be different per location or country and because of the good existing gas infrastructure, the power plant is not fixed to a specific location.

Table 10: Capital and operational expenditures for natural gas combined-cycle power plants

Plant type	**LCOE [€/MWh]**	**Reference**
Combined-cycle gas fired power plant in the US	33	(Tiseo, 2019)
Combined-cycle gas fired power plant in the US	28	(U.S. Energy Information Agency, 2019)
Natural gas combined cycle power plant	45	(Breeze, 2010)
Combined Cycle natural gas power plant	35	(JRC, 2014)
Combined-cycle gas fired power plants in the US	38	(EIA, 2010)

As shown in Table 10, the levelized cost of electricity for a gas fired power plant is around 35 €/MWh. Compared to our MSMP energy system, we notice that these costs are lower than the balance shown in Table 8. Therefore we can say that, as long as the unknown costs are lower than 34.8 €/MWh$_p$ our system is economically competitive with a gas fired power plant.

6.4 Discussion

In this chapter we have analyzed the economical aspect of the proposed MSMP energy system. The economic analysis was limited by the fact that the concept does not exist in practice, so there is no data available of possible costs of the whole system. If we consider the individual components, both the solar reactor and the DCFC are not operational on an industrial scale. So an individual economic analysis of these components cannot be done completely.

We could only determine the value of both the sources and products, based on the modelling results and the current or expected prices of the sources and products in a specific country. Based on the current price of hydrogen, natural gas and electricity in Algeria we calculated that the balance is 38.0 €/MWh$_p$. We could argue that it is reasonable to say that our MSMP energy system will not be operational earlier than 2030, given the fact that a lot of technological development is needed for especially the DCFC and solar reactor receiver. Possibly the global demand for hydrogen would be higher in 2030, increasing the price and thus the revenue of our system. Also the price of renewable electricity could decrease over time, reducing the revenue. Price changes would certainly have an effect on the balance.

Although both the costs of our solar reactor and DCFC are unknown, we have determined the costs of several related components. We determined the manufacturing and O&M costs of the heliostat mirrors in a CSP plant, which are basically identical in our solar reactor. We determined the manufacturing costs of an MCFC, which has the same electrolyte as our DCFC. And we took the manufacturing costs of a WGS reactor in a fuel processor for the WGS reactor in our MSMP energy system. With these assumptions we calculated that all unknown costs need to be lower than 37.8 €/MWh$_p$ for the MSMP energy system to be profitable. The unknown costs are the developing costs of the MSMP energy system, the manufacturing cost of the solar reactors receiver, the extra manufacturing costs of a DCFC compared to an MCFC, pumps, valves, blowers, pipes, O&M costs of the system and possible costs or revenue by increase/decrease of methane, hydrogen or electricity price.

We also analyzed the costs of competing technologies to know what the maximum costs of our MSMP energy system need to be in order to be competitive.

Our system produces both H2 and generates electricity, so we have analyzed methods for hydrogen production and electricity generation. It seemed that the cost of hydrogen production need to be lower than 29.8 €/MWh to be competitive with steam reforming and as long as our balance remained positive it would be competitive with electrolysis. It would be competitive with gasification when the unknown costs are lower than 20.6 €/MWh_p.

For electricity generation gas fired power plants are taken into account as competing technology, because they also use natural gas as source to generate electricity. We calculated that the unknown costs of our MSMP energy system need to be lower than 34.8 €/MWh_p.

Gasification and pyrolysis are less renewable hydrogen production methods than our MSMP energy system and also a gas fired power plant is less renewable. We could argue that the reduction is CO2 has also an economic value. In fact, based on the modelling results a common combined-cycle power plant emits 48% more CO2 than the proposed MSMP energy system at 800 °C (TNO, 2002). Of course, we have to take into account that the produced hydrogen in the MSMP energy system is included in our combined power generation, while it is impossible to convert hydrogen into power with 100% efficiency and without costs. Our model also neglects several other losses, such as pump and heat exchange losses. But the 48% reduction of CO2 shows the renewable potential of our MSMP energy system.

The economic value of the CO2 reduction is hard to determine, because CO2 emission has an indirect and long-term impact on our environment and health. Given the fact that through global warming on the long term we can expect more instable weather, more drought in large areas, flood in crowded coastal area's and more and more health problems by polluted air, the indirect cost of CO2 emission is enormous. Estimation of these costs falls beyond the scope of research in this thesis and is therefore not taken into account. Although we will not give an economic quantity to CO2 reduction, we will acknowledge that CO2 reduction has a significant economic value on the long term.

Ultimately our economic feasibility study results in an estimation of what the unknown costs for our MSMP energy system need to be in order to be profitable and competitive with competing technologies. The unknown costs need to be lower than 29.8 €/MWh_p to be competitive with the most common hydrogen production method, steam reforming. To be competitive with a gas fired power plant, the unknown costs need to be lower than 34.8 €/MWh_p. And to be profitable without comparing other technologies, the unknown costs need to be lower than 37.8 €/MWh_p.

The unknown costs include the developing costs of the MSMP energy system, developing and manufacturing costs of the solar receiver, the difference in O&M and manufacturing costs between the DCFC and MCFC (which are quite similar) and smaller components such as pumps, valves, blowers, pipes and heat exchangers. The known costs include the manufacturing costs of the mirrors and tower of the solar reactor, MCFC and WGS reactor, the feedstock costs and the revenue by hydrogen production and electricity generation. The margin left for the unknown costs is such, that we can say when our market prices and assumed costs are valid, our MSMP energy system has good potential to be economically feasible.

7 Social feasibility

This chapter will present an analysis which answers the sub question whether our proposed MSMP energy system is socially feasible or not.

7.1 Introduction

The social feasibility explores the applicability of a new or an improved technique at a non-technical and non-economical perspective.

The main goal of the MSMP energy system is to propose a sustainable and stable method for electricity generation and hydrogen production compared to conventional methods. We will analyze, based on the modelling results presented in Chapter 5, if the MSMP energy system is more sustainable than conventional methods and therefore reach its goal. Similar to this, we will analyze if the input sources and the materials can be sustainably produced.

Another important factor is the location where our MSMP energy system can be applied. We could propose such a high-tech and interesting energy system, but if the system is dependent on environmental conditions that are not possible to find on earth the system would not be socially feasible. Given the fact that our system is highly dependent on solar irradiation, we will analyze if and where the ideal places on earth are to create ideal environmental conditions for the system. The location will be analyzed in terms of current and prospected infrastructure and geo politics.

With the help of this social analysis we try to answer the third sub question:

3. Is the MSMP energy system socially feasible?

First we will analyze the sustainable potential of the concept, followed by a research where we try to find the ideal location for implementation of the MSMP energy system.

7.2 Sustainable energy

This paragraph will analyze the modelling results to make a comparison with conventional technology. We will compare the CO2 emission from the MSMP system with CO2 emissions from fossil fueled technology to determine if our method is more sustainable. We will also compare it with conventional sustainable technologies, because our MSMP energy system would not be interesting if conventional and cheaper technologies would be more sustainable than ours.

For a better understanding of which in- and output variables are relevant to analyze the sustainable potential, the earlier presented modelling results are summarized in Table 11.

Table 11: Modelling results relevant for determining sustainable potential

DCFC Temperature		**700 °C**	**750 °C**	**800 °C**
In				
Q_{sun}	MW	16.0	17.6	19.0
M_{CH4}	kg/s	1.18	1.38	1.40
Out				
P_{DCFC}	MW	20.5	20.7	24.1
M_{H2eq}	kg/s	0.55	0.59	0.63
M_{CO2}	kg/s	3.39	3.86	3.95
Overall				
CO2 emission	kg_{co2}/kWh	0.155	0.160	0.153

CO2 emission $H2_{eq}$	kg_{co2}/kg_{H2}	5.90	6.08	5.83

The CO2 emission $H2_{rq}$ is calculated by converting the generated electricity to hydrogen (HHV). In practice this is not the case, since hydrogen production via electricity (electrolysis) has no efficiency of 100%. But for simplicity we do want to know the total CO2 emission per H2 equivalent in order to compare this with other technologies.

Now that all in- and output variables are known, we can determine what the carbon emission per unit of produced hydrogen is from our modelled MSMP energy system and compare it with conventional fossil fueled systems. (Muradov, 2017) performed a techno-economic analysis towards industrial hydrogen production technologies, which is shown in Table 12.

Table 12: CO2/H2 ratio for conventional industrial hydrogen production methods (Muradov, 2017)

Proces	**Feedstock**	**CO2/H2 ratio [kg/kg]**
Steam reforming	Natural gas	8.7 – 10.4
Partial oxidation	Natural gas	9 – 10
Plasma pyrolysis	Natural gas	12
Steam / O2 gasification	Coal	19 - 24
Water electrolysis*	H2O	24 - 28

*Assuming fossil fueled electricity

Table 12 shows that our MSMP energy system emits approximately 37% less CO2 than steam methane reforming. (Muradov, 2017) reports that steam methane reforming is currently the most common method for hydrogen production, which makes it even more interesting that our proposed MSMP energy system is emitting less CO2. This shows the sustainable potential of our concept. If this potential can be realized in practice, the concept would definitely be socially feasible in terms of sustainability.

7.3 Location

This paragraph analyzes the geographical aspect of the proposed MSMP energy system. At first we will investigate where the solar reactor can be located, taking into account that the solar reactor needs to have a certain level of solar irradiance for the thermal decomposition of methane. Secondly, the system is dependent on input sources (natural gas) and it is necessary that the products (electricity and hydrogen) can be utilized. Therefore the infrastructure and source abundancy at the location where the system can be applied needs to be at such a level, that there will be no barriers for the sources and products that cannot be overcome. Thirdly, the locations left after the second subparagraph will be analyzed in terms of geo politics.

7.3.1 Solar Irradiation

The solar reactor in our MSMP energy system uses concentrated solar power to heat methane at a temperature where the methane is converted into hydrogen and solid carbon particles. The waste heat of this process is used for preheating the air entering the cathode, the heat necessary to enable the Boudouard reaction and for the WGS reaction. Based on these facts, we can conclude that the MSMP energy system suits best at places with a high annual solar irradiance yield and where the irradiance level is high.

Figure 23 shows the global annual solar irradiance at the ideal tilt level, indicating where the irradiance level is maximized. The darkest places receive the highest irradiance level, highlighting the west side of the Andes mountain area (around the border of Chile, Bolivia and Argentina), the west side of Namibia, the whole Sahara desert, the southern part of the Middle-East and Australia.

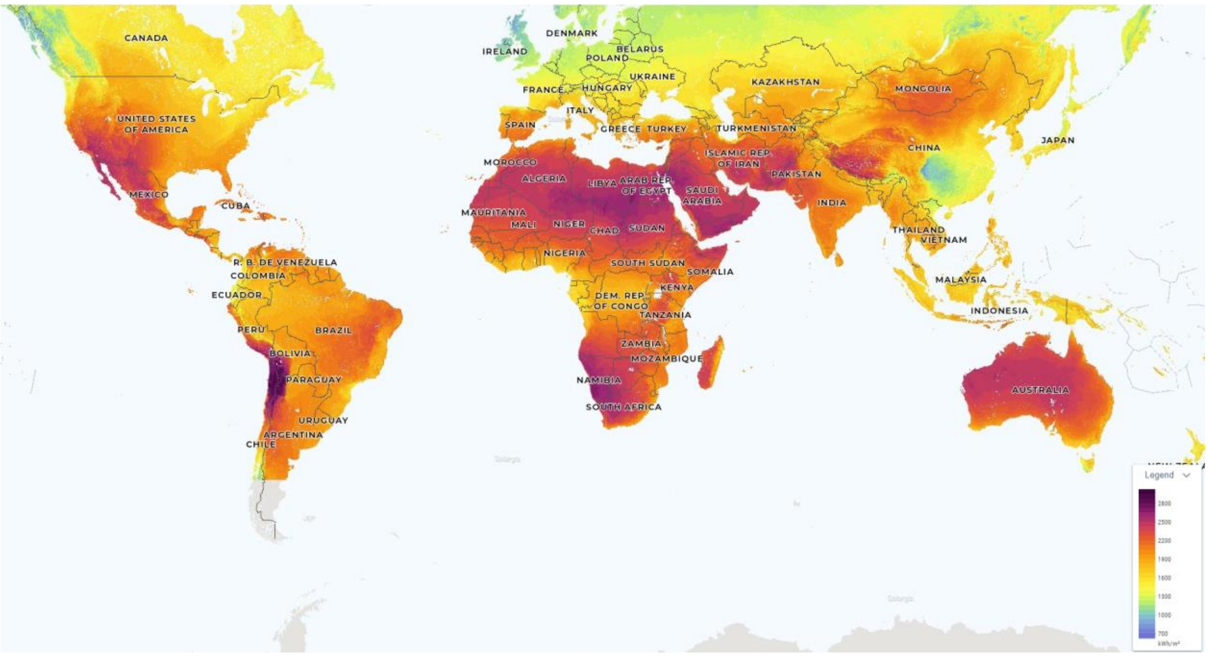

Figure 23: Global annual solar irradiance at ideal tilt level [kWh/m2] (Energydata.info, no date)

A high solar irradiance is not the only indication for a suitable location for our MSMP energy system, because if this peak moment happens only once a year and on average the sky is cloudy the location is not suited at all. Therefore Figure 24 is presented, showing the world map with the annual amount of sunlight. This map highlights a small part on the western US-Mexican border, the Sahara region and the Middle-East.

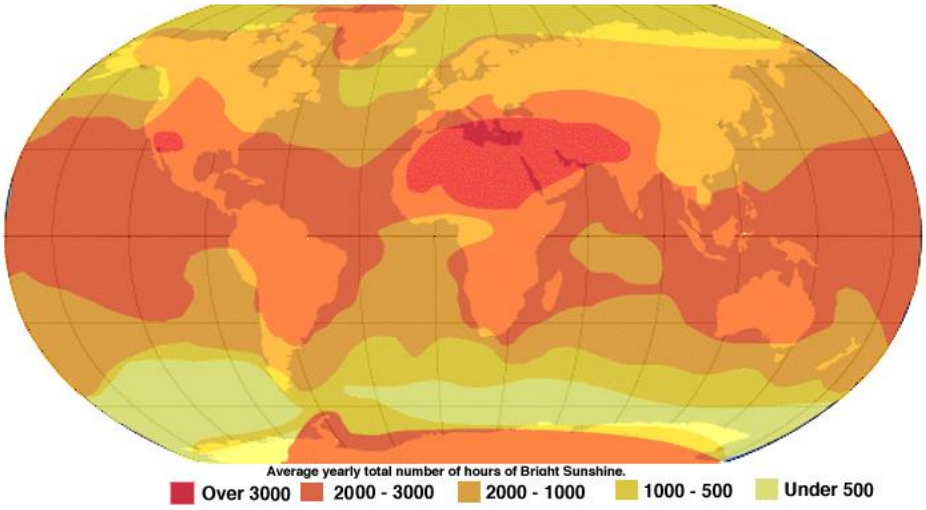

Figure 24: World map with the annual amount of sunlight [h/year] (Institute, no date)

If we combine Figure 23 and Figure 24 we can conclude that the Sahara region and the Middle-East receive the highest solar irradiance and have the most sunlight hours. This makes these regions most suitable for our MSMP energy system in terms of solar irradiation.

7.3.2 Infrastructure

Now that we have selected the ideal region in terms of maximum solar irradiation, we can analyze the infrastructure in this specific region. The MSMP energy system is dependent on natural gas (in this thesis methane) as input so at the ideal location there needs to be a proper source of natural gas. This can be in the form of a local gas field and/or a good connection with the gas grid. Secondly, the our MSMP energy system produces hydrogen which needs to be transported to other regions in the world with hydrogen demand. Currently, there is no hydrogen infrastructure so we assume that either existing gas pipelines can be used for hydrogen transportation or that it is easier to build a hydrogen pipeline next to an existing gas pipeline. Both assumptions include that an existing gas pipeline is beneficial for hydrogen infrastructure.

It is commonly known that the northern part of Africa and the Middle-East have good supplies of fossil fuels, which is shown in Figure 25 and Figure 26.

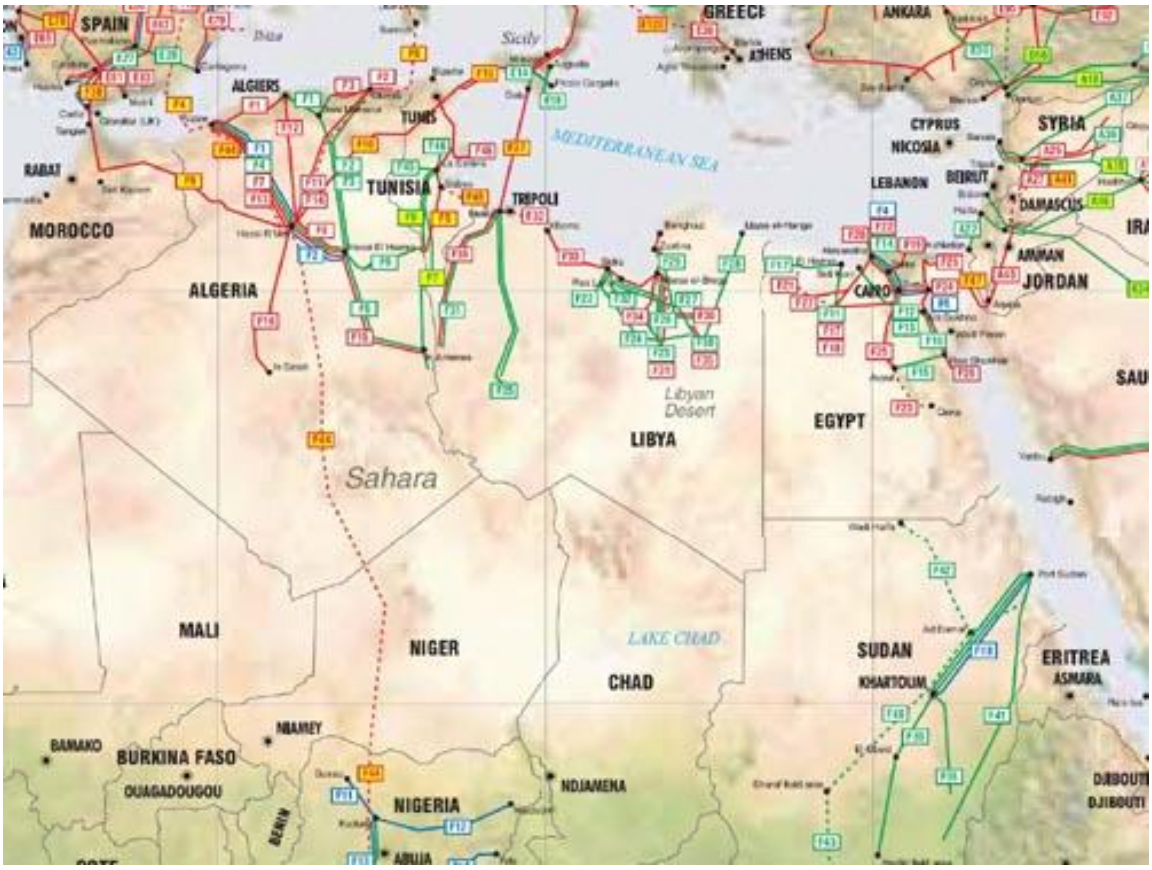

Figure 25: Map of North Africa with oil (green) and gas (red) pipelines highlighted (Theodora, 2017)

Figure 25 shows gas resources and pipelines (marked in red) in Algeria, Tunisia, Libya and Egypt. These countries are also in the high solar irradiation zone presented in Figure 24 and therefore suited for our MSMP energy system with respect to the supply of natural gas.

From the product hydrogen perspective, it is of importance that the existing gas grid (thus the possible hydrogen grid) is connected to the European grid. The European marked is more developed than the African and Middle-Eastern marked and therefore have a higher demand for hydrogen. Figure 25 shows that the Algerian grid is via Morocco connected to Spain. Libya and Tunisia are connected to Italy. Egypt is not directly connected to Europe, because their grid is only connected to Jordan. Furthermore Egypt has good maritime connection via ports in the Mediterranean sea towards Europe and the red see towards Asia.

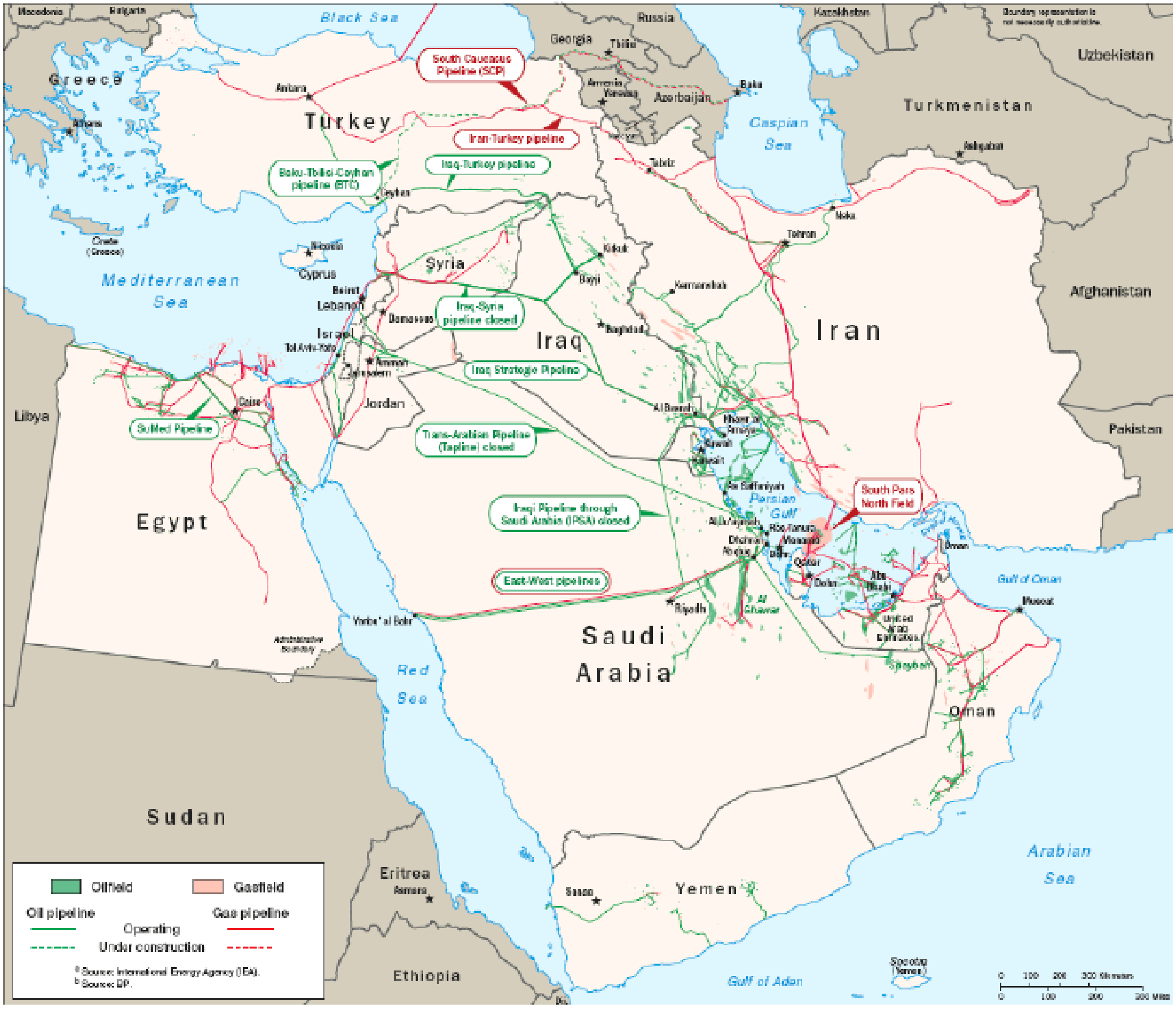

Figure 26: *Map of the Middle-East with oil (green) and gas (red) pipelines highlighted* (Campos, 2013)

Figure 26 shows that Jordan, Saudi-Arabia, Syria, Iraq and Iran have proper gas resources. Although the gas reserves in the Middle-East are abundant and there is an existing infrastructure, Figure 26 shows that the whole grid has one connection with Europe via Turkey. It has a connection with the Russian oriented grid and with ports in the Persian Gulf for maritime transportation to Asia.

If we combine the findings with respect to solar irradiation and the findings in terms of gas resources and gas grid possibilities, we can list the countries suited to apply our MSMP energy system. The countries that have abundant gas resources and are directly connected to the European grid are Algeria, Tunisia and Libya. Morocco is also directly connected to the European grid but has no abundant gas and is therefore dependent on foreign gas resources.

Egypt, Saudi-Arabia, Iraq, Iran, Syria and Jordan have also good gas resources and gas infrastructure but are dependent on Turkey for the connection with the European grid.

7.3.3 Geo politics

Based on the location of where the MSMP energy system can be applied we have to analyze if this specific region is stable and safe and have proper political relations with foreign countries. A politically instable country is not in favor to apply our MSMP energy system, because we have to maintain a long lifetime of the system with reliable supply and distribution of the input source output product respectively. Stable politics means a stable and long term policy, with a low chance of varying policy towards sustainable energy and towards distribution partners where the output product is transported to. From a European perspective we do not want to be dependent on an unreliable hydrogen supply.

In this subparagraph we will determine the political relation with Europe and gas grid connection from the potential countries and if the country is stable and safe. We will analyze the political stability and safety of the country where we can apply the MSMP energy system.

Given the fact that all Middle-Eastern countries with a proper solar irradiation and gas infrastructure are connected to Europe via Turkey, we have to analyze the European-Turkish political relation in order to determine whether the Middle-East is suited to apply our MSMP energy system.

Turkey has the strategy to become a major hub in the international gas distribution, connecting the Middle-East, Asia, Russia and Europe. Their strategy is to privatize a significant part of the gas market in order to stimulate innovations (Austvik and Rzayeva, 2017). Contrary to this strategy, the Turkish regime is not transparent and forbids private parties to sign new contracts with foreign countries. The business-to-government relation is currently not good enough for businesses to have mutual economic advantages. Furthermore the Russian intervention in Ukraine, Syrian crises, Arab spring and other political and civil uncertainties are heavily effecting the reliability of Turkey as a central hub of gas distribution (Austvik and Rzayeva, 2017). Also the strengthening of the centralizing power, the bolstering control over military forces and the Kurdish and DAESH military conflicts do not make Turkey a very stable country.

If we analyze the middle eastern countries with gas resources and infrastructure, we can conclude that Iran and Saudi-Arabia have a stable regime, although this regime conflicts with European politics. It is commonly known that these regimes are in conflict in terms of Women rights and that minorities are not accepted. We can ask ourselves the question whether we (Europe) want to be dependent on these countries for their supply of hydrogen.

Syria and Iraq are countries which have a brief history of war conflicts. Syria is still in a war between DAESH radicals, Russian forces, Kurdish forces and Turkish forces. Iraq has similar conflicts. These countries are very instable and are certainly unreliable for hydrogen dependency and the safety of a long lifetime of the MSMP energy system.

The only country without much recent conflicts is Jordan, but is has to be taken into account that their gas grid only leads to Europa via Syria and Turkey.

If we take a look at the northern African countries, Algeria, Libya, Tunisia and Morocco we see more potential than in the Middle-East.

Algeria has no international or civil conflicts since 1988 (Abada and Bouharkat, 2018). The country has a so called controlled democracy, where the President is head of state and the Prime Minister is head of government. Although freedom of speech is not common, opposition is unofficially permissioned and a free market economy has official support from the government. The relative stability of Algeria makes this country a suited place for the MSMP to be applied.

In terms of politics, Libya is very unreliable. Ever since Muammar Khadaffi has been taken down during the Arab spring, Libya is nowadays a country without a ruling government. The country is in civil war and the gas sources are controlled by different rebellion parties. Although Libya is directly connected Italy, the unsafety and politically uncertainty of this country makes it no good place for our MSMP energy system.

In Tunisia, concentrated solar power is already applied in the southern part of this country. (Omri, Chtourou, *et al.*, 2019) did a Global Risk Analysis towards CSP in Tunisia and they conclude that the technique is exposed to political, financial, legal and strategic hazards. They showed that the major barrier would be the preparation phase of the technique. The risk of not receiving a permit to build the CSP plant is high and there is a risk to conflicts with local residents. Politically, Tunisia is stable although (Omri, Chtourou, *et al.*, 2019) concludes that the public-private partnership needs to be improved in order to have a proper environment for a new technology to be implemented.

Now that we have seen what regions in the world receive the highest level of solar radiation combined with the most sun hours and we have analyzed which countries in these regions have gas resources and proper infrastructure towards a grid connection with Europe and are politically stable, we have Algeria and Tunisia as best possible countries where our MSMP energy can be applied.

7.4 Discussion

In this chapter we have analyzed the social aspect of the proposed MSMP energy system. Earlier we presented the theory, modelling results, technical and economic feasibility and in this chapter our goal was to determine social feasibility.

First we analyzed the sustainable potential of the concept, which we will compare with competing technologies. Based on the modeling results we determined that our concept emits around 0.155 kg_{co2}/kWh. If we consider hydrogen production we noticed that our method produces hydrogen with 37% less CO2 emission than the method of steam reforming, which is currently the most common hydrogen production method. However, we have to take into account that our MSMP energy system is producing hydrogen and generating electricity simultaneously. Therefore we chose to combine the electricity and hydrogen, so every kWh produced is a combination of the energy content in hydrogen and the generated electricity. We also have to notice that our modelling results presented in Chapter 4 are based on assumptions and design choices, and that we neglect several losses in the system. The reduction of CO2 emission compared to conventional methods would therefore probably decrease, but the 37% lower CO2 emission shows that our MSMP energy system certainly has the potential to be more sustainable.

We also explored where in the world our MSMP energy system could be installed. Since our concept is highly dependent on solar irradiation, locations with a high solar density are favored. It seemed that the Sahara region in northern Africa and the Middle-East receive the highest annual amount of sunlight.

Furthermore the MSMP energy system is dependent on natural gas and produces hydrogen, so a proper infrastructure of gas pipelines is desired. Taking this into account, Algeria, Tunisia, Morocco, Egypt, Saudi-Arabia, Iraq, Iran, Syria and Jordan turned out to have a good gas infrastructure.

Considering these countries, we have analyzed geo politics. We favor a country with stable politics, so the gas connection is secured. It seemed that Egypt, Saudi-Arabia, Iraq, Iran, Syria and Jordan have a proper gas infrastructure, but are dependent on Turkey for the connection with the European gas grid. Since Turkey is currently not a stable country, with many international conflicts, dependency on Turkey is not desired. Algeria, Libya, Tunisia and Morocco have a gas connection with Europa via Spain or Italy so this connection is more secured than the connection via Turkey. Considering these countries, Libya and Morocco are not favored. Libya is currently at civil war, which is the worst environment for our technology. Morocco has good gas infrastructure, but gas there is not abundant which make them dependent on neighboring countries. Although Tunisia is a stable country, the view on implementing new technologies seemed not very positive. Therefore we select

Algeria as desired country for our MSMP energy system. It has stable politics, renewable targets, good connection with the European gas grid and has an abundancy of natural gas.

By highlighting that our MSMP energy system has the potential to be a more sustainable hydrogen producer and electricity generator than conventional methods and by finding a country where our system could be implemented where it is functional and without high risks of failing, we can say that our MSMP energy system has a high potential to be socially feasible.

8 Discussion

We started this thesis with the knowledge that our proposed MSMP energy system has two components based on immature technologies. Part of the solar reactor is based on CSP technology, but the receiver of the solar reactor involves besides heat transfer also a chemical reaction (thermal decomposition). Although the solar reactor is not operational at an industrial scale, there are some experimental setups where successful conversion of methane into hydrogen and carbon was established. However, this is at small scale and our MSMP energy system is desired to operate at industrial scale to act as a power plant and industrial hydrogen producer. In the technical feasibility we analyzed the technical challenges we would face at industrial scale and solutions in heat handling and mass transfer are available particularly in the process industry. But in Chapter 2: Technology we noticed that especially the receiver of the solar reactor is the most complex component, which has only been tested in experimental setups. At industrial scale, similar to the scale of our computer model, a methane mass flow of almost 1.5 kg/s is needed. In the experimental setup of (Dahl, Buechler, *et al.*, 2004) the solar receiver was tested with mass flows between $8.74e^{-6}$ and $2.41e^{-5}$ kg/s, so at industrial scale the mass flow of methane would be a factor 65.000 higher. Although we have presented solutions for heat handling and mass transfer in the technical feasibility, we have to acknowledge that we cannot say if the receiver of the solar reactor would show similar results as the solar reactors at experimental scale.

The lack of practical results accounts even more for the DCFC. There are practical results available, but they are all focused on a DCFC where the production of CO2 at the anode is desired. No experiments are known where the production of CO is favored. As explained in Chapter 3: Theory, there are experiments documented where a DCFC was tested at temperatures where CO was expected, but where CO2 was dominant in the product gas mix. Based on the theory, when the produced CO is close to the current collector it can be electrochemically oxidized to CO2. This could be prevented by increasing the overpotential, which decreases the rate of this reaction. The fact that multiple (electro)chemical reactions take place and that the few existing experiments report unexpected results, highlights that controlling the reactions in the DCFC is very complex. Therefore we have to take into account that the results from our model are very theoretical and that there is a chance that in practice the desire to favor CO production is hard to achieve.

Furthermore, the model presented in Chapter 4: Modelling is a simplified simulation of reality based on assumptions and design choices. Because of limitations in the Cycle Tempo software not all possible (electro)chemical reactions taking place at the fuel cell could be implemented in the fuel cell apparatus of Cycle Tempo, so we had to fix some variables that in reality depend on operating conditions. This resulted that in our model 40% of the carbon in the fuel cell is electrochemically oxidized to CO2, 40% of the carbon is electrochemically oxidized to CO and CO2 (molar ratio 1:1) and 20% of the carbon reacts with the produced CO2 by the Boudouard reaction. Based on the theory CO would be more dominant with increasing temperature, but this is not included in our model. If this was included in the model, it would have significant effect on the modelling results. When the CO/CO2 ratio increases, it means that the endothermic (electrochemical) reactions that produce CO are more dominant so the fuel cell demands more heat to stabilize the cell voltage. More CO production means that more CO is fed to the WGS reactor, so more steam needs to be produced to react with CO. This means that also more heat is necessary to produce the steam. So more heat is necessary at both the fuel cell and WGS reactor, affecting the total system thermal efficiency according to equation (18) of the MSMP energy system negatively. On the other hand, when CO becomes more dominant, the DCFC has a higher energy efficiency according to equation (17) because the extra heat is converted directly into power. Also more CO production means that more

H2 can be produced by the WGS reactor. The higher energy efficiency of the DCFC and the increased H2 production affect the total system thermal efficiency of the MSMP energy system positively.

Because the 2-electron DCFC and the 4-electron DCFC were based on a different fuel cell subroutine, it was not possible to run both fuel cells simultaneously, as Cycle Tempo can only run on one fuel cell subroutine. Therefore we choose to model and run the total MSMP energy system in individual components. The modelling results of the solar reactor, 2-electron DCFC, 4-electron DCFC, Boudouard reactor and WGS reactor are individually collected and combined as the results of the total MSMP energy system. This modelling method was very time consuming and limited Cycle Tempo to calculate the mass and energy balances of the total MSMP energy system. If we did succeed to model the complete MSMP energy system as one model the exergy analysis would be more accurate, because then all components would be analyzed in terms of exergy losses. The data would be more accurate, since there was no chance of inaccuracies or human error by collecting the data of the individual components manually to calculate the results of the total MSMP energy system. This does not mean that our method of modelling is inaccurate, but a complete model is preferred to make the modelling process less complex.

Other design choices we made for our model are neglecting the losses by pumps, blowers, valves and heat exchangers. In practice the pumps and blowers are energy consumers, which is neglected in our model. Also heat losses to the environment will be present in practice, but are neglected in our model. We can estimate roughly what the losses of heat exchanging equipment, blowers and valves would be by taking the research of Houwing et al. into account. Although they modelled a solar reactor with a DCFC that only included the electrochemical oxidation of C to CO2, they have included heat exchangers, a blower and a valve (Houwing, Hemmes, *et al.*, 2005). They performed an exergy analysis and the blowers in their model accounted for 0.22% of the total exergy loss in the system. For the valves this was 3.62% and for the heat exchanging equipment this was 8.58%. So in total in their system, blowers, heat exchangers and valves accounted for almost 12.5% of the total exergy loss. The model of Houwing et al. does not include a WGS reactor, so in our model more blowers, pumps, valves and heat exchanging equipment would be necessary. This means that this equipment will have a significant contribution to the total losses in the system.

The technical feasibility showed that solutions to challenges in heat and mass are available in the process industry. We did not find an available solution for the mass transfer of the molten carbonate at our desired temperature, although we did find an experimental setup where molten carbonate was transported by a pump at the desired temperature. On the other hand, molten carbonate is also being used as thermal storage in CSP plants. Although this is at lower temperature than our system, we can say that currently high mass transfer of molten carbonate is possible.

We proposed a solution where the electrolyte is multifunctional, as it functions as the electrolyte, heat transferring medium and transports the carbon particles to the anode. This seems like a viable solution, but it has not been tested in practice. We did not explain how the carbon particles will be present in the molten carbonate and we have to take into account that the carbon particles are also needed in the methane, since the methane itself cannot absorb the solar irradiation. So the carbon particles formed by thermal decomposition are firstly needed in the methane and secondly need to be present in the molten carbonate to be transported to the fuel cell. And thirdly, hydrogen is also formed by thermal decomposition and needs to be separated from the methane, carbon particles and molten carbonate. This process has not been studied in the technical feasibility and could possibly be a challenge.

As explained, the losses that are neglected in the Cycle Tempo model will contribute to the total losses in the system. Consequently, these losses will have an effect on the economic and social feasibility. For the economic feasibility, these losses cause that the maximum unknown costs of our MSMP energy system (37.8 €/MWh$_p$) are in fact lower than we calculated. Because pumps, valves, blowers and heat exchangers account for heat losses to the environment and pumps and blowers use electricity to operate the net power output will decrease and the heat necessary in the system will increase.

The losses we neglected in the Cycle tempo model would account for an increase of CO2 emission (kg$_{co2}$/kWh) in the system. It would have a negative impact on the sustainable potential of our system, so would decrease the social feasibility. The losses cause a decrease in net produced electricity, so the same amount of CO2 is emit for less produced kWh. This would increase the kg$_{cO2}$/kWh ratio. However, we calculated that our MSMP energy system emits 37% less CO2 than conventional hydrogen production methods. Taking into account that Houwing et al. calculated that these losses contribute to approximately 12.5% of the total exergy losses, the neglected losses will not eliminate the sustainable benefit compared to conventional hydrogen production methods.

For the economic feasibility study we used the modelling results from Chapter 4 and we determined costs and revenue from literature. We selected Algeria as the preferred country where our MSMP energy system could be implemented, but Algeria would not be the only country with high annual solar irradiation. As explained in Chapter 7, the whole northern African region and the Middle-East has a high solar density. But also California, Spain, Italy and parts of South-America (i.e. Chile) have high solar density, which is supported by the fact that CSP plants can be found in these countries. The input variables for the economic feasibility will vary per country in terms of gas price, hydrogen price, electricity price, labor cost, permits, etc. For example, for our economic feasibility we took into account the gas price in Algeria. Since Algeria has one of the biggest gas reserves in the world, gas is relatively cheap which is advantageous for the economic feasibility. On the other hand, the electricity price is relatively cheap in Algeria compared to other countries (Globalpetrolprices.com, 2020) which is disadvantageous for the economic feasibility.

We could argue that we can optimize the economic feasibility. We could select a country with high solar density and with the highest electricity price. Then import the necessary gas for the MSMP energy system from the country with the lowest gas price. And export the produced hydrogen to the country with the highest hydrogen price. Parts of Chile, for example, have a very high solar density and in Chile the electricity price for households without subsidy for renewable energy is almost 5 times higher than the non-subsidized electricity price in Algeria (Globalpetrolprices.com, 2020). By transporting cheap Algerian natural gas by ship to Chile, there could be a chance that the economic feasibility improves compared to our results. On the other hand, this suggestion will have a negative impact on the social feasibility. We determined the sustainable potential of our MSMP energy system as a factor of social feasibility. The transportation of cheap Algerian gas to Chile is only possible by ship and it is commonly known that large ships are very polluting. Therefore the MSMP energy system should be built in a country with its own natural gas reserves, to limit the need for polluting transportation of resources.

In terms of sustainable energy we can also discuss why we would consider a system with CO2 emission at all. We could propose a solution with solar panels and electrolyzers, where the solar irradiation is converted to electricity by photovoltaics and with electricity water is converted to hydrogen by electrolysis. Both processes do not involve CO2 emission so this method is in essence more sustainable than our proposed method. However, it is arguable that it is not energy efficient to produce hydrogen by electricity and use the hydrogen later to generate electricity again. The efficiency of a Proton Exchange Membrane (PEM) electrolyzer is around 70% for the production of hydrogen, and a PEM fuel cell for electricity generation has a similar efficiency (RVO, 2006) (Shiva Kumar and Himabindu, 2019). Therefore in this process more than 50% of energy is lost, while there would be no losses when the electricity generated by the solar panels would be used directly. We can fairly say that photovoltaics is an excellent sustainable technology for electricity generation, but will be inefficient when the electricity is used for the production of hydrogen.

In the social feasibility we determined that our proposed MSMP energy system is socially feasible, based on the sustainable potential and based on the fact that we found a suitable location where our system could be implemented. We determined that Algeria would be the best location, since it has a very high solar density, good infrastructure and is relatively stable in terms of politics. But we did not analyzed if Algeria would benefit from the implementation of our MSMP energy system. If we consider electricity demand in Algeria, we notice that the increase in demand is around 3% per year (Haddad, Díaz-Cuevas, *et al.*, 2021). In 2018, the share of renewables in Algeria was only 1% of the total electricity capacity. The government targets to increase the renewable share to approximately 40% in 2035 (Haddad, Díaz-Cuevas, *et al.*, 2021). Given the fact that our system is more sustainable than conventional gas fired power plants, it would contribute to the increase of renewable share in the electricity grid in Algeria, so it would contribute to the renewable energy target of the Algerian government.

Algeria has an abundancy of natural gas reserves, which is an important export product regarding their economy. Our proposed MSMP energy system would not only increase the renewable energy share, but would also not have an effect on current gas consumption because the source for our system is natural gas. So local parties involved in the gas industry would not be negatively affected by our MSMP energy system. Therefore our MSMP energy system would not affect the important gas industry in Algeria.

Our focus in the social feasibility study was to find a suitable country where our MSMSP energy system could be implemented, based on solar density, available resources and geopolitics. Although the northern African region has the highest solar density, we find CSP plants in many countries such as the US, Spain, Italy and China (Omri, Chtourou, *et al.*, 2019). Since CSP plants have a similar dependency on solar irradiation as our MSMP energy system, we could say that our system would work in these countries too if we assume that there would be available necessary resources. It is fair to say that in the coming decades the demand for green hydrogen will increase especially in more developed countries. Hydrogen transportation is an energy consuming process, because it needs to be pressurized significantly. It can be transported by trucks or via pipelines, but it is estimated that hydrogen transportation consumes approximately 3 kWh per kg of hydrogen (Rödl, Wulf, *et al.*, 2018). Therefore it would be beneficial for the social feasibility to reduce the need for transportation of hydrogen. This could be established by building the MSMP energy system as close as possible to a location with high (green) hydrogen demand, such as the US or Europe.

Now that we have performed all feasibility studies and discussed all findings, we will present the final conclusion and answers to the research- and sub questions in Chapter 9.

9 Conclusion

This thesis analyzes multiple angles of approach of electrochemical gasification in a direct carbon fuel cell, based on the multi-source multi-product concept. The MSMP concept is a combination of a solar reactor, direct carbon fuel cell and water-gas-shift reactor. The system consumes multiple sources (methane, solar heat) and produces multiple products (hydrogen, electricity).

By considering literature we have determined the current state of relevant technologies, which highlighted that both the solar reactor and the DCFC are no mature technologies. Although the solar reactor is based on the same working principle as a CSP plant, the receiver of the solar reactor is more complex than in a CSP plant. Where in a receiver of a CSP plant only heat transfer occurs, in the receiver of the solar reactor both heat transfer and thermal decomposition takes place. Experimental setups showed that > 99% thermal decomposition of methane can be accomplished at temperatures > 1500 K, which seemed possible to achieve in a solar tower configuration.

An even less mature technology is the DCFC, because our desired DCFC which favors CO production has not (yet) been tested in practice. At DCFC temperatures higher than 700 °C, multiple (electro)chemical reactions take place simultaneously. Since the 2-electron electrochemical reaction is endothermic, an external thermal source is demanded to stabilize the cell voltage. This means that heat is directly converted into electricity, so theoretically a reversible efficiency >100% would be possible to achieve in the DCFC. In our case, the thermal source is the solar reactor.

The produced CO is fed to a WGS reactor, where it reacts with steam to form H2 and CO2. The WGS reaction favors a temperature of 200 °C with a high steam to CO ratio. With these operating conditions, almost a 100% conversion of H20 and CO to H2 and CO2 can be achieved. The WGS reactor is operational at an industrial scale, so we can say that this is a mature technology.

We modelled the MSMP energy system in Cycle Tempo. Because of software limitations we had to rewrite the Cycle Tempo fuel cell subroutine to add the 2-electron electrochemical reaction. Given the complexity of the model, we neglected pumps, valves, heat exchangers and blowers in the model. Losses by these components are therefore not taken into account. Unfortunately we were not able to tune the input variables such, that the expected I-V curve of the DCFC was shown which would allow us to determine the maximum power density. Therefore we chose to determine the maximum power density based on literature and to tune the input variables such that the DCFC operates at this maximum power density. With these input variables our model showed what was expected. This was a measure of reliability, so that we could use the modelling results for the feasibility studies.

We also performed an exergy analysis. Although a negative exergy loss was shown, which is not possible in practice, we can say that the solar reactor showed the highest contribution to the total exergy loss of the system. This tells us that this is the part where most significant improvements are to be found.

In the technical feasibility we analyzed if the MSMP energy system can be built and operated in practice. By using graphite and stainless steel alloys as materials for the components, the heat in both the solar reactor and the DCFC could be handled since these materials have proper thermal resistance. We presented a stepwise heat exchange solution for an efficient heat exchange in the system. As thermal source for the fuel cell we proposed a solution where the molten carbonate electrolyte is heated by the solar reactor and transferred to the fuel cell. By adding the carbon particles to the carbonate melt, the molten carbonate functions as electrolyte, as heat transferring medium and transports the carbon fuel to the anode of the DCFC. Considering the fact that the WGS reactor is a mature technology, the solar reactor is based on existing technology (CSP) and we presented solutions to challenges in heat handling and mass transfer, we conclude that our MSMP energy system has high potential to be technically feasible.

Based on the modelling results we analyzed the economic feasibility. Since no MSMP energy system is operational, we could not calculate or determine the developing, manufacturing and operation and maintenance costs based on practical data. Therefore we calculated the costs and revenue of the sources and products, based on current and local market prices (in our case in Algeria, based on the social feasibility). We determined the cost of parts in our MSMP energy system which we were able to determine, such as the mirrors of the solar reactor, WGS reactor and the MCFC (which shares the same electrolyte with the DCFC). All other non-determinable costs were called unknown costs. It turned out that the unknown costs need to be lower than 37.8 €/MWh for the MSMP energy system to stay profitable. We then analyzed the costs of competing hydrogen producers and electricity generators, in order to determine what the maximum unknown costs need to be for the MSMP energy system to compete with these competing technologies. We determined that the unknown costs need to be lower than 29.8 €/MWh$_p$ to compete with the most common hydrogen production method, steam reforming. To compete with gas fired power plants the unknown costs need to be lower than 34.8 €/MWh$_p$. We have to acknowledge that our modelling results neglect certain losses in the system and that the we had to make some design choices which can be beneficial for the economic feasibility. But based on current market prices for methane, hydrogen and electricity in Algeria and based on the fact that we were able to determine the costs of the majority of components in the MSMP energy system, it is likely that the unknown costs will not exceed our determined maximum unknown costs. Therefore we can conclude that our proposed MSMP energy system has the potential to be economically feasible.

For the social feasibility study, we analyzed the sustainable potential and we analyzed where our MSMP energy system could be preferably implemented. Based on the modelling results we calculated that our model emitted 37% less CO2 for hydrogen production than steam reforming, which is currently the most common method of hydrogen production. It is fair to say that the neglected losses by our model would account for a higher CO2 emission. However, the losses by this equipment were calculated by Houwing et al. in a similar MSMP energy system and the contribution of these losses were approximately 12.5% to the total exergy loss in the system. Therefore the contribution of these losses will probably not eliminate the 37% reduction of CO2 emission, compared to steam reforming. We also explored where our MSMP energy system could be installed. Since our system highly depends on solar power, a country with high solar density was desired. We also desire a country with good gas infrastructure and stable politics. It turned out that Algeria meets all demands of our MSMP energy system. They do not have significant international conflicts, have an abundancy of natural gas resources, have good connection with the European gas grid, have renewable energy targets and have a very high solar density. Based on the modelling results we calculated that our MSMP energy system is more sustainable than conventional technology and we found a country that meets all demands for the MSMP energy system to be operational. Therefore we can conclude that our MSMP energy system has high potential to be socially feasible.

Based on existing technologies, the theory and modelling results we performed a technical, economic and social feasibility study. We presented and discussed our findings. Based on our research we conclude that our proposed MSMP energy system has high potential to be feasible.

9.1 Answers to research questions

1. Is the MSMP energy system technically feasible?

We determined that the major technical challenges were to be found in heat handling and large mass transfer. Especially in the process industry we found solutions for these challenges. We presented materials with high thermal resistance of which the components of the solar reactor and DCFC can be made of. We proposed a method of efficient heat exchange based on solutions present in the process industry. We proposed a multifunctional electrolyte, also functioning as thermal source and as carrier for the carbon particles. Although the mass transfer of molten carbonate is not present on an industrial scale, we found experiments proving that it is technically possible to establish a mass flow of molten carbonate at our desired temperature. Given the fact that we can use existing technologies and we were able to present logical solutions for challenges without a ready solutions, it is highly likely that our MSMP can be built in practice. Therefore we conclude that the MSMP energy system has high potential to be technically feasible.

2. Is the MSMP energy system economically feasible?

Based on the modelling results and current market prices, we calculated the costs and revenues of the sources and products of the system. This allowed us to calculate what the maximum of all other costs need to be in order for the MSMP energy system to be profitable. We determined based on literature the costs of multiple MSMP energy system components, so the unknown costs became more specific. Based on current market prices for methane, hydrogen and electricity in Algeria and based on the fact that we were able to determine the costs of the majority of components in the MSMP energy system, it is likely that the unknown costs will not exceed our determined maximum unknown costs. Therefore we conclude that our proposed MSMP energy system has the potential to be economically feasible.

3. Is the MSMP energy system socially feasible?

We analyzed the social feasibility in terms of the sustainable and geographical potential. We calculated that our MSMP energy system emits 37% less CO2 than conventional hydrogen production methods. We determined that our MSMP energy system desires a geographical location with high solar density, proper gas infrastructure, stable politics and a government with renewable targets. Algeria turned out to be the favored country for our MSMP energy system to be implemented. Based on the modelling results we calculated that our MSMP energy system is more sustainable than conventional technology and we found a country (Algeria) that meets all demands for the MSMP energy system to be operational. Therefore we conclude that our MSMP energy system has high potential to be socially feasible.

Now that we have answered the sub questions, we can answer the main research question:

Is a Direct Carbon Fuel Cell – Multi-Source Multi-Product energy system feasible?

We analyzed related state-of-the art existing technologies and we presented the detailed theory of the solar reactor and DCFC. We modelled the MSMP energy system and we used our findings in these chapters to perform a technical, economic and social feasibility study. We presented our findings and discussed the uncertainties. We concluded that our MSMP energy system has high potential to be technically, economically and socially feasible. Based on our research we conclude that our proposed MSMP energy system has high potential to be feasible.

9.2 Contribution to science

In this final paragraph we will explain the contribution of this thesis to science. We will explain on which studies our research is based and what the differences are between our and other findings.

As explained in the introduction of this thesis, limited research has been done towards the DCFC. Although the interest in this type of fuel cell has increased over the last two decades, there are just a few documented experimental setups. Most research towards the DCFC focuses on operating temperatures < 700 °C and aim on pure CO2 production at the anode, other than our research. We focused in this thesis on a DCFC at higher operation temperature in order to produce as much CO as possible, instead of just pure CO2 production. As far as we know our research is the first that modelled a DCFC with all possible (electro)chemical reactions included.

We based our Cycle Tempo model on the model of Houwing, which is described in Chapter 4: Modelling. Similar to literature, the model of Houwing took a DCFC into account that produces only CO2 at the anode. Our model is able to run the DCFC at higher operation temperature, where other (electro)chemical reaction can take place. Although we were not able to make a dynamic model, where the occurring reactions are dependent on operating conditions, it still contributes to a better understanding of the possibilities with the DCFC. We were able to compare our results with the results of Houwing, to determine the differences between the MSMP energy system with a DCFC with pure CO2 production and the MSMP energy system with a DCFC that also produces CO which is used in a WGS reactor. Our results showed an improved total system thermal efficiency compared to Houwing, indicating the potential of our proposed MSMP energy system.

Another contribution to science is the feasibility study based on the modelling results. As far as we know there are no reported feasibility studies towards the DCFC, or towards a similar MSMP energy system. We were not able to determine the costs of the whole system, but we were able to determine what the costs need to be in order to be competitive with competing technology. We were also able to determine that the system has high potential to be manufacturable and operatable in practice. We were able to determine that the system can be a sustainable alternative for conventional hydrogen production methods and we were able to find a country that meets all demands for our MSMP energy system. The feasibility studies contributed to science, by highlighting the potential to be technically, economically and socially feasible. Our findings could be a motivation for further research towards the DCFC, solar reactor and/or the total MSMP energy system with the ultimate goal to be operational in practice.

10 Recommendations for further research

Now that we have drawn the conclusions and discussed the findings of our thesis, we will present recommendations elaborating on this thesis.

In Chapter 2: Technology we explained that the proposed MSMP energy system has two components that have not been operated at an industrial scale. Therefore the both the solar reactor and the DCFC are immature technologies. The receiver of the solar reactor has been tested successfully at an experimental scale, but has not been developed further unfortunately. We would recommend further testing of the receiver, but we would also recommend further research towards the effect of increasing the size of the receiver at a size where it can be operated at an industrial scale.

Although the interest in the DCFC has been increased in the last two decades, most studies and experiments focus on CO2 production at the anode. We would recommend to experiment with a DCFC where CO production is desired. This would help analyzing how the (electro)chemical reactions taking place in the fuel cell can be controlled, which allows us to optimize the DCFC in such a way that CO will be dominant in the product gas stream at the anode.

More practical testing of the DCFC will also help to simulate the system in a computer model. For example, the model presented in this thesis has a fixed power density based on experimental results. Since the power density values found in literature aren't very consistent, more testing of the DCFC would help to determine the maximum power density more precisely. We would also recommend to model the DCFC with software that includes all possible (electro)chemical reactions, without a fixed ratio of the reactions taking place in the fuel cell. When the reactions are dependent on operation conditions, it would be a more reliable simulation of reality.

As described in Chapter 4: Modelling our modelling results showed a temperature dependency of the open circuit voltage of the 4-electron DCFC, while in Chapter 3: Theory we explained that the electrochemical reaction taking place at the anode is nearly temperature independent. A similar contrast was shown by the modelling results of the 2-electron DCFC, where the OCV seemed temperature independent while in theory a temperature dependency was expected. Since we were unable to explain the difference between the modelling results of the OCV and the theory, one of our recommendations for further research is to analyze and test the fuel cell subroutine in Cycle Tempo.

In Chapter 4: Modelling we presented an exergy analysis and Cycle Tempo showed a negative exergy loss in the DCFC, which is impossible in practice. We were not able to explain properly what caused this negative exergy loss, so we would recommend a more detailed exergy analysis towards our presented model.

We presented an economic feasibility study in Chapter 6, but it was not possible to determine all costs for our MSMP energy system because of lack of research. Since our desired DCFC has not been tested in practice and the solar reactor is has not been operated at an industrial scale, it was impossible to determine manufacturing, development and operation and maintenance costs. We would recommend further research towards the economic feasibility of our concept, with a more detailed analysis of the possible costs and lifetime of our system. This would help determine more realistically if the MSMP energy concept is commercially interesting.

In the social feasibility study we concluded based on the modelling results that our system is a more sustainable hydrogen producer than conventional methods. In the model we neglected certain losses and we only calculated the CO_2 emission with our static configuration of the fuel cell (as described in Chapter 8: Discussion). We recommend for further research to include the losses we neglected and to use a model that does include all possible (electro)chemical reactions in the fuel cell without the software limitations we had. In this way modelling would be less time consuming and can be optimized in terms of low CO_2 emission in the system. In this way the sustainable potential of our MSMP energy system would be more accurate.

With a more realistic and dynamic model we would recommend for further research to analyze the possibility to implement our MSMP energy system at locations closer to locations where the demand of green hydrogen is expected to increase in the coming decades. As described in Chapter 8: Discussion, transportation of hydrogen is energy consuming, so it would be beneficial for the social feasibility to have the MSMP energy system as close to the place where the hydrogen is needed to reduce losses by transportation.

Another location than Algeria means that the economic feasibility would be different, so we recommend for further research to analyze the effect on the economic feasibility if another location is selected. In this way it would be possible to make a balance between an optimized economic feasibility and social feasibility.

11 Bibliography

'1996 THERMOECONOMIC OPERATION OPTIMIZATION OF THE' (no date).

Z. Abada and M. Bouharkat (2018) 'Study of management strategy of energy resources in Algeria', *Energy Reports*, 4(2018), pp. 1–7. doi: 10.1016/j.egyr.2017.09.004.

S. Abanades and G. Flamant (2005) 'Production of hydrogen by thermal methane splitting in a nozzle-type laboratory-scale solar reactor', *International Journal of Hydrogen Energy*, 30(8), pp. 843–853. doi: 10.1016/j.ijhydene.2004.09.006.

M.A. Abaza,W.M. El-Maghlany,M. Hassab,and F. Abulfotuh (2020) '10 MW Concentrated Solar Power (CSP) plant operated by 100% solar energy: Sizing and techno-economic optimization', *Alexandria Engineering Journal*, 59(1), pp. 39–47. doi: 10.1016/j.aej.2019.12.005.

J.M. Andújar and F. Segura (2009) 'Fuel cells: History and updating. A walk along two centuries', *Renewable and Sustainable Energy Reviews*, 13(9), pp. 2309–2322. doi: 10.1016/j.rser.2009.03.015.

Asimptote (2018) 'Introduction of A program for thermodynamic modeling and optimization of energy conversion systems', p. 9. Available at: http://www.asimptote.nl/assets/media/4275c9cd-5032-4937-ad1e-03420680bf24.pdf.

O.G. Austvik and G. Rzayeva (2017) 'Turkey in the geopolitics of energy', *Energy Policy*, 107(October 2016), pp. 539–547. doi: 10.1016/j.enpol.2017.05.008.

S.P.S. Badwal,H. Ju,S. Giddey,and A. Kulkarni (2017) 'Direct Carbon Fuel Cells', *Encyclopedia of Sustainable Technologies*, 3, pp. 317–329. doi: 10.1016/B978-0-12-409548-9.10119-8.

E. Bellini (2019) *PV-magazine*. Available at: https://www.pv-magazine.com/2019/10/30/algerian-150-mw-solar-tender-concludes-with-final-price-of-0-069-kwh-but-only-a-third-of-capacity-assigned/ (Accessed: 10 January 2021).

S. Boukhari,Y. Djebbar,A. Guedri,and A. Guebail (2011) 'The impact of actual water pricing in Algeria on the environmental dimension of sustainable development', *Journal of Materials and Environmental Science*, 2(SUPPL. 1), pp. 427–432.

P. Breeze (2010) 'The Cost of Power Generation', *Business Insight*, p. 147.

P. Breeze and P. Breeze (2016a) 'Chapter 5 – Solar Towers', *Solar Power Generation*, pp. 35–40. doi: 10.1016/B978-0-12-804004-1.00005-1.

P. Breeze and P. Breeze (2016b) 'Chapter 6 – Solar Dishes', *Solar Power Generation*, pp. 41–46. doi: 10.1016/B978-0-12-804004-1.00006-3.

J. Campos (2013) *Selected oil and gas pipeline infrastructure in the middle east*. Available at: https://www.researchgate.net/figure/Oil-and-Gas-Pipeline-Infrastructure-in-the-Middle-East-35_fig2_260056385 (Accessed: 28 November 2020).

M. Cassir and K. Hemmes (2004) 'A Theoretical Study of the Carbon / Carbonate / Hydroxide (Electro-) Chemical System in a Direct Carbon Fuel Cell', (January). doi: 10.1115/1.4003750.

C. Chen and J.R. Selman (2017) 'Anode modeling of a molten-carbonate based direct carbon fuel cell', *Journal of Power Sources*, 353, pp. 312–322. doi: 10.1016/j.jpowsour.2017.03.078.

G. Cinti and K. Hemmes (2011a) 'Integration of direct carbon fuel cells with concentrated solar power', *International Journal of Hydrogen Energy*, 36(16), pp. 10198–10208. doi: 10.1016/j.ijhydene.2010.11.019.

G. Cinti and K. Hemmes (2011b) 'Integration of direct carbon fuel cells with concentrated solar power', *International Journal of Hydrogen Energy*, 36(16), pp. 10198–10208. doi: 10.1016/j.ijhydene.2010.11.019.

J.K. Dahl,K.J. Buechler,A.W. Weimer,A. Lewandowski,and C. Bingham (2004) 'Solar-thermal dissociation of methane in a fluid-wall aerosol flow reactor', *International Journal of Hydrogen Energy*, 29(7), pp. 725–736. doi: 10.1016/j.ijhydene.2003.08.009.

Daniels-Fans (2021) *High Temperature Fans*. Available at: https://www.danielsfans.com/high-temperature-fans/ (Accessed: 9 January 2021).

A.W. Dowling,T. Zheng,and V.M. Zavala (2017) 'Economic assessment of concentrated solar power technologies: A review', *Renewable and Sustainable Energy Reviews*, 72(June 2016), pp. 1019–1032. doi: 10.1016/j.rser.2017.01.006.

EIA (2010) 'Updated Capital Cost Estimates for Electricity Generation Plants', *US Energy Information Administrations*, (November), p. 189. Available at: http://www.eia.gov/oiaf/beck_plantcosts/pdf/updatedplantcosts.pdf.

A. Elleuch,A. Boussetta,and K. Halouani (2012a) 'Analytical modeling of electrochemical mechanisms in CO 2 and CO / CO 2 producing Direct Carbon Fuel Cell', *Journal of Electroanalytical Chemistry*, 668, pp. 99–106. doi: 10.1016/j.jelechem.2012.01.010.

A. Elleuch,A. Boussetta,and K. Halouani (2012b) 'Analytical modeling of electrochemical mechanisms in CO2 and CO/CO2 producing direct carbon fuel cell', *Journal of Electroanalytical Chemistry*, 668, pp. 99–106. doi: 10.1016/j.jelechem.2012.01.010.

N. Energy (2019) *No Title*, *05-11-2019*. Available at: https://www.nsenergybusiness.com/features/worlds-biggest-gas-fired-power-plants/#:~:text=Located in the Russian city,the Tyumen region oil fields. (Accessed: 9 January 2021).

Energydata.info (no date) *Global Solar Atlas*. Available at: https://globalsolaratlas.info/map?s=78.937708,-48.164063&m=site&c=18.062312,6.328125,3 (Accessed: 25 November 2020).

A.E. Gheribi,J.A. Torres,and P. Chartrand (2014) 'Recommended values for the thermal conductivity of molten salts between the melting and boiling points', *Solar Energy Materials and Solar Cells*, 126, pp. 11–25. doi: 10.1016/j.solmat.2014.03.028.

S. Giddey,S.P.S. Badwal,A. Kulkarni,and C. Munnings (2012) 'A comprehensive review of direct carbon fuel cell technology', *Progress in Energy and Combustion Science*, 38(3), pp. 360–399. doi: 10.1016/j.pecs.2012.01.003.

Globalpetrolprices.com (2020) *Algerian natural gas price*. Available at: https://www.globalpetrolprices.com/Algeria/natural_gas_prices/.

B. Haddad,P. Díaz-Cuevas,P. Ferreira,A. Djebli,and J.P. Pérez (2021) 'Mapping concentrated solar power site suitability in Algeria', *Renewable Energy*, 168, pp. 838–853. doi: 10.1016/j.renene.2020.12.081.

K. Hemmes (2009) 'Towards multi-source multi-product and other integrated energy systems', *International Journal of Integrated Energy Systems*, 1(1), pp. 1–15. Available at: http://wiki-app2.tudelft.nl/pub/Education/IndustrialEcology/RenewableEnergySystems4413RENESY/LectureFuelCellIntegration/2010__K_Hemmes_IJIES_Towards_Multi-source____xid-7105672_2.pdf.

K. Hemmes,J.F. Cooper,and J.R. Selman (2013) 'Recent insights concerning DCFC development : 1998 e 2012', *International Journal of Hydrogen Energy*, 38(20), pp. 8503–8513. doi: 10.1016/j.ijhydene.2013.02.117.

T. Hijikata,K. Kionoshita,K. Uozumi,and T. Koyama (2013) ‘Development of transport technologies for high-temperature fluid in pyrometallurgical reprocessing’, *Energy Procedia*, 39, pp. 127–140. doi: 10.1016/j.egypro.2013.07.199.

D. Hirsch and A. Steinfeld (2004) ‘Solar hydrogen production by thermal decomposition of natural gas using a vortex-flow reactor’, *International Journal of Hydrogen Energy*, 29(1), pp. 47–55. doi: 10.1016/S0360-3199(03)00048-X.

Houwing (2003) ‘Modelling and Analysis of Energy Systems Based on Biomass Gasifiers and Solid Oxide Fuel Cells’, (October).

M. Houwing,K. Hemmes,and N. Woudstra (2005) ‘Thermodynamic equilibrium modeling of Direct Carbon Fuel Cell systems’, 31(0).

Hydrogen Council (2020) ‘Path to hydrogen competitiveness: a cost perspective’, (January), p. 88. Available at: www.hydrogencouncil.com.

A. Ido and M. Kawase (2020) ‘Development of a tubular molten carbonate direct carbon fuel cell and basic cell performance’, *Journal of Power Sources*, 449(November 2019), p. 227483. doi: 10.1016/j.jpowsour.2019.227483.

O.B. Inal and C. Deniz (2020) ‘Assessment of fuel cell types for ships: Based on multi-criteria decision analysis’, *Journal of Cleaner Production*, 265, p. 121734. doi: 10.1016/j.jclepro.2020.121734.

W.R. Institute (no date) *World Sunshine Map*. Available at: http://earth.rice.edu/mtpe/geo/geosphere/hot/energyfuture/Sunlight.html.

N.M. Isa,C.W. Tan,and A.H.M. Yatim (2016) ‘A comprehensive review of cogeneration system in a microgrid: A perspective from architecture and operating system’, *Renewable and Sustainable Energy Reviews*, (February 2016), pp. 1–28. doi: 10.1016/j.rser.2017.06.034.

S. Jia,X. Cao,X. Yuan,and K.T. Yu (2020) ‘Multi-objective topology optimization for the solar thermal decomposition of methane reactor enhancement’, *Chemical Engineering Science*, (xxxx), p. 116265. doi: 10.1016/j.ces.2020.116265.

JRC (2014) ‘ETRI 2014 - Energy Technology Reference Indicator projections for 2010-2050’, *Publication Office of the European Union*, 57(3), p. 108. doi: 10.2790/057687.

C.M. Jubayer,K. Siddiqui,and H. Hangan (2016) ‘CFD analysis of convective heat transfer from ground mounted solar panels’, *Solar Energy*, 133, pp. 556–566. doi: 10.1016/j.solener.2016.04.027.

S. Karagöz,T.T. Tsotsis,and V.I. Manousiouthakis (2020) ‘Multi-scale model based design of membrane reactor/separator processes for intensified hydrogen production through the water gas shift reaction’, *International Journal of Hydrogen Energy*, 45(12), pp. 7339–7353. doi: 10.1016/j.ijhydene.2019.05.118.

M. Kayfeci,A. Keçebaş,and M. Bayat (2019) *Hydrogen production*, *Solar Hydrogen Production: Processes, Systems and Technologies*. doi: 10.1016/B978-0-12-814853-2.00003-5.

T. Keipi,V. Hankalin,J. Nummelin,and R. Raiko (2016) ‘Techno-economic analysis of four concepts for thermal decomposition of methane: Reduction of CO2emissions in natural gas combustion’, *Energy Conversion and Management*, 110, pp. 1–12. doi: 10.1016/j.enconman.2015.11.057.

T. Keipi,H. Tolvanen,and J. Konttinen (2018) ‘Economic analysis of hydrogen production by methane thermal decomposition: Comparison to competing technologies’, *Energy Conversion and Management*, 159(December 2017), pp. 264–273. doi: 10.1016/j.enconman.2017.12.063.

B. Kilkovsky,P. Stehlik,Z. Jegla,L.L. Tovazhnyansky,O. Arsenyeva,and P.O. Kapustenko (2014) ‘Heat exchangers for energy recovery in waste and biomass to energy technologies - I. Energy recovery from flue gas', *Applied Thermal Engineering*, 64(1–2), pp. 213–223. doi: 10.1016/j.applthermaleng.2013.11.041.

X. Li,Z. Zhu,J. Chen,R. De Marco,A. Dicks,J. Bradley,and G. Lu (2009) 'Surface modification of carbon fuels for direct carbon fuel cells', *Journal of Power Sources*, 186(1), pp. 1–9. doi: 10.1016/j.jpowsour.2008.09.070.

Y. Li,D. Li,and G. Wang (2011) 'Methane decomposition to COx-free hydrogen and nano-carbon material on group 8-10 base metal catalysts: A review', *Catalysis Today*, 162(1), pp. 1–48. doi: 10.1016/j.cattod.2010.12.042.

Q. Liu,Y. Tian,H. Li,L. Jia,C. Xia,L.T. Thompson,and Y. Li (2010) 'High efficiency chemical energy conversion system based on a methane catalytic decomposition reaction and two fuel cells : Part I . Process modeling and validation', *Journal of Power Sources*, 195(19), pp. 6539–6548. doi: 10.1016/j.jpowsour.2010.04.047.

T.S. Moraes,H.N. Cozendey da Silva,L.P. Zotes,L.V. Mattos,L.E. Pizarro Borges,R. Farrauto,and F.B. Noronha (2019) 'A techno-economic evaluation of the hydrogen production for energy generation using an ethanol fuel processor', *International Journal of Hydrogen Energy*, 44(39), pp. 21205–21219. doi: 10.1016/j.ijhydene.2019.06.182.

N. Muradov (2017) 'Low to near-zero CO2 production of hydrogen from fossil fuels: Status and perspectives', *International Journal of Hydrogen Energy*, 42(20), pp. 14058–14088. doi: 10.1016/j.ijhydene.2017.04.101.

NASA (2020) *Global Climate Change*, *Nov 2020*. Available at: https://climate.nasa.gov/vital-signs/carbon-dioxide/ (Accessed: 20 January 2021).

OBG (2018) *The Report: Algeria 2018*. Available at: https://oxfordbusinessgroup.com/overview/efficient-expansion-aims-include-building-more-water-related-infrastructure-and-growing-natural-gas (Accessed: 25 January 2021).

E. Omri,N. Chtourou,and D. Bazin (2019) 'Risk management and policy implications for concentrating solar power technology investments in Tunisia', *Journal of Environmental Management*, 237(February), pp. 504–518. doi: 10.1016/j.jenvman.2019.02.049.

N. Ozalp,A. Kogan,and M. Epstein (2009) 'Solar decomposition of fossil fuels as an option for sustainability', *International Journal of Hydrogen Energy*, 34(2), pp. 710–720. doi: 10.1016/j.ijhydene.2008.11.019.

H. Park and M.S. Kim (2014) 'Thermodynamic performance analysis of sequential Carnot cycles using heat sources with finite heat capacity', *Energy*, 68, pp. 592–598. doi: 10.1016/j.energy.2014.02.073.

W.H.A. Peelen,K. Hemmes,and J.H.W. De Wit (1998) 'Carbon a major energy carrier for the future? Direct carbon fuel cells and molten salt coal/biomass gasification', *High Temperature Material Processes*, 2(4), pp. 471–482. doi: 10.1615/HighTempMatProc.v2.i4.30.

A. Pizzolato,F. Donato,V. Verda,M. Santarelli,and A. Sciacovelli (2017) 'CSP plants with thermocline thermal energy storage and integrated steam generator – Techno-economic modeling and design optimization', *Energy*, 139, pp. 231–246. doi: 10.1016/j.energy.2017.07.160.

G.K. Reddy and P.G. Smirniotis (2015) 'Homogeneous WGS Reaction', *Water Gas Shift Reaction*, pp. 169–205. doi: 10.1016/B978-0-12-420154-5.00007-3.

A. Rödl,C. Wulf,and M. Kaltschmitt (2018) 'Assessment of selected hydrogen supply chains-factors determining the overall GHG emissions', *Hydrogen Supply Chain: Design, Deployment and Operation*, pp. 81–109. doi: 10.1016/B978-0-12-811197-0.00003-8.

F. Rosner,Q. Chen,A. Rao,S. Samuelsen,A. Jayaraman,and G. Alptekin (2019) ‘Thermo-economic analyses of IGCC power plants employing warm gas CO2 separation technology’, *Energy*, 185, pp. 541–553. doi: 10.1016/j.energy.2019.07.047.

RVO (2006) *PEMFC-Efficiency*. Available at: https://www.rvo.nl/subsidies-regelingen/projecten/pemfc-efficiency (Accessed: 28 January 2021).

S. Saeidi,F. Fazlollahi,S. Najari,D. Iranshahi,J.J. Klemeš,and L.L. Baxter (2017) ‘Hydrogen production: Perspectives, separation with special emphasis on kinetics of WGS reaction: A state-of-the-art review’, *Journal of Industrial and Engineering Chemistry*, 49, pp. 1–25. doi: 10.1016/j.jiec.2016.12.003.

S.Z. Saw,J. Nandong,and U.K. Ghosh (2018) ‘Optimization of steady-state and dynamic performances of water–gas shift reaction in membrane reactor’, *Chemical Engineering Research and Design*, 134, pp. 36–51. doi: 10.1016/j.cherd.2018.03.045.

A. Segal and M. Epstein (2003) ‘Optimized working temperatures of a solar central receiver’, *Solar Energy*, 75(6), pp. 503–510. doi: 10.1016/j.solener.2003.08.036.

S. Shiva Kumar and V. Himabindu (2019) ‘Hydrogen production by PEM water electrolysis – A review’, *Materials Science for Energy Technologies*, 2(3), pp. 442–454. doi: 10.1016/j.mset.2019.03.002.

J.D. Slater,T. Chronopoulos,R.S. Panesar,F.D. Fitzgerald,and M. Garcia (2019) ‘Review and techno-economic assessment of fuel cell technologies with CO2 capture’, *International Journal of Greenhouse Gas Control*, 91(October 2018), p. 102818. doi: 10.1016/j.ijggc.2019.102818.

P. Stehlík (2011) ‘Conventional versus specific types of heat exchangers in the case of polluted flue gas as the process fluid - A review’, *Applied Thermal Engineering*, 31(1), pp. 1–13. doi: 10.1016/j.applthermaleng.2010.06.013.

A. Steinfeld,M. Brack,A. Meier,A. Weidenkaff,and D. Wuillemin (1998) ‘A solar chemical reactor for co-production of zinc and synthesis gas’, *Energy*, 23(10), pp. 803–814. doi: 10.1016/S0360-5442(98)00026-7.

T. van der Stelt (2018) ‘Technical Notes’.

Theodora (2017) *North Africa pipelines map*. Available at: https://theodora.com/pipelines/north_africa_oil_gas_products_pipelines_map.html (Accessed: 28 November 2020).

I. Tiseo (2019) *Project CAPEX of US CC power plant*, *Statista*. Available at: https://www.statista.com/statistics/243707/capital-costs-of-a-typical-us-combined-cycle-power-plant/.

TNO (2002) ‘CO 2 emission factors for fuels in the Netherlands’.

U.S. Energy Information Agency (2019) ‘Annual Energy Outlook 2019 with projections to 2050’, *Annual Energy Outlook 2019 with projections to 2050*, 44(8), pp. 1–64. doi: DOE/EIA-0383(2012) U.S.

D. Vallentin and P. Viebahn (2010) ‘Economic opportunities resulting from a global deployment of concentrated solar power (CSP) technologies-The example of German technology providers’, *Energy Policy*, 38(8), pp. 4467–4478. doi: 10.1016/j.enpol.2010.03.080.

V. Verda and F. Nicolin (2010) ‘Thermodynamic and economic optimization of a MCFC-based hybrid system for the combined production of electricity and hydrogen’, *International Journal of Hydrogen*

Energy, 35(2), pp. 794–806. doi: 10.1016/j.ijhydene.2009.10.104.

W.C. Wang,Y. Zhang,Y.X. Li,C. Liu,and S. Han (2020) ‘Vulnerability analysis of a natural gas pipeline network based on network flow’, *International Journal of Pressure Vessels and Piping*, 188(April), p. 104236. doi: 10.1016/j.ijpvp.2020.104236.

L. Xiaowei,R. Jean-Charles,and Y. Suyuan (2004) ‘Effect of temperature on graphite oxidation behavior’, *Nuclear Engineering and Design*, 227(3), pp. 273–280. doi: 10.1016/j.nucengdes.2003.11.004.

R. Yukesh Kannah,S. Kavitha,Preethi,O. Parthiba Karthikeyan,G. Kumar,N.V. Dai-Viet,and J. Rajesh Banu (2021) ‘Techno-economic assessment of various hydrogen production methods – A review’, *Bioresource Technology*, 319(August 2020), p. 124175. doi: 10.1016/j.biortech.2020.124175.

12 Appendix

12.1 Cycle Tempo subroutine

Original part of the DCFC subroutine

```
*---------------------------------------------------------------------------*
*    Determine anode outlet composition, no equilibrium.     *
*---------------------------------------------------------------------------*
ELSE IF (TYPE == 'DCFC') THEN
            YAN(CO2) = YAN(CO2) + YAN(C) * 3 * UFLH
            YAN(C)   = YAN(C) * (1 - UFLH)
```

Changed part of the DCFC subroutine

```
*---------------------------------------------------------------------------*
*    Determine anode outlet composition, no equilibrium.    *
*---------------------------------------------------------------------------*
ELSE IF (TYPE == 'DCFC') THEN
            YAN(CO2) = YAN(CO2) + YAN(C) * UFLH
            YAN(CO) = YAN(CO) + YAN(C) * UFLH
            YAN(C) = YAN(C) * (1-UFLH)
```

Original part of the DCFC subroutine

```
*----------------------------------------------------------------------*
*    3. Calculation of reversible potential                          *
*----------------------------------------------------------------------*
ELSE IF (TYPE == 'DCFC') THEN
        IF (YAN(CO2) > 0) THEN
          ERev = E0C + R * TK / ( 2 * FAR) *
    &           XLOG( XSQRT(YCA(O2)) * YCA(CO2) * XSQRT(PFCELL) /
    &           (YAN(CO2) * XSQRT(YAN(CO2))))
```

```
    ELSE
      ERev = 1.d20
    ENDIF
```

Changed part of the DCFC subroutine

```
*----------------------------------------------------------------------*
*    3. Calculation of reversible potential                            *
*----------------------------------------------------------------------*
ELSE IF (TYPE == 'DCFC') THEN
    IF (YAN(CO2) > 0) THEN
      Erev = E0C + R * TK / ( 2 * FAR) *
&        XLOG( XSQRT(YCA(O2)) * YCA(CO2) * XSQRT(PFCELL) /
&        (YAN(CO2) * YAN(CO)))       ELSE
      ERev = 1.d20
    ENDIF
```

12.2 Modelling results

In the following tables, the modelling results are presented in detail.

Table 13: Relevant variables of the solar reactor in the MSMP energy Cycle Tempo model at fixed power density and temperature

DCFC = 700 °C	$\dot{m}_{CH4_{in}}$	1.18 kg/s
	$\dot{Q}_{sun}$	8.24 MW
	$\dot{m}_{H2_{out}}$	0.32 kg/s
	$\dot{m}_{C_{out}}$	0.87 kg/s
	$\dot{Q}_{H2_{\Delta T=700-25}}$	3.12 MW
DCFC = 750 °C	$\dot{m}_{CH4_{in}}$	1.34 kg/s
	$\dot{Q}_{sun}$	9.67 MW
	$\dot{m}_{H2_{out}}$	0.37 kg/s
	$\dot{m}_{C_{out}}$	0.97 kg/s
	$\dot{Q}_{H2_{\Delta T=750-25}}$	3.83 MW
DCFC = 800 °C	$\dot{m}_{CH4_{in}}$	1.39 kg/s
	$\dot{Q}_{sun}$	10.4 MW
	$\dot{m}_{H2_{out}}$	0.38 kg/s
	$\dot{m}_{C_{out}}$	1.01 kg/s
	$\dot{Q}_{H2_{\Delta T=800-25}}$	4.26 MW

Table 14: Relevant variables of the CO2-DCFC in the MSMP energy Cycle Tempo model at fixed power density and temperature

DCFC = 700 °C	$\dot{m}_{cath_{in}}$	16.6 kg/s
	$\dot{m}_{an_{in}}$	0.43 kg/s
	P_{DCFC}	1.00 MW
	$\dot{Q}_{sun}$	9.68 MW
	$\dot{m}_{an_{out}}$	3.85 kg/s
	$\dot{m}_{cath_{out}}$	13.2 kg/s
	T_{out}	800 °C
	$\dot{Q}_{cat_{\Delta T=800-25}}$	8.84 MW
DCFC = 750 °C	$\dot{m}_{cath_{in}}$	20.7 kg/s
	$\dot{m}_{an_{in}}$	0.49 kg/s
	P_{DCFC}	8.82 MW
	$\dot{Q}_{sun}$	13.0 MW
	$\dot{m}_{an_{out}}$	4.37 kg/s
	$\dot{m}_{cath_{out}}$	16.8 kg/s
	T_{out}	850 °C
	$\dot{Q}_{cat_{\Delta T=850-25}}$	11.9 MW
DCFC = 800 °C	$\dot{m}_{cath_{in}}$	16.3 kg/s
	$\dot{m}_{an_{in}}$	0.51 kg/s
	P_{DCFC}	11.0 MW
	$\dot{Q}_{sun}$	10.9M kW
	$\dot{m}_{an_{out}}$	4.55 kg/s
	$\dot{m}_{cath_{out}}$	12.3 kg/s
	T_{out}	900 °C
	$\dot{Q}_{cat_{\Delta T=900-25}}$	9.28 MW

Table 15: Relevant variables of the CO-CO2-DCFC in the MSMP energy Cycle Tempo model at fixed power density and temperature

DCFC = 700 °C	$\dot{m}_{cath_{in}}$	63.3 kg/s
	$\dot{m}_{an_{in}}$	0.43 kg/s
	P_{DCFC}	10.5 MW
	$\dot{Q}_{sun}$	36.9 MW
	$\dot{m}_{an_{out}}$	2.14 kg/s
	$\dot{m}_{cath_{out}}$	61.6 kg/s
	T_{out}	600 °C
	$\dot{Q}_{cat_{\Delta T=600-25}}$	30.6 MW
DCFC = 750 °C	$\dot{m}_{cath_{in}}$	71.2 kg/s
	$\dot{m}_{an_{in}}$	0.49 kg/s
	P_{DCFC}	11.9 MW
	$\dot{Q}_{sun}$	44.6 MW
	$\dot{m}_{an_{out}}$	2.43 kg/s
	$\dot{m}_{cath_{out}}$	69.2 kg/s
	T_{out}	650 °C

	$\dot{Q}_{cat_{\Delta T=650-25}}$	37.4 MW
DCFC = 800 °C	$\dot{m}_{cath_{in}}$	79.6 kg/s
	$\dot{m}_{an_{in}}$	0.51 kg/s
	P_{DCFC}	13.2 MW
	$\dot{Q}_{sun}$	53.3 MW
	$\dot{m}_{an_{out}}$	2.53 kg/s
	$\dot{m}_{cath_{out}}$	77.6 kg/s
	T_{out}	700 °C
	$\dot{Q}_{cat_{\Delta T=700-25}}$	45.2 MW

Table 16: Relevant variables of the Boudouard reactor in the MSMP energy Cycle Tempo model at fixed power density and temperature

DCFC = 700 °C	$\dot{m}_{in}$	6.00 kg/s
	$\dot{Q}_{sun}$	2.53 MW
	T_{out}	730 °C
	$\dot{Q}_{\Delta T=730-25}$	2.85 MW
DCFC = 750 °C	$\dot{m}_{in}$	6.80 kg/s
	$\dot{Q}_{sun}$	2.86 MW
	T_{out}	780 °C
	$\dot{Q}_{\Delta T=780-25}$	3.54 MW
DCFC = 800 °C	$\dot{m}_{in}$	7.08 kg/s
	$\dot{Q}_{sun}$	3.00 MW
	T_{out}	830 °C
	$\dot{Q}_{\Delta T=830-25}$	4.38 MW

Table 17: Relevant variables of the WGS-reactor in the MSMP energy Cycle Tempo model at fixed power density and temperature

DCFC = 700 °C	T_{in}	200 °C
	$\dot{m}_{H2O_{in}}$	2.00 kg/s
	$\dot{m}_{gasmix_{in}}$	5.99 kg/s
	$\dot{Q}_{sun}$	1.04 MW
	T_{out}	400 °C
	$\dot{Q}_{out}$	3.72 MW
	$\dot{m}_{H2_{out}}$	0.11 kg/s
	$\dot{m}_{CO2_{out}}$	6.80 kg/s
DCFC = 750 °C	T_{in}	200 °C
	$\dot{m}_{H2O_{in}}$	2.27 kg/s
	$\dot{m}_{gasmix_{in}}$	6.80kg/s
	$\dot{Q}_{sun}$	1.19 MW
	T_{out}	400 °C
	$\dot{Q}_{out}$	4.23 MW
	$\dot{m}_{H2_{out}}$	0.12 kg/s
	$\dot{m}_{CO2_{out}}$	7.75 kg/s

DCFC = 800 °C	T_{in}	200 °C
	$\dot{m}_{H2O_{in}}$	2.34 kg/s
	$\dot{m}_{gasmix_{in}}$	7.03 kg/s
	$\dot{Q}_{sun}$	1.22 MW
	T_{out}	400 °C
	$\dot{Q}_{out}$	4.37 MW
	$\dot{m}_{H2_{out}}$	0.13 kg/s
	$\dot{m}_{CO2_{out}}$	7.99 kg/s